DEPARTAMENTO DE MEDICINA
FACULTAD DE MEDICINA
UNIVERSIDAD DE SALAMANCA

TESIS DOCTORAL

Analysis of Autophagy in Lung Cancer

RUSLAN IBRAHIM AL-ALI

2016

TESIS DOCTORAL

Analysis of Autophagy in Lung Cancer

RUSLAN IBRAHIM AL-ALI

2016

DIRECTOR

PROF. DR. ROGELIO GONZÁLEZ SARMIENTO

DEPARTAMENTO DE MEDICINA
FACULTAD DE MEDICINA
UNIVERSIDAD DE SALAMANCA

El Prof. Dr. ROGELIO GONZÁLEZ SARMIENTO, Catedrático del Departamento de Medicina, Universidad de Salamanca.

CERTIFICA:

Que el trabajo titulado “ANALYSIS OF AUTOPHAGY IN LUNG CANCAER”, que representa el Licenciado en Farmacia Don Ruslan Al-Ali, ha sido realizado bajo su dirección en el Departamento de Medicina y reúne, a su juicio, todos los requisitos necesarios, para ser presentado ante el tribunal correspondiente, a fin de optar al **Grado de Doctor** por la Universidad de Salamanca.

Para que así, se expide el presente certificado.

En Salamanca, a 13 de Julio de 2016

Fdo. Dr. Rogelio González Sarmiento

VNiVERSiDAD D SALAMANCA
CAMPUS DE EXCELENCIA INTERNACIONAL

800 AÑOS
1218 - 2018

DEPARTAMENTO DE MEDICINA

D. Rogelio González Sarmiento, Catedrático de Medicina de la Universidad de Salamanca y director de la tesis de D. Ruslan Al Ali pone en conocimiento de la Comisión de doctorado que D. Ruslan Al Ali es de nacionalidad ruso-siria y que ha desarrollado su tesis doctoral financiado por una beca Erasmus Mundi. Aunque durante estos años ha mejorado sus habilidades en castellano, todavía tiene problemas para una correcta expression escrita en este idioma, motivo por el cual el manuscrito se ha redactado en ingles. La presentación oral de la tesis se hará en ese idioma y la discussion en castellano, circunstancia conocida y aceptada por los miembros del tribunal.

Para que así conste a los efectos orpotunos

En Salamanca a 18 de Julio de 2016-07-18

Rogelio González Sarmiento

El presente trabajo ha sido co-financiado por el Proyecto FIS PI 10/00213

“This project has been funded with support of the European Commission. This publication reflects the view only of the author, and the Commission cannot be held responsible for any use which may be made of the information contained therein.”

ACKNOWLEDGMENT

- Firstly, I would like to thank my supervisor Prof. Dr. Rogelio González Sarmiento for his patience and support. I wish someday I will be able to make him proud.

-Secondly, I would like to thank EPIC program and Ms. Susana Verde for the support I got. With them, I felt that I belong.

- Thirdly, I would like to thank University of Salamanca, IBSAL, and the laboratories of J.J. García Marín, I. Sánchez-García, J. de Las Rivas and E.M. Sánchez Tapia for the help and guidance that I got.

-Fourthly, I thank all my colleagues and friends that stood by me. And all those who stood against me… I don't think I could have done it without you.

-Finally, to my parents. You wanted me to be better, helped me even when it was hard and got worried about every single detail. Nothing can explain how I feel.

Thank you all

Título:

Análisis de autofagia en cáncer de pulmón

Introducción

El cáncer del pulmón tiene la segunda prevalencia más alta entre los tumores y la mortalidad más alta. La resistencia a los fármacos es común. Por eso, la vía de autofagia puede presentar una diana alternativa de terapia en este tipo del cáncer.

La autofagia es un mecanismo celular de reciclaje de proteínas y de protección contra las toxinas y el estrés. Este proceso empieza con la formación de una doble membrana (Fagofora-Phagophore) por los complejos ULK1-ATG13-FIP200 y Beclin1-ATG14L1-VPS15-VPS34. Luego forma una esfera (autofagosoma) por ATG16-ATG5-ATG12 y LC3B, y que contiene las proteínas y orgánulos que están destinados a ser destruidos. Finalmente, se fusionó con una lisosoma y forma el autolisosoma.

La autofagia tiene relación con la vía del apoptosis por Beclin1-Bcl2 y posiblemente, por Caspasa-8 y P62. Esta relación puede ser útil en terapias anti-tumorales, en particular el bloqueo de autofagia en células resistentes a los fármacos inductores de apoptosis.

Para evaluar la participación autofágica en el cáncer del pulmón, hemos estudiado factores genéticos que pueden cambiar la predisposición a la enfermedad (i.e. polimorfismos), cambios que afectan la expresión de las proteínas, el papel de las isoformas y el efecto de los tratamientos que modifican la autofagia.

Resumen

Nuestra hipótesis del trabajo es que la autofagia juega un papel esencial en el desarrollo y el crecimiento del cáncer de pulmón. Modular la autofagia y la expresión de sus mRNAs y proteínas es una diana terapéutica potencial en esta enfermedad.

Nuestro estudio ha evaluado los factores genéticos que afectan autofagia y la expresión de sus proteínas. Además, hemos realizado un análisis bioinformático de los cambios en la expresión de isoformas en las vías de autofagia y apoptosis que pueden afectar las enfermedades del pulmón. Finalmente, hemos estudiado el efecto de tratamientos diferentes que afectan la vía de autofagia.

El genotipado se realizó para cuatro polimorfismos de genes relacionados con la autofagia. Los polimorfismos son ATG2B (rs3759601), ATG10 (rs1864183), ATG5 (rs2245214) y ATG16L1 (rs2241880). El análisis de estos polimorfismos se realizó en una muestra de 165 fumadores con cáncer de pulmón y 145 fumadores sanos. El 30% de la muestra tenía EPOC y el 44% tenía una historia de un cáncer en la familia.

Nuestros resultados han revelado que el alelo G del gen ATG16L1 (rs2241880) tiene un papel protector frente al desarrollo del cáncer del pulmón, en particular en pacientes sin EPOC. El alelo G del gen ATG16L1 (rs2241880) produce una disminución de la autofagia debido a un aumento de la degradación de ATG16L1 por Caspasa-3 y una interacción reducida con moléculas del dominio WWD necesarias para la función de ATG16L1.

Los polimorfismos que hemos estudiado están en la zona codificante del gen, excepto el de ATG5 (rs2245214) que está en un intrón. Nuestro estudio ha investigado la región 5' no-codificante (5'UTR) para mutaciones que afectan la expresión proteica de genes relacionados con autofagia. Hemos encontrado que la presencia de secuencias "AUG" en la zona promotora (uAUG) tiene un efecto supresor sobre la expresión proteica. En el gen ATG16L2, la distancia entre uAUG y el codón de inicio está relacionado con el efecto inhibidor, efecto que se incrementa al aumentar el número de uAUG.

El "dogma central" clásico de biología teoriza "un gen- una proteína". Aunque después del proyecto del genoma humano se ha descubierto que la mayor parte de eucariotas pueden producir múltiples mRNAs de un gen por un proceso de splicing alternativo. Los mRNAs que resultan se llaman isoformas, y pueden tener la misma función biológica o una función diferente. Los niveles de isoformas cambian con el consumo de tabaco y enfermedades como el cáncer y EPOC.

La secuenciación masiva (NGS) es muy útil en los estudios del RNA. Para los biólogos, usar de NGS no es fácil y cuesta mucho su análisis bioinformático. Los resultados se agrupan en tablas de miles de millones de números que no sirven de mucho en el laboratorio molecular. Así, hemos seleccionado los datos para analizar las vías de autofagia y apoptosis de 87 archivos de RNA-Seq de tejido pulmonar de sujeto sanos y pacientes de EPOC y de tumores del pulmón no-microcíticos (ENA/EBI). El análisis se realizó por TopHat/Cufflinks y la plataforma usegalaxy.org. Se utilizaron textos de programación de R3.2.1 para analizar la expresión de genes e isoformas.

Hemos encontrado que la vía de la autofagia en el cáncer del pulmón está sobreexpresada (ULK1, ATG13, ATG16L1, Beclin1, P62/SQSTM, ATG7, ATG4B, ATG9A y ATG2A). El inhibidor mTOR presenta niveles altos de expresión total, lo que no es consistente con una autofagia activa. En el cáncer del pulmón, mTOR tiene niveles normales de mTOR canónico (MTOR-001), pero sobreexpresa una

isoforma corta (MTOR-002) que puede tener un efecto inhibidor sobre el mTOR canónico, así que la autofagia aumenta. Hemos encontrado una expresión baja de MTOR-002 y de genes de autofagia en EPOC, así como cambios de isoformas en apoptosis han ocurrido en Caspasa-10 (cáncer de pulmón) y Caspasa-3 (EPOC).

Nuestros resultados sugieren un posible papel de las isoformas en las enfermedades. Estos cambios en las isoformas pueden servir como biomarcadores en biopsias liquidas o como dianas terapéuticas.

Nuestro estudio incluye tres tratamientos que modifican la autofagia. La cloroquina que bloquea los últimos pasos de autofagia; el Panobinostat (LBH589) que inhibe histona deacetilasas (HADCi) y aumenta la autofagia y, finalmente, la metformina que activa la vía del AMPK y aumenta la autofagia.

Hemos usado dos líneas-celulares de cáncer de pulmón (H1299 y COR-L23p). El estudio ha utilizado técnicas para medir el crecimiento celular (MTT), las fases del ciclo celular y la muerte (FACS), la morfología de las células y la distribución de las proteínas (microscopía confocal, 3D cultivos y inmunofluorescencia) y estudio de cambios en proteínas relacionadas con autofagia por Western-blot (mTOR, P62/SQSTM1, LC3B y Beclin1) .

Nuestros resultados indican que las células que tienen niveles iniciales altos de autofagia (COR-L23p) mueren cuando se tratan con HDACi y eso puede ser por la toxicidad autofagica. Por otro lado, la cloroquina mata a las células con autofagia normal (H1299) y el HDACi baja el nivel del crecimiento celular, pero no produce muerte. La metformina no produzca muerte, pero baja el crecimiento celular con concentraciones altas de fármaco. Las combinaciones diferentes de los fármacos no han producido ganancia en el efecto terapéutico.

La vía de la autofagia tiene potencial para ser una diana de fármacos anti-tumorales tan importante como la vía del apoptosis. Sin embargo, se necesitan más estudios de combinaciones posibles de fármacos relacionados con autofagia y más información sobre interacciones entracelulares de proteínas y RNAs.

Conclusiones

1. En nuestro estudio, el alelo G del gen ATG16L1 rs2241880 juega un papel protector frente el desarrollo del cáncer de pulmón, en particular en los pacientes sin EPOC.
2. La existencia de uAUG en la región 5' no-traducida inhibe la expresión proteica, y esta inhibición depende de la distancia la codón iniciador y el número de uAUGs.
3. La expresión diferente de las isoformas del gen mTOR puede jugar un papel en la patologenica del cáncer y EPOC.
4. Líneas celulares del cáncer del pulmón responden de formas diferentes a tratamientos que modifican la autofagia. Las células que tienen niveles altos de autofagia presentan toxicidad celular cuando son tratados con inhibidores de histona deacetilasa como panobinostat. Las células que tienen niveles normales pueden ser tratadas con bloqueadores de autofagia como la cloroquina. En el cáncer de pulmón no-microcítico, el uso de metformina o la combinación de moduladores de autofagia no proporcionan ninguna mejora en el resultado.

El índice:

INDEX

1. INTRODUCTION

1.1. AUTOPHAGY

Autophagy is a natural mechanism where the cell recycles some unnecessary, toxic and dysfunctional components. The degradation of cytoplasmic materials consists of several sequential steps: sequestration, transport to lysosomes, degradation, and utilization of degradation products [1].

Generally, autophagy is classified into three types: macroautophagy, microautophagy, and chaperone-mediated autophagy. Microautophagy is a non-selective lysosomal degradative process which involves direct engulfment of cytoplasm by the lysosome (in mammals) or the vacuole (in plant and fungi). It can be induced by nitrogen starvation or rapamycin [2]. Chaperone-mediated autophagy selectively degrades cytosolic proteins in lysosomes. It is activated in response to stressors such as prolonged starvation, exposure to toxic compounds, or oxidative stress [3]. Macroautophagy is the sequestration of cargo within cytosolic double-membrane vesicles. It is an evolutionarily conserved process from yeast to mammals. Macroautophagy is the primary catabolic mechanism for degrading and recycling long-lived proteins and organelles such as the endoplasmic reticulum, mitochondria, peroxisomes, the nucleus and ribosomes. It occurs as a cellular response to both extracellular stress conditions (e.g., nutrient starvation, hypoxia, overcrowding and high temperature) and intracellular stress conditions (e.g., accumulation of damaged or superfluous organelles and cytoplasmic components) [4]. We will focus on macroautophagy in our work and referred to it as autophagy.

The steps of autophagy are described in Figure 1, were elongation and nucleation of a membrane form the phagophore. The expanding double-membrane vesicle is called “autophagosome”, which contains the targeted-for-autophagy molecules. Finally, the outer membrane of the autophagosome fuses with a lysosome and form an autolysosome. The inner membrane and its cytoplasmic cargo are degraded and recycled. [5]

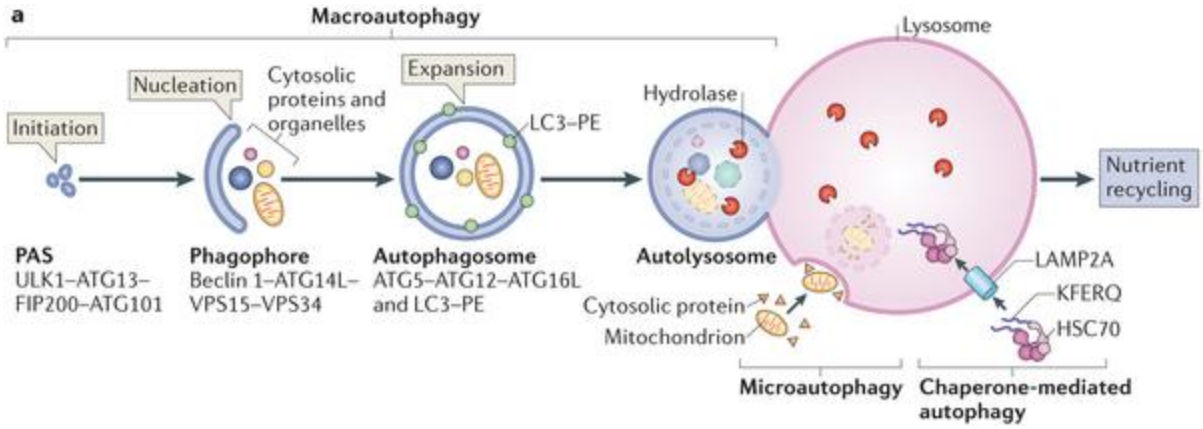

Figure 1: A brief description of autophagy process. The steps of initiation, nucleation, expansion and merge with lysosomes.

Over 20 genes were described to participate in mammalian autophagy. The initiating process starts with the formation of ULK1-ATG13-FIP200 complex. The elongation requires another complex of Beclin1-ATG14L-VPS15-VPS34. The phagophore is expanded with ATG5-ATG12-ATG16L complex from one hand, and LC3B-PE and P62/SQSTM1 from the other hand.

One of the most important genes involved in autophagy control is mTOR, which forms a complex called MTORC1 that inhibits the complex ULK1-ATG13-FIP200, providing a negative control on autophagy [6].

1.2. PROTEINS INVOLVED IN AUTOPHAGY

1.2.1. MTOR complexes

The mechanistic target of rapamycin or mammalian target of rapamycin (mTOR) is also known as FKBP-Rapamycin Associated Protein or FKBP12-Rapamycin Complex-Associated Protein (FRAP). It is coded in humans by MTOR gene (ENSG00000198793) at chromosome1. mTOR is a regulator of cellular metabolism, growth and survival. It regulates the phosphorylation of more than 800 proteins directly and indirectly.

mTOR is arguably considered the single most potent control of autophagy. mTOR is a kinase that forms two known complexes MTORC1 and MTORC2, the latter related to organization of cytoskeleton. MTORC1 is a complex composed of mTOR, Raptor, mLst8/GβL. Another molecule involved in this complex is PRAS40, which plays a role as a regulatory component that disassociates after growth factor stimulation [7, 8].

Growth factors activate mTOR and inhibit autophagy. The two main pathways affecting the function of MTORC1 are PI3K/Akt and AMPK pathways. The PI3K/Akt is activated via growth

factors, leading to inhibition of GTPase activity of TSC2, which finally ends activating Rheb. Energy depletion leads to activating AMPK (AMP-activated protein kinase) and increased activity of TSC2. Rheb binds gently to MTORC1 and is considered an activator (Figure 2) [8].

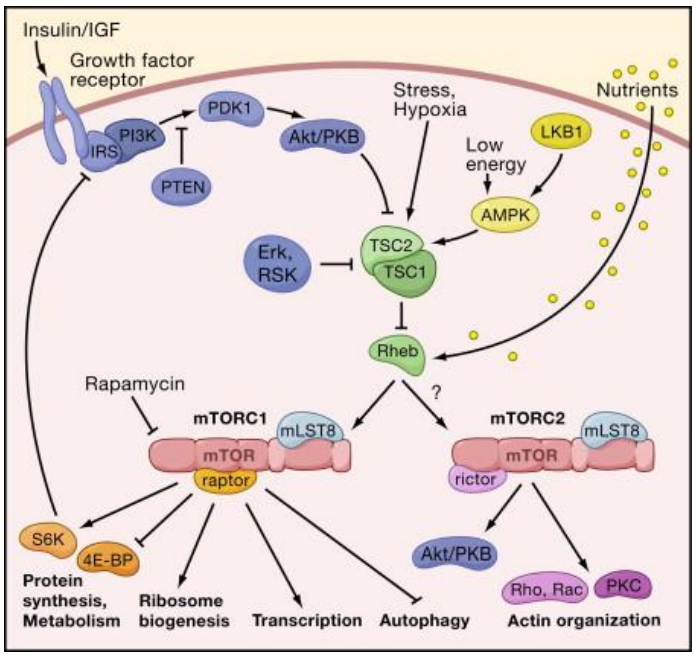

Figure 2: mTOR two complexes, both of them have mLST8 on their mTOR kinase domain. mTORC1 interacts with Raptor, while mTORC2 interacts Rictor protein instead. [7]

AMPK phosphorylates ULK1 on Ser317 and Ser777 activating it. Under nutrition sufficiency, mTOR phosphorylates ULK1 at Ser757; this interferes with ULK1/AMPK, and eventually disturbs the activation of autophagy [6].

1.2.2. ULK1-ATG13-FIP200

ULK1 (unc-51 like autophagy activating kinase 1) is the only serine/threonine kinase in the core autophagy pathway. It is activated by AMPK directly and inhibited by MTORC1. Both ATG13 and FIP200 can enhance ULK1 kinase activity separately, but to get the full activation, both of them are required [9]. Another protein that plays a role in this complex is ATG101, which is essential for the phosphorylation and stabilization of ATG13. [10]

ULK1 is thought to induce the phosphorylation of P62/SQSTM1 under proteotoxic stress. Also, both ULK1 and ATG13 have LIR domain that allows the interaction with LC3. [11]

1.2.3. Beclin1

ULK1 is responsible for Beclin1 activation through Ser14 phosphorylation. ATG14L promotes Beclin1 phosphorylation by enhancing association with ULK1. Phosphorylation of Beclin-1 is required for induction of autophagy in response to amino-acid starvation [12]. Beclin1 role as autophagy-inducing protein is now being seriously questioned because it appears to exercise several non-autophagy functions. [13]

Beclin1 is part of a complex that contains ATG14L, VPS34 and VPS15 among others. But it may worth more to mention its relationship to Bcl2 family. Beclin1 get its name from interacting with Bcl2 (Bcl-2-interacting myosin-like coiled-coil protein). Beclin1 has BH3 domain that interacts with Bcl2 (Figure 3) [14]. Bcl2, a well-known anti-apoptotic protein, binds to Beclin1 BH3 domain, preventing the assembly of pre-autophagosomal structure, thereby inhibiting autophagy. There is no evidence that this binding affects Bcl2 anti-apoptotic function. [13]

The dissociation of Bcl2-Beclin 1 complex can occur after phosphorylation of Bcl-2 by JNK1. Once Bcl2 is phosphorylated and dissociates from Beclin1, autophagy can occur [14].

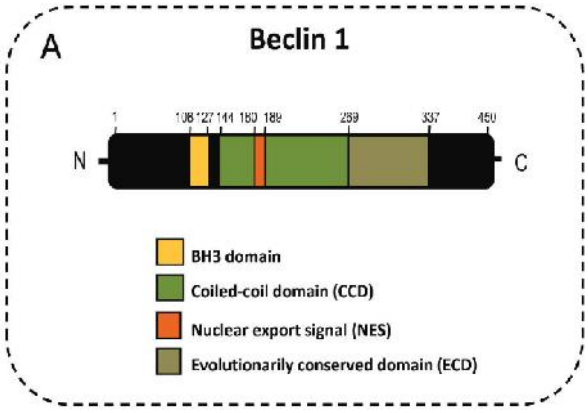

Figure 3: Beclin1 structure. BH3 domain helps interacting with Bcl2 protein.

1.2.4. ATG5-ATG12-ATG16L1

The activation of ATG12 starts with ATG7 (Figure 4). ATG7 shows homology with E1 ubiquitin-activating enzyme. Most ATG7 exists as homo-dimer and interacts with ATG12 at Cys572. ATG7 transfers the activated ATG12 to the E2-like enzyme ATG10 via the C-terminal thioester linkage. The function of ATG10 is likely equivalent to that of E2 ubiquitin-conjugating enzymes. Finally, the carboxy-terminal glycine of ATG12 is covalently attached to lysine 149 of ATG5 via an isopeptide bond between the carboxyl group of a glycine residue and a ε-amino group of the lysine residue. After the formation of the ATG5-ATG12 conjugate, ATG16L1

associates with the complex, binding non-covalently with ATG5 and forming a tetrameric complexes. [15, 16]

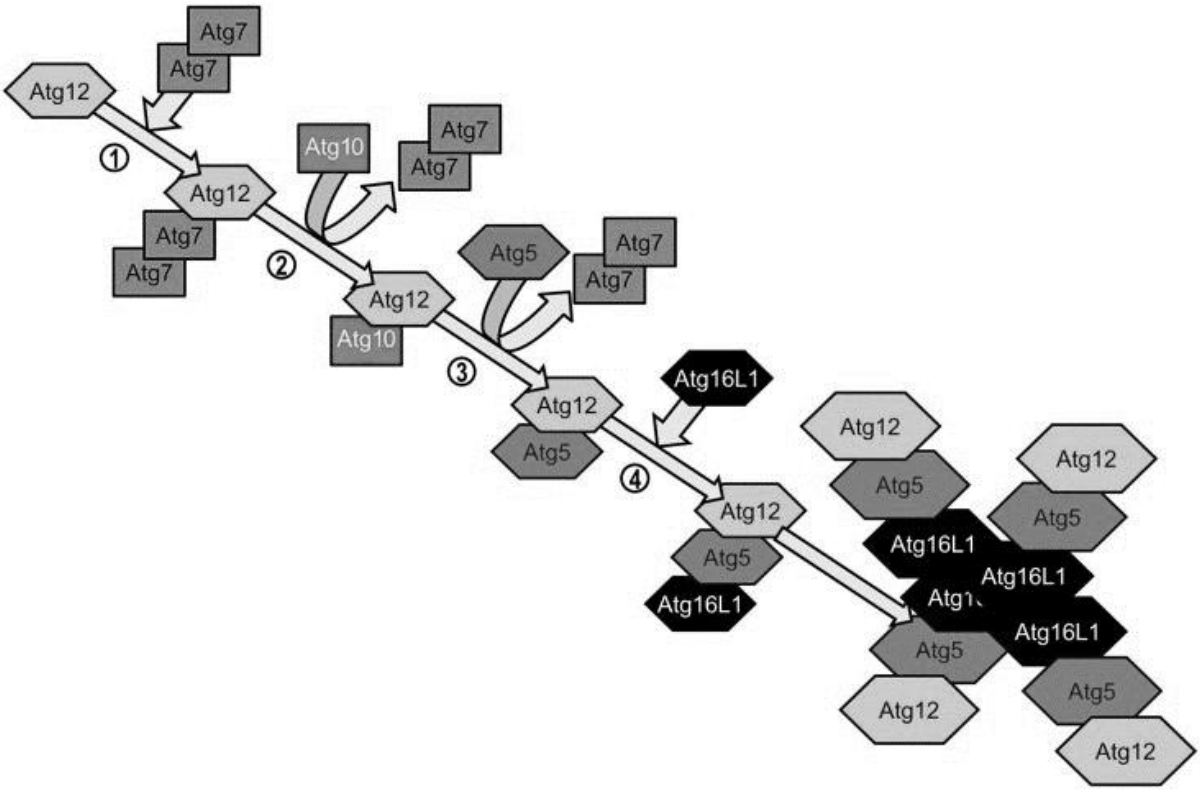

Figure 4: the formation of ATG5-ATG12-ATG16L1 complex. It start with ATG12 interacting with ATG7, then ATG10 removes ATG7, and later replaced with ATG5. The last molecule that is involved is ATG16L1. The final composition is a quarto-mere of ATG5-ATG12-ATG16L1.

1.2.5. ATG8 system

Atg8 is a yeast protein that acts as E1-like enzyme. It has several homologs in mammals. The most important are LC3 and GABARAP.

LC3 is considered the best-characterized autophagosome marker in mammalian cells. ATG2B removes the amino acids located on the C-terminal region from last glycine residue in newly synthesized LC3 (pro-LC3) to form LC3-I. ATG7 activates LC3-I via conjugation to phosphatidylethanolamine (PE) to form the membrane-associated LC3-II.

LC3 is considered one of the best markers for the activity of autophagy, especially the ratio of LC3I/LC3II. Western-blot analysis show two bands can be distinguished easily in 12% SDS-PAGE.

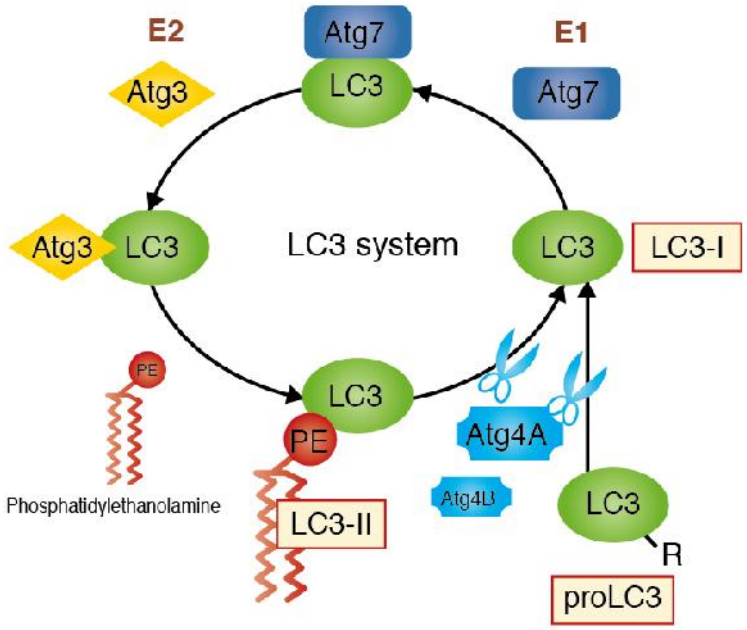

Figure 5: LC3 system. The pro-LC3 molecule is cut by ATG4 and converted into LC3I. Later, two other proteins (ATG7/ATG3) helps the molecule to be transferred into the head group of its substrate phosphatidylethanolamine (PE) and turn to LC3II. LC3II is recycled by ATG4 back into LC3I by deconjugating it from PE. [17]

While LC3 plays a role in the elongation of the phagophore, GABARAP is responsible for a later stage in autophagosomal maturation. [18]

1.2.6. P62/SQSTM1

Proteins are selected for autophagy by chaperones and ubiquitinated, then aggregated by P62/SQSTM1 [19]. P62 is the protein responsible of carrying the selected proteins into the autophagosome. Its reaction with LC3 helps to locate it with the selected proteins inside the autophagosome that later will be catabolized in the autolysosome.

P62 is composed of three domains: the N-terminal Phox and Bem1 (PB1), a zinc finger domain (zinc) and C-terminal ubiquitin associated domain (UBA). While PB1 domain exhibits self-oligomirization, the UBA domain binds to the ubiquitinated proteins targeted for autophagy [20, 21].

A small region of 11 amino acids is located between the zinc finger and UBA domain called LRS (LC3 recognition sequence). It is essential for P62-LC3 interaction, and this domain is shared through many autophagy receptors that react directly with ATG8 (ATG19, ATG32,

ATG34, P62, NBR1, NDP52, OPTN and Nix). The domain is highly conserved and involves an acidic cluster (337-339: DDD or DEE) and hydrophobic residues (340-343: WXXL or WXXV). [22]

P62 is degraded via autophagy and interaction with LC3 and self-oligomerization are needed for affective degradation [23].

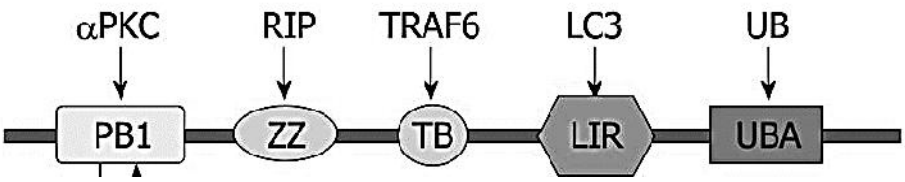

Figure 6: Domains of P62/SQSTM1 and the proteins that interact with.

1.2.7. Other genes

While many more genes can be associated with autophagy, some important genes need to be high-lightened. ATG2A and ATG2B genes are paralogs, located on chromosomes 11 and 14 respectively. They are required for autophagosome formation and knocking both causes a block in autophagic flux and accumulation of unclosed autophagic structures [24].

ATG9A is an integral membrane protein required for autophagosome formation and a membrane carrier in the autophagy pathways. It has been suggested that ATG9A transports membranes during autophagosome formation and dynamically cycles between trans-Golgi network and late endosomes [25]. ATG9A overexpression was correlated with poor survival in patients with oral squamous cell carcinoma [26].

1.3. RELATED PATHWAYS

1.3.1. Apoptosis

Apoptosis is the *type I of programmed cell death* (PCD type I). Over exposure to stress and pro-autophagy factors leads to autophagy programmed death (PCD type II). Many proteins play a role controlling both autophagy and apoptosis, some of them are listed in Table 1.

Autophagy may be able to kill a cell either by actively degrading necessary cellular components (e.g. mitochondria) or by non-selectively degrading cellular components to the point that the cell can no longer survive. However this does not mean that autophagy is directly responsible for activating apoptosis. [27]

Exogenous apoptosis is initiated with Fas receptor activation (Fas/Fas L complex). The signal is transferred via FADD to activate Caspase8-10 and release cytochrome C from mitochondria. Cytochrome C recruits Apaf1 and Caspase9 to form apoptosome. All this leads to activation of the executing caspases 3,6 and 7. (Figure 7) [28]

During apoptosis, morphological and biochemical changes occurs in the cell. Morphological changes include cell shrinkage, nuclear condensation and fragmentation, dynamic membrane blebbing, and loss of adhesion. The biochemical changes include DNA cleavage into fragments, phophatidylserein externalization and cleavage of several intracellular substrates by proteolysis. [29]

As mentioned before, Beclin1 and Bcl2 are strongly related. Bcl2 is a known inhibitor of apoptosis that also affect autophagy. The autophagy is only induced with the release of Beclin1 from Bcl2 by pro-apoptotic BH3 proteins. In addition to that, Caspase3 cleaves Beclin1 leading to overall inhibition of autophagy. The kinase DAPK phosphorylates Beclin1, decreasing the inhibitory relation with Bcl2, and promoting autophagy [27]. JNK can trigger both apoptosis and autophagy by virtue of its capacity to phosphorylate Bcl2 in its flexible loop between the BH4 and BH3 domains (at Thr69, Ser70 and Ser87) which decreases its inhibitory interaction with Beclin1 and with pro-apoptotic members of the BCL2 family. [30]

Bcl2-family is a big family of proteins that includes molecules that activate apoptosis and others that inhibit it. In order to release cytochrome C and produce apoptosis, multi-BH3 domain proteins Bax/Bak are required. Pro-survival Bcl2 family members (Bcl2, Bcl-XL and Mcl1) block this effect. [29]

A second apoptosis-autophagy relationship might exist between Caspase8 and P62/SQSTM1. P62 plays a crucial role in activation of Caspase8. However, Caspase8 cleaves P62 in response to death receptor activation. In addition, Caspase8 is degraded by autophagy (presumably via P62) [27]. This degradation is thought to be part of mechanism of resistance

against apoptotic inducing TRAIL (TNF-related apoptosis-inducing ligand) in colon cancer lacking pro-apoptotic Bax. [30]

The relationship between autophagy and apoptosis is shifting according to cell situation and interaction between the proteins, and rarely controlled by stress alone (see Figure 8)

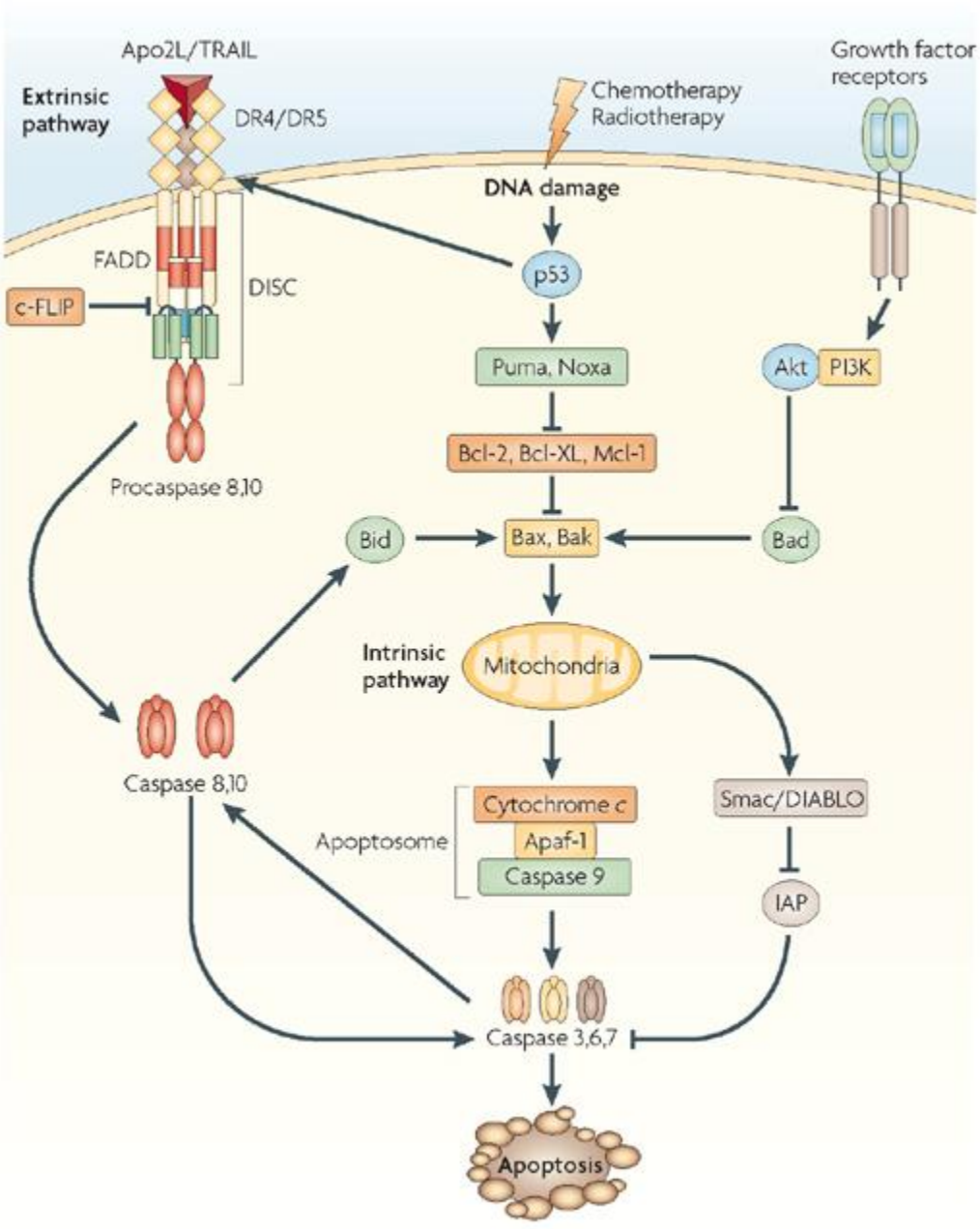

Figure 7: [28] Apoptosis pathway presenting different receptors and their contribution till executing apoptosis with Caspase 3,6 and 7.

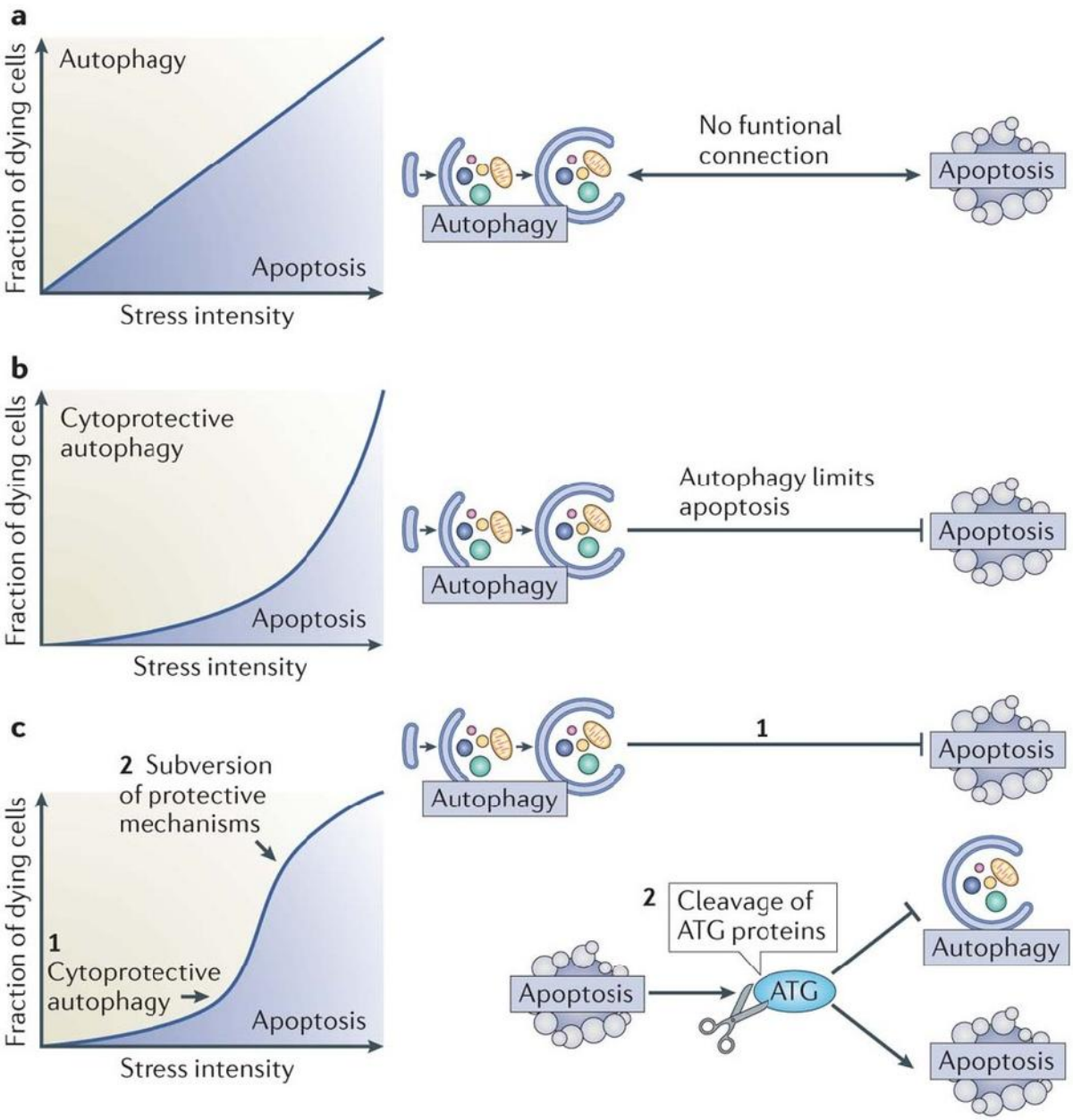

Figure 8: [30] The balance between autophagy and apoptosis. a | Hypothetical scenario of an absent interplay between autophagy and apoptosis. If no functional connection between apoptosis and autophagy existed, the percentage of cells activating the autophagic pathway or instead succumbing to apoptosis would be solely determined by stress intensity over time. b | Effect of cytoprotective autophagy on a dose-response curve. If autophagy inhibits apoptosis, the cell population becomes relatively resistant to cell death, unless the intensity of the stressor overcomes the protective barrier of autophagy. c | Cytoprotective autophagy, followed by lethal subversion of the apoptotic machinery. In this scenario, autophagy would constitute an initial barrier against apoptosis when stress intensity is low (1). As stress intensity increases (2), the induction of apoptosis results in the subversion of cytoprotective mechanisms, including autophagy, and the conversion of cytoprotective molecules into cytotoxic ones. For example, cleavage of essential ATG proteins does not only inactivate the autophagic machinery but also leads to the generation of protein fragments with novel pro-apoptotic properties.

Table 1: Proteins with dual roles in autophagy and apoptosis [27]

Protein	Function
DAPK	Phosphorylates Beclin1; activates DISC
NF-kB	Regulates survival pathways – inhibits apoptosis activates autophagy
JNK	Positively regulates both apoptosis and autophagy
p62	Crucial for activation of Caspase-8; regulates selective autophagy of many substrates
Beclin1	Primary cellular activator of autophagy; regulated by Bcl-2
Bcl-2	Inhibits both autophagy and apoptosis by binding Beclin-1 and Bax/Bad/Bak
Caspase-8	Activates apoptosis via extrinsic pathway; cleaves p62 during apoptosis
Caspase-3	May cleave Beclin-1 to inhibit autophagy during terminal stages of apoptosis
p53	Induces mitochondrial outer membrane permeabilization in response to stress; positively and negatively regulates autophagy
Atg5	Crucial autophagy gene; activates apoptosis via FADD and MOMP upon calpain cleavage
FLIP	c-FLIP inhibits autophagy through inhibition of Atg3-LC3 conjugation
Atg12-Atg3	Novel regulator of mitochondria and apoptosis with no known function in autophagy

1.3.2. P53 and autophagy

P53 is one of the most important proteins regarding DNA damage and cell death. The role of P53 is not simple in autophagy. Cytoplasmic P53 produce an inhibitory effect over autophagy, while nuclear P53 abets autophagy by interacting with its targets Sestrin1/2 and DRAM (the P53-regulated autophagy and cell death gene) [31]. Sestrin1 and Sestrin2 are negative regulators of MTORC1 and activate AMPK and TSC1/2 [29]. P53 is usually present in the cytosol but translocates to the nucleus upon DNA damage following its phosphorylation by a number of distinct stress-activated kinases. [30]

P53 loss of function in a cell induces autophagy, which suggests that cytoplasmic P53 is a player in this pathway. P53(-/-) cells had high levels of autophagy represented by depletion of P62/SQSTM1, LC3 lipidation and accumulation of autophagosomes and autolysosomes. It also seems that several distinct autophagy inducers (e.g., starvation, rapamycin, lithium, tunicamycin and thapsigargin) stimulate the rapid degradation of P53 [32].

1.3.3. RAS subfamily and autophagy

RAS is a small GTPase family ubiquitously expressed in all cell lineages and organs. They are involved in signal transduction and their activation lead to cell growth, differentiation and survival.

There are three proteins in this family: KRAS, NRAS and HRAS that are very similar in structure and function. Active mutations in RAS are found in 20-25% of total cancers, and KRAS mutations are associated with the most lethal cancers (lung colon and pancreatic cancer) [33]. The most pathogenic mutations are at residues 12, 13 and 61, that render RAS insensitive to deactivation by GAP.

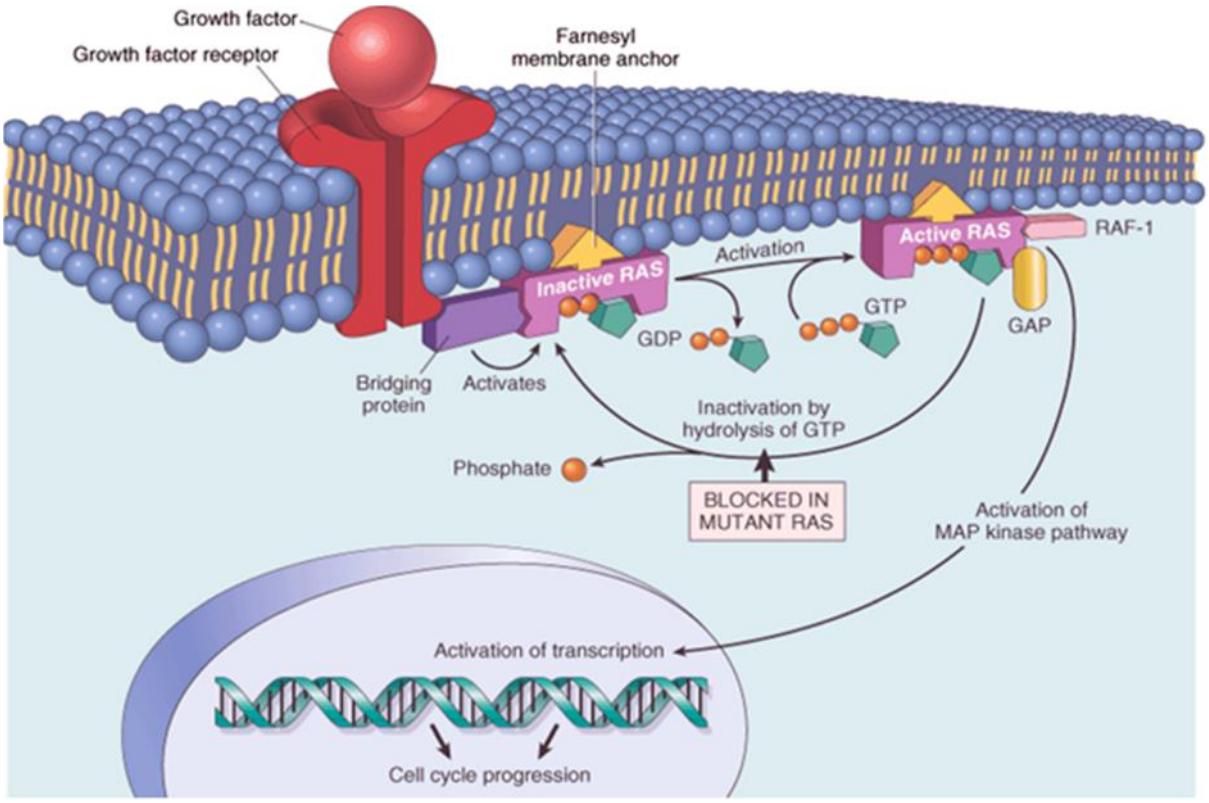

Figure 9: Model for RAS action. RAS proteins are activated by receptors. RAS family they act as GTPases, and phosphorylate many proteins. GAP is a protein that deactivated RAS, and when a mutation in RAS is preventing this action, RAS stays always active.

Of the many pathways that are controlled by RAS genes, PI3K/AKT/mTORC1 is related to autophagy. The activation of PI3K/AKT/mTORC1 leads to inhibition of autophagy, but the vast effects of RAS means that the final result depends upon the cell type and cellular contents. The classical mutation G12V in KRAS inhibits autophagy in fibroblasts via PI3K/AKT/mTORC1,

but a mutation in the same location in HRAS induces autophagy via Raf1/MEK1/ERK pathway. [33]

1.4. AUTOPHAGY AND DISEASE

Autophagy is responsible of basic removal of toxins and cell survival under stress. So it is not uncommon to relate mutations in this pathway with a wide variety of diseases (see Table2).

Table 2: Diseases related to mutations in the genes of autophagy [34]

Genes	Functions in autophagy	Associated human diseases
ATG5	Autophagosome formation	Genetic polymorphisms are associated with asthma and enhanced risk of systemic lupus erythematosus
ATG16L1	Autophagosome formation	T300A mutation is associated with increased risk of Crohn's disease
BECN1	Autophagosome formation	Monoallelic deletion is associated with risk and prognosis of human breast, ovarian, prostate, and colorectal cancers
SQSTM1/p62	A selective substrate An adaptor protein for selective autophagy	Mutations are associated with Paget disease of bone and amyotrophic lateral sclerosis

1.4.1. Lung cancer

Lung cancer is the second most common cancer in the world, but it is the most lethal [35]. The treatment varies depending on lung cancer type; non-small cell lung carcinoma (NSCLC) can be treated with surgery, while small cell lung carcinoma (SCLC) usually responds better to chemotherapy and radiation.

Almost 85% of lung cancer are classified as non-small-cell lung cancer (NSCLC) [36]. Survival differs greatly depending on the stage of NSCLC. 5-year survival equals 49% at stage IA, 45% at stage IB, 30% at stage IIA, 31% at stage IIB, 14% at stage IIIA, 5% at stage IIB and 1% at stage IV (metastatic stage) [37]. Studies showed that autophagy inhibition delays early but not late stage metastatic disease [38].

NSCLC is a histological classification. However, it is composed of non-homogenous group of tumors that includes adenocarcinomas (ADCs), squamous cell carcinomas (SCC), large cell, and anaplastic carcinomas [39].

Smoking tobacco is the most important risk factor of lung cancer. Smoking increases the risk of lung cancer in men and women about 25 folds. Between years 2005-2009, around 87% of lung cancer deaths were associated with smoking [40].

The treatment offers limited success as the majority of lung cancer patients start with advanced stage of the disease. Standard therapeutic regimens hit a problem of the dysregulation of cell death signaling. Different reports have demonstrated that deficits in apoptotic machinery can lead not only to abnormal proliferation as well as to insensitivity to cytotoxic therapy [41].

Autophagy, as a response to starvation, is less pronounced in cancer cells, but it is up-regulated in many tumor types suggesting that it could play an important survival mechanism. Some studies reported that cancer cells that are unable to undergo apoptosis secondary to genetic mutations are still susceptible to autophagic cell death [41].

The two most common mutations in lung cancer are KRAS and P53. 45.5% of lung cancer patients have mutations in KRAS, and 32.5% have mutations in P53. These mutations were present in both tumor and normal tissue. The presence of these mutations were higher in currently smokers comparing to ex-smokers. [42]

Autophagy inhibitors such as hydroxychloroquine have been tested for therapeutic efficacy in NSCLC. Genetic deletion of ATG5 results in impaired progression of KRAS(G12D)-driven lung cancer and promoted the survival of mice bearing such tumors. However, the initiation of KRAS(G12D)-driven lung tumors in these mice was accelerated by ATG5 deletion, suggesting that autophagy may prevent oncogenesis but promote tumor growth. [43]

Age can be a very important factor in lung cancer susceptibility and 5-years survival. About 2 out of 3 people diagnosed with lung cancer are 65 or older, while less than 2% are younger than 45. [37]

1.4.2. COPD

Chronic obstructive pulmonary disease (COPD) is an inflammatory lung disease that causes obstructed airflow. Symptoms include breathing difficulty, cough, sputum production and wheezing. It's caused by long-term exposure to irritating gases or most often from cigarette smoke. People with COPD are at an increased risk of developing heart disease, lung cancer and a variety of other conditions [44].

It has been reported elevated levels of autophagy in human bronchial epithelial (HBE) in smokers with COPD. Samples from normal lungs and COPD showed a dramatic increase in autophagic vacuoles (autophagosomes /autolysosomes) under electron microscope. In addition to that, the ratio of LC3B-II/LC3B-I and the expression of ATG4B, ATG5-ATG12 and

ATG7 were significantly increased in COPD lung [45]. Other studies argue that the effect of autophagy might not be enough to remove smoking-induced toxins and, based on the levels of LC3II, the increase in autophagy due to smoking toxins is transient (12-24 hours). However, mTOR inhibitor (Torin1) improves autophagy and reduces accumulated ubiquitinated protein and P62. This suggests mTOR could be a target for COPD therapies. [46]

There is growing evidence that pulmonary and systemic inflammation, key events in COPD, may change in nature as the disease progresses. Apoptosis is a mechanism of protection for the cells. But constant smoking and inflammation might cause an over-apoptotic response. Adding to the cancer-initiation properties of tobacco, this response triggers cigarette smoke–induced cancer. [47]

1.5. GENOMICS AND CANCER

1.5.1. Bases of tumorigenesis

It is widely thought that all cancers are a result of a sequence of mutations. The first mutations to occur are called driver mutations, and they establish a suitable environment for further mutagenesis and DNA instability. It has been reported that epigenetic changes alone can be the initial cause of cancer, which opens the possibility for a different etiology that does not include exclusive DNA damage [48]. However, mainstream science at this moment still focuses at DNA as the underlying pathological reason for cancer.

1.5.2. Polymorphism in genes of autophagy

As autophagy is a process of survival and cell death, genes implicated in autophagy might play a role in tumor development. We investigated several important single nucleotide polymorphisms (SNPs) related to autophagy genes:

1. *ATG2B (rs3759601)* is located at chromosome 14. ATG2 proteins participate in autophagosome formation and regulation of lipid droplet morphology and dispersion, knocking down both ATG2A and ATG2B is known to affect autophagy [24]. This polymorphism results from a substitution of C for G, where allele C is present in 25-35.5% in all cases [49]. It is a missense mutation where a substitution Q1383E occur.
2. *ATG5 (rs2245214)* is located at chromosome 6. It results from a substitution of C for G in the intronic region, where the allele G is present in 45.6% of the cases [49]. This SNP can, in theory, decrease indirectly the autophagy due to modifications in RNA stability and folding. [50]

3. *ATG10 (rs1864183)* is located at chromosome 5. It functions as type E2 ligase and plays crucial role in formation ATG5-ATG12-ATG16L1 complex [51]. It results from a substitution of G for T, where G allele exist in 48-49% and the allele T is present in 37.7% [49]. The TT genotype was associated with changes in IL-8 synthesis [52]. It is a missense mutation where a substation T212M takes place.

4. *ATG16L1 (rs2241880)* is located at chromosome 2. It is a missense mutation where a substitution T300A takes place. The amino acids 296-299 in ATG16L1 form a domain that can support the union with Caspase3. The T300A mutation makes ATG16L1 more sensitive towards the effects of Caspase3 and causes its degradation. The degradation of ATG16L1 decreases the levels of autophagy [53]. A recent study revealed that this mutation reduces the engagement of ATG16L1 with molecules that include a WDD-binding motif (e.g. TMEM59) [54]. This SNP results from a substitution of A for G, where the allele G is present in 39-45% of the cases [49].

1.5.3. SNPs controlling protein expression

Besides the effects of SNPs on protein primary structure and splicing, SNPs may affect a promotor, enhancer or inhibitor region of a gene. The change affects the quantity of protein expression without any change in the protein structure. These mechanisms of action are not investigated with sufficient detail. The sequence upstream to the start codon affects ribosomal annealing to the mRNA, the 3D mRNA structure and nucleotide context.

5'UTR region ranges in length in human with an average of 125bp [55]. As much as 72% of 5' UTRs include introns [56]. 5' UTR plays a crucial role in post-transcriptional regulation of gene expression by modulation of mRNA transport out of the nucleus, sub-cellular localization and stability [57].

As early as 1987, sequences in 5'UTR region were studied and its importance identified. The most famous of them is Kozak sequence. The sequence includes one nucleotide in the coding region (G), and at least 6 nucleotides in 5'UTR (gccRcc) [58]. The Kozak sequence is thought to improve the effectiveness of ribosomal complex in starting protein translation. The region around start codon has low number of "AUG" sequences, especially 16-27 codon upstream and 5-11 codon downstream [59]. Bioinformatics' studies revealed an inhibitory role for alternative initiation codon sequence in 5' UTR or upstream "AUG" (abbreviated hereafter as uAUG). The number of the uAUG was the factor most relevant to protein expression. [60] In yeast and plants, results showed an important inhibitory in the nearest 10bp in 5'UTR [61] [56]. While in human, several studies pointed to the rule of SNPs that create de novo uAUG in pathogenesis. [62, 63, 64, 65]

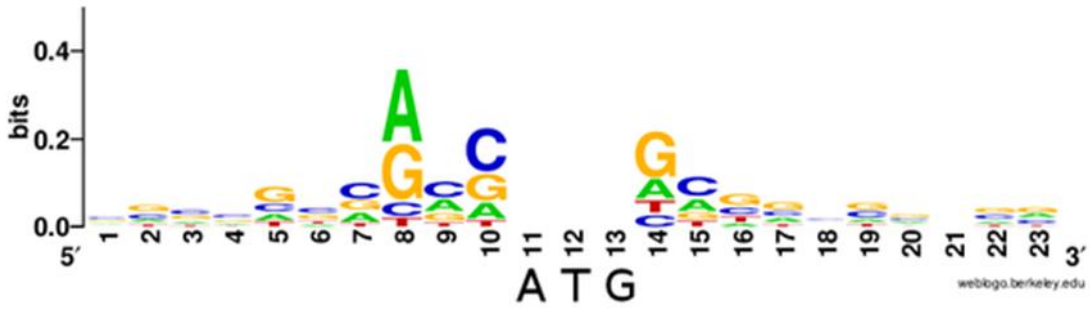

Figure 10: A sequence logo presenting the counts of bases around initiation codon from 10000 human mRNA.

1.5.4. Patterns of isoform expression

The classic central dogma of biology was the theory of “one gene-one protein”. But since the end of the human genome project in early 2000s, the dogma was challenged with new data. Most of eukaryotic cells are able to produce several mRNAs from each gene and thus one gene might be responsible for several proteins.

The different isoforms could have the same biological function, different function or contradictory functions. Those various roles suggested that isoforms are important players in pathology. For now, studies reported wide changes in isoform expressions in smokers and tumor samples [66, 67, 68, 69].

Next generation sequencing (NGS) are the main players nowadays in isoform detection, quantification and new isoform recognition. The process of massive isoform recognition depends heavily on complex algorithms on one hand and clean genomic data on the other. The genomic data needed consists of genome sequence (genome build) and metadata related to the location and length of exons described for each isoform (annotation). While it is easier to study RNAs in simple organisms such as bacteria, this process is error-prone in higher eukaryotes especially when studying low number of samples or a single cell.

Genomic sequence build (template) is published in several versions, the last version is GRC38 (biomart.org). However, the previous version (GRC37/hg19) is used more often as it is better annotated. Most of the data about isoforms come from massive studies and are published in different databases. Ensembl.org, UCSC and NCBI are the most common sources to identify isoform sequences.

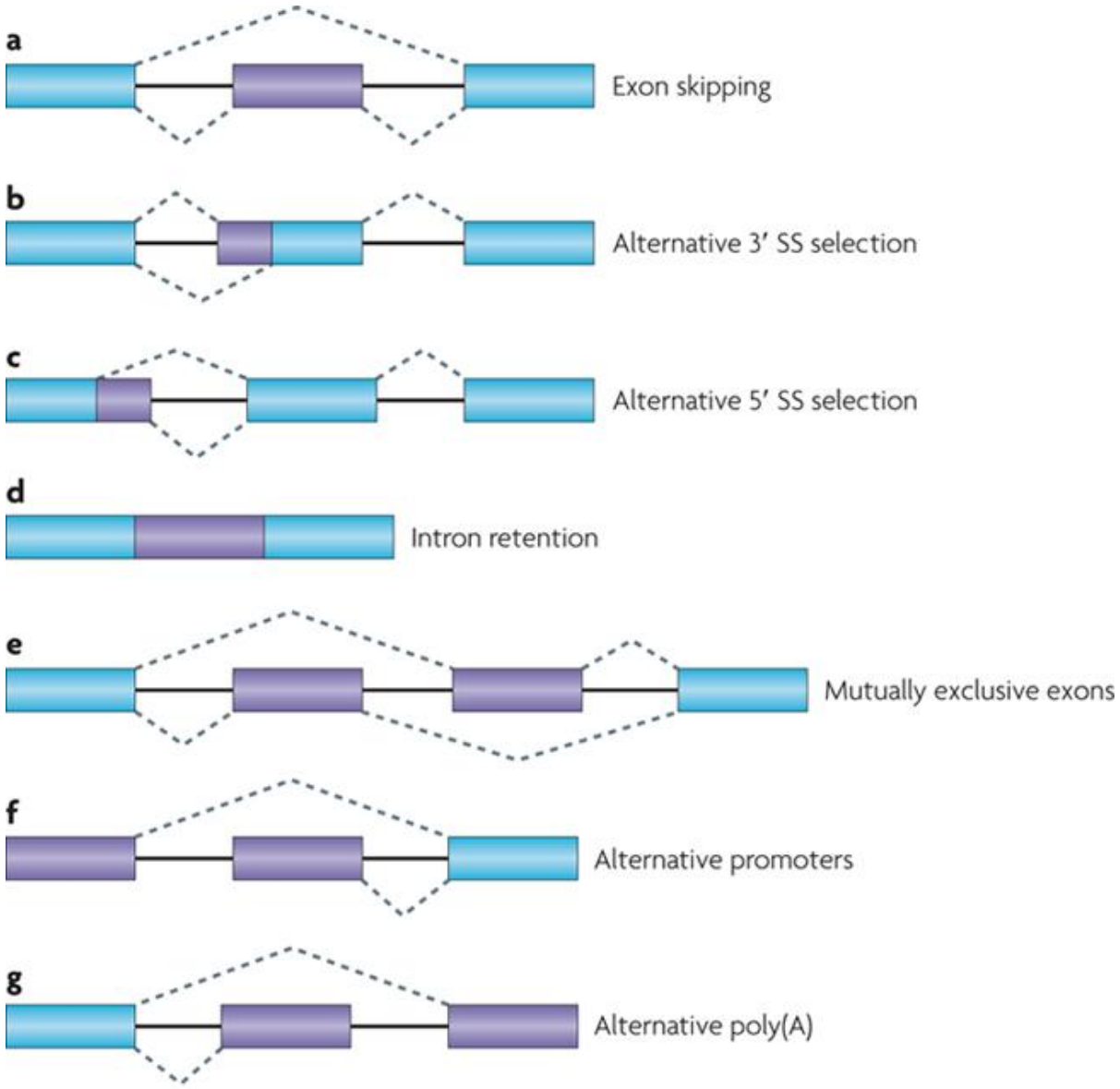

Figure 11: There are several different types of alternative splicing (AS) events, which can be classified into four main subgroups. The first type is exon skipping, in which a type of exon known as a cassette exon is spliced out of the transcript together with its flanking introns (part a). Exon skipping accounts for nearly 40% of AS events in higher but is extremely rare in lower eukaryotes. Less frequent, complex events that give rise to alternative transcript variants include mutually exclusive exons (part e), alternative promoter usage (part f) and alternative polyadenylation (part g).

The difference in the quantity and sequence are a huge problem when studying isoforms. Adding to that, independent studies report new isoforms that are not included in any annotation and rarely checked.

Moreover, NGS report RNA quantities not protein expression. The difference between the final products of two isoforms is not only related to their quantities, but it also related to the ability to be translated into proteins (e.g. difference in uAUG content).

Some of the most common differences between isoforms that come from one gene is skipping an exon (cassette exon) or losing one or more 5'end exons (Figure 11, a and f). The latter case produces two isoforms with different 5'UTR which in turn may affect their ability to be translated into proteins.

An example of isoform complexity is mTOR. The main mTOR isoform is mTORα (MTOR-001:ENST00000361445), which is 8677bp long and codes a protein of 2549aa with a molecular weight 289KD. It has 58 exons, and a rich CpG island around exon1, but no AUG in its 5'UTR. Structurally, mTOR possesses up to 20 tandem HEAT repeats (a protein-protein interaction structure of two tandem anti-parallel α-helices found in huntingtin, elongation factor 3, PR65/A and TOR) at the amino-terminal region, followed by an FAT domain (FRAP, ATM, and TRRAP, all PIKK family members) (Figure 12). The kinase domain is between the FRB (FKBP12/rapamycin binding) domain, which is C-terminal to the FAT domain, and the FATC (FAT C-terminus) domain, located at the C-terminus of the protein. [70]

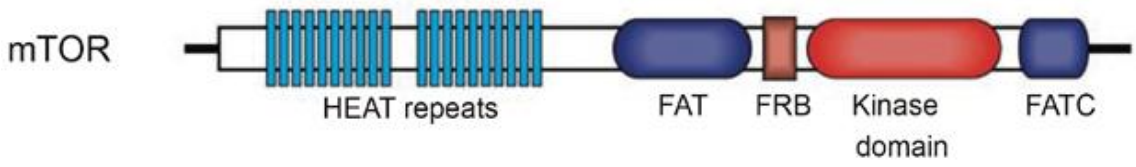

Figure 12: The domains of full mTOR protein (isoform 001). HEAT domain provides the possibility to interact with other proteins such as Raptor.

Ensembl database lists 6 more isoforms, two of which code proteins. MTOR-002: ENST00000376838 is a 4017bp transcript that produces a 754aa protein of 85.9KD (UniProt: B1AKP8). This transcript starts basically from exon39 in MTOR001 and continues till the end. It includes some of the intronic region between exons 38-39 as new 5'UTR with high presence of "AUG" sequence. This isoform lose all Heat and FAT domains, so it is not expected to show activity as it cannot interact with proteins such are Raptor and Rictor. The third protein-coding transcript is MTOR-005: ENST00000455339 (694bp, 161aa and 18KD). It starts in exon51 of MTOR-001, and continues to exon56.

An article by *Panasyuk et al* reported an isoform that they called mTORβ [71]. The isoform is very similar to MTOR002, but it has the same 5'UTR as MTOR001. This means it retains a small HEAT domain that the authors claim to be sufficient for the kinase to be effective. MTOR002 and mTORβ share most of the sequence and more work need to confirm their existence as two different isoforms.

Other isoforms published in Alharbi 2015 [72] and NCBI show no functional domains.

1.6. TREATMENTS RELATED TO AUTOPHAGY

1.6.1. Chloroquine

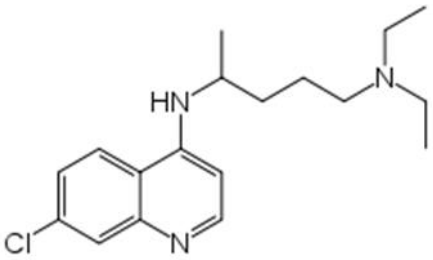

Chloroquine (CQ) is an FDA-approved antimalarial drug with an established history of generally well-tolerated clinical use. It has been used to treat rheumatoid arthritis and other autoimmune diseases due to its mild immunosuppressive properties. It is on the World Health Organization's List of Essential Medicines.

CQ is a weak base with hydrophobic characteristics that diffuses into the lysosomes of cells where it becomes protonated and trapped, thus leading to a rise in lysosomal pH. These CQ-loaded lysosomes can no longer fuse with autophagosomes, blocking autophagy at a late stage. Chloroquine and its derivative hydroxychloroquine are the only drugs currently approved by FDA to inhibit autophagy in humans [73]. Some pancreatic and other cancers with RAS mutations have been described as being particularly susceptible to autophagy inhibition and CQ treatment [73].it could be possible that RAS mutations lead cancer cells to become “addicted” to autophagy, and blocking it is a possible target for pharmacological treatments [73]. Chloroquine treatment has no effect on cancer cell lines that lacks autophagy such as prostate cell-line DU145 that lacks ATG5 [73].

Recently, a new connection between chloroquine and mTOR levels were published in osteoclasts. Chloroquine increases levels of mTOR by affecting its lysosomal degradation [74].

Autophagy has a protective role against erlotinib in NSCLC cells with wild-type EGFR. Knocking down ATG5 or using chloroquine in combination to erlotinib can overcome the innate resistance [75]. This drug combination is currently in Phase II for NSCLC treatment [76].

1.6.2. LBH-589

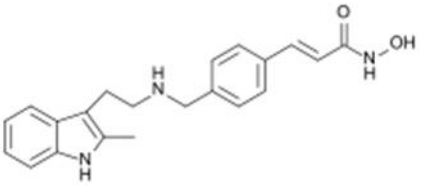

LBH-589 (Panobinostat or Farydak) is a drug developed by Novartis for the treatment of various cancers. It acts as a non-selective histone deacetylase inhibitor (pan-HDAC inhibitor), and it is considered a hydroxamic acid derivative. LBH is the first HDAC inhibitor approved to treat multiple myeloma. It is intended for patients who have received at least two prior standard therapies, including bortezomib and an immunomodulatory agent. [77]

In Hodgkin lymphoma cell lines, LBH induced cell death and autophagy [78]. The tumor suppressor death-associated protein kinase (DAPK) seems to play a role in LBH activity. LBH inhibit cell proliferation, reduce the long-term survival and up-regulate and activate DAPK in colorectal cancer cells. LBH589-induced autophagy seems to be caused by DAPK protein kinase activity. [79]

HDAC6 interaction with tubulin and dynein (motor protein) is critical to the transport of these protein aggregates for autophagy degradation. Inhibition of HDAC6 by LBH leads to hyper-acetylated microtubules and inefficient autophagy degradation [80].

1.6.3. Metformin

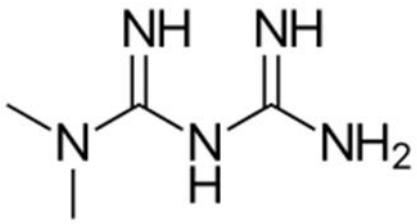

Metformin (Glucophage) is a biguanide class medication for the treatment of type 2 diabetes. It decreases glucose production in the liver and increasing glucose use by body tissues.

Although metformin has an AMPK-independent mechanisms for the improvement of the metabolic profile, most investigators agree that metformin activates AMPK [81]. Metformin is reported to affect both autophagy and apoptosis in esophageal squamous cell carcinomas by downregulating Stat3 and Bcl2 [82]. Reports indicated that metformin inhibit cell proliferation in different breast cancer cell lines, but that it had no effect on a breast epithelial cell line. Metformin induced a caspase-dependent cell death, and this apoptosis was enhanced when autophagy was blocked using chloroquine. [83]

In melanoma cells, the effects of metformin started by arresting cell-cycle at G0/G1 after 24 hours, prompted autophagy after 72 hours, and autophagy-induced apoptosis after 96 hours. [84]

1.6.4. Paclitaxel (Taxol®)

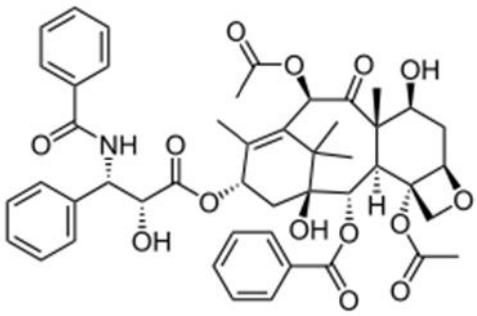

Paclitaxel is a taxane drug. Its mechanism of action involves the interference with microtubules breakdown during cell division. It is licensed for the treatment of ovarian, breast, lung, bladder, prostate, melanoma, esophageal, and other types of solid tumor cancers as well as Kaposi's sarcoma [85]. It is developed by Bristol-Myers Squibb and commercially known as Taxol®.

Unlike other tubulin-targeting drugs such as colchicine that inhibit microtubule assembly, paclitaxel stabilizes the microtubule polymer and protects it from disassembly. Chromosomes are thus unable to achieve a metaphase spindle configuration. This blocks the progression of mitosis. The prolonged activation of the mitotic checkpoint triggers apoptosis or reversion to the G-phase of the cell cycle without cell division. [86]

Paclitaxel not only activates apoptosis but it is reported to stop autophagy by two different mechanisms depending on the state of the cell. In mitotic cells, paclitaxel blocked activation of the class III phosphatidyl inositol 3 kinase, Vps34, a critical initiator of autophagosome formation. In non-mitotic paclitaxel-treated cells, autophagosomes were generated but their movement and maturation was inhibited. [87]

2. HYPOTHESIS AND OBJECTIVES

Autophagy is involved in cell survival under stress and protects the cell from chemotherapy and radiotherapy by eliminating ROS factors. On the other hand, a prolonged exposure to autophagy drives the cells to programmed death via apoptosis or independently. Thus, both increase and decrease in autophagy can play a role in lung cancer treatment.

Non-small cell Lung cancer is resistant to chemotherapy and radiotherapy. It could be related to changes in autophagy. We think that the study of lung cancer development could reveal potential therapeutic targets related to autophagy.

Our aim was to study autophagy in lung cancer at various levels. We studied the link of genetic changes in autophagy with increased risks of lung cancer. We also investigated modifications in autophagy gene expression and isoforms. Finally, we studied the effects of treatments that modify autophagy on lung cancer cell lines.

We hypothesized that SNPs in autophagy-related genes would affect the development of lung cancer. So we aimed to evaluate the role of autophagy as a protector or risk factor in smoker with and without lung cancer. We also assessed the role of autophagy in lung cancer patients with and without COPD.

Protein expression of genes and isoforms differ greatly in cancer patients. We hypothesized that sequences in 5' untranslated region could play a regulatory role. Upstream open reading frames (uORFs) are the focus of many studies of protein expression. It has been reported that a stop codon near uAUG diminishes transcription [59]. Several basic questions are still to be answered, one of them is the relation between uAUG and distance. No study have been able until now to address this relation [88, 63].

We also hypothesized that isoform changes in lung cancer and other diseases (i.e. COPD) are more than collateral products. A change in isoform expression may control a change in the biological pathway. To evaluate this hypothesis, we used RNA-Seq data to understand the changes that happens in autophagy and apoptosis.

Finally, we hypothesized that the state of autophagy in lung cancer cells will affect the response to autophagy-modulating treatments.

The objective of our study are:

1- To characterize genotype distribution in ATG2B, ATG5, ATG10 and ATG16L1 SNPs between healthy smokers and lung cancer smokers.
   Null hypothesis H_0:
   No relationship is exist between lung cancer and allelic variations of genes related to autophagy (ATG2B, ATG5, ATG10 and ATG16L1).
   Alternative Hypothesis H_a:
   H_{a1}: The relationship between lung cancer and one allelic variant of genes related to autophagy makes the latter a risk factor.
   H_{a2}: The relationship between lung cancer and one allelic variant of genes related to autophagy makes the latter a protection factor.

2- To assess the effects of uAUG on the quantity of protein expression in ATG16L2.

3- To search for key isoform changes in autophagy and apoptosis pathways.

4- To study the role of autophagy in NSCLC cell lines using autophagy-modulating drugs (Chloroquine, LBH587 and metformin).

3. MATERIAL AND METHODS

3.1. PATIENTS AND CONTROLS

3.1.1. Sample collection

The patients included in this study were collected in two previous studies conducted at the University of Salamanca by D. S. de Prado Otero (2008) and A.E. Jiménez Massa (2011) [89, 90]. Which in total comprises 165 patients with lung cancer and 145 healthy subjects.

Samples were collected mainly from the University Hospital of Salamanca that receives patients from all the province of Salamanca. Samples were collected between 2005 and 2010.

3.1.2. Ethics

The samples was collected from peripheral blood according to basic ethical principles of investigation and the principles established by law.

The ethical principles were respected as declared in declaration of Helsinki, Belmont report and the universal declaration of the UNESCO regarding human genome. The project had been approved by the research committee and ethical committee in the clinical hospital of Salamanca.

3.2. DNA EXTRACTION

Peripheral blood samples were collected from peripheral blood of patients and controls, and DNA were extracted in the laboratory of Molecular Medicine at the Faculty of Medicine/University of Salamanca via a method based on organic solvents. [91]

Each sample had 10ml of blood and the white blood cells were separated by using 50ml of cold hypotonic solution (dH_2O, 4°C). The samples were centrifuged at 1500rpm for 15 minutes, and rewashed.

To complete washing off the red blood cells, 5 ml of Fornace buffer was used (0.25M sucrose, 50mM Tris-HCl pH7.5, 25mM KCl and 5mM $MgCl_2$), the samples were centrifuged at 1500rpm for 20 minutes.

The lower layer of cell was re-suspended in 5ml Fornace buffer (estimated $5x10^6$ cell/ml), 10mM EDTA (Ethylenediaminetetraacetic acid), 1% SDS (Sodium dodecyl sulfate) and 20µl Proteinase K (Boehringer Mannheim 50µg/ml). The mixture was incubated at 55°c for 8-16 hours.

Then, the proteins were separated with phenol and chloroform-isoamyl alcohol (CIA). The DNA was precipitated with absolute ethanol, and washed two times with 70% ethanol.

The DNA was measure with Nanodrop® 260/280nm to check its purity from proteins. The values between 1.7 - 2.0 were considered pure. DNA was suspended in TE buffer or ddH_2O. And the sample stored at -20°c.

The final concentration of DNA was 1000-1500µg/ml, and was measured by the following equation:

$$\mu g \text{ of DNA/ml} = (OD_{260}) \times (\text{dilution factor}) \times 50$$

Where OD_{260} is optical density at 260nm, and 50 is a correction factor.

Isolation of DNA was strictly done with Good Practice (GP) in mind, as the extraction process and the amplification with PCR were done in two physically separate locations.

3.3. ANALYSIS OF ALLELIC VARIANTS VIA PCR WITH TAQMAN® PROBES

Genotyping of allelic variants (SNPs) was performed using Taqman® probes. It is a cheap fast way to amplify and detect simultaneously in a closed tube, with no special preparation steps.

The use of Taqman's probes provides a method to track the reaction in real time. And it is considered a golden standard for gene expression quantification around the world.

The principle behind this techniques is fairly simple. It uses polymerase chain reaction (PCR) to amplify the target. As the temperature raises, the DNA denaturates into two separate chains. This separation allows a specific probe to anneal with the targeted region. Each kit has two probes: VIC and FAM. That target different alleles.

The design of each probe is consistent with a DNA chain, a fluorescent dye on 5' and of the chain and a quencher (MGB-non florescent quencher) on 3' end. VIC and FAM have different florescent dyes attached to them.

As the PCR continues, the polymerase synthesize a new chain. Its 5' nuclease activity leads to the cleavage of the probe and the release of the dye. The type of the dye and its quantity is related to the type and amount of amplicon synthesized (Figure 13).

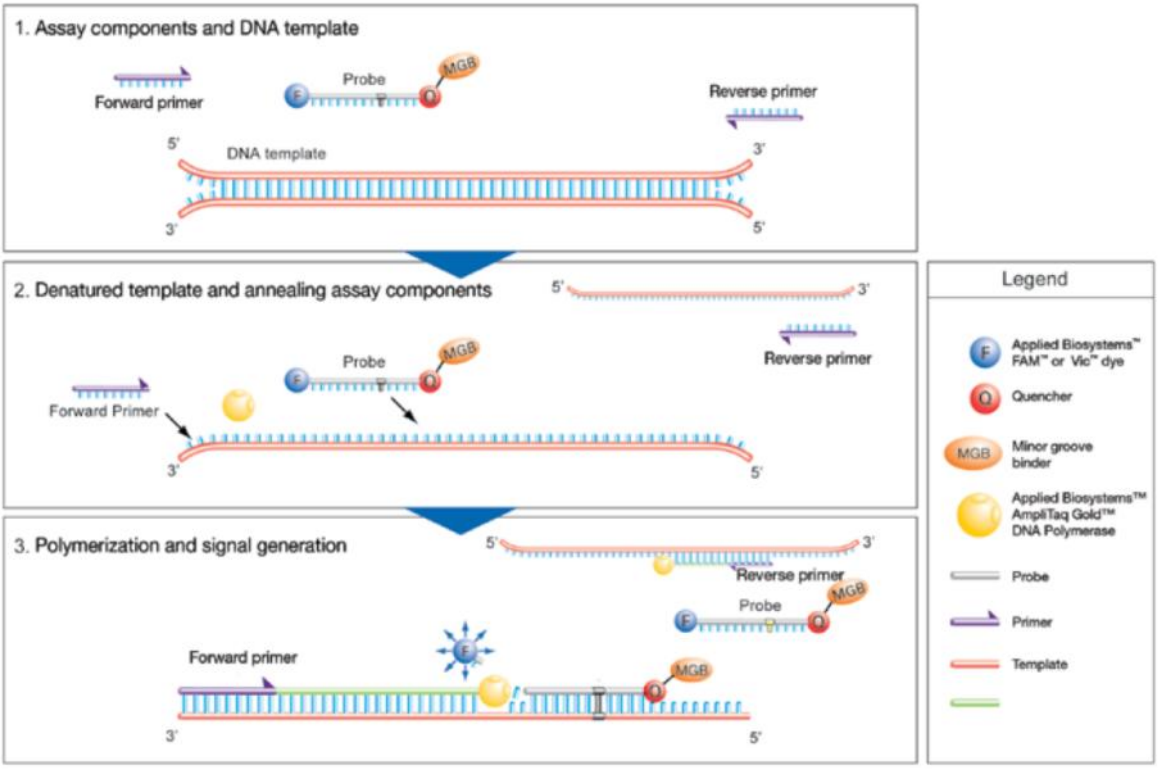

Figure 13: the principle of Taqman® kit for allelic variants. The separation of two DNA strands allow for a probe to anneal. The probe has one of two florescent dye that is quenched. The polymerase cleaves the probe releasing the dye and informing the type of SNP and the quantity of DNA.

Each sample was inspected for ATG2b, ATG10 and ATG16L1 using 5µl of Master Mix (Promega®), 0.5µl of *allelic discrimination* mix (primers and probes), 4µl of free-nuclease water and 0.5µl of sample DNA. For ATG5, the master mix was AB TaqMan® Genotyping Master Mix®.

The program used to amplify the DNA was:

- Temp=60°c for 30sec (read the background noise)
- Temp=95°c for 10 minutes (eliminate protein residues)
- Cycle 40 times:
  - Temp=95°c for 15sec (denaturation)
  - Temp=60°c for 1min (annealing)
- Temp=60°c for 1min (elongation)

For the test, 96-well optic plats (applied Biosystems) were used with a negative control in each row. And the results were read by StepOne™ Real-Time PCR Systems software. (Figure 14)

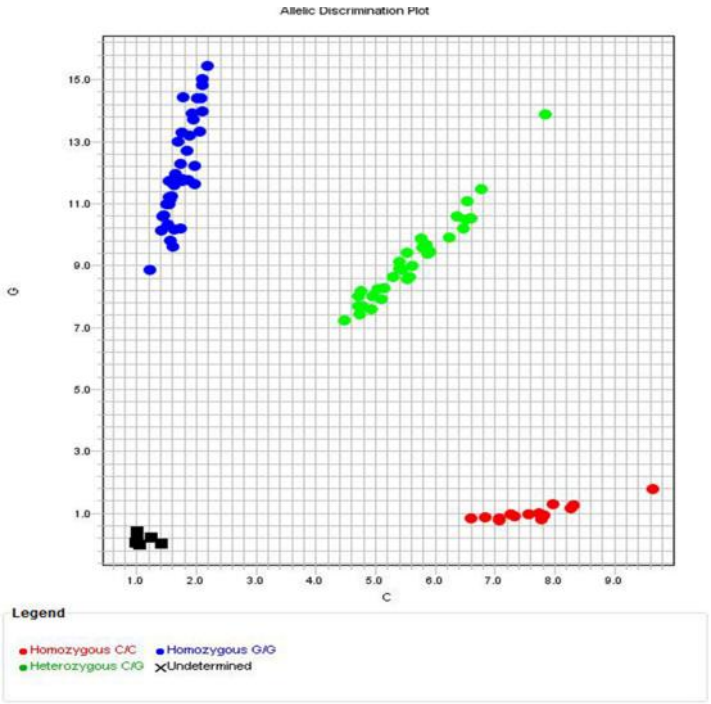

Figure 14: An example for the distribution of allelic variants of ATG2B. The red dots are samples with C/C, the green are C/G and the blue are G/G. The black dots are the negative controls.

3.4. ANALYSIS OF GENE EXPRESSION

3.4.1. Amplifying target gene

We have cloned 253bp upstream of ATG16L2 initiation codon. The sequence was amplified by PCR using two primers. *FW1_ATG16B*: CTCTAAGCTT CCACAGGAGCCCCCACTTAGG, and *BK1_ATG16B:* ATATCCATGGCCGCGCTCTCCC. The amplification mix included 2µl Genomic DNA (300ng) from a healthy subject, 9.5µl dH_2O and 12.5µl PCR Master Mix (Ref:M7505-Promega) on a Veriti Thermal cycler (Applied biosystems). The amplification program was:

- 95°C 2 min.

- 30 cycles of (95°C 30 sec, 55°C 30 sec, 72°C 2 min)

- 10 min at 72°C. Using 50ng of each primer

The PCR product was sequenced to check its complete match to genomic reference.

3.4.2. Mutagenesis

The sequence was initially cloned into pGEM-T Easy plasmid (Promega) (Figure 15). Four new mutations in (pGEM-T+ATG16L2) were created using QuikChange® Site-Directed Mutagenesis Kit from Stratagene (Figure 17).

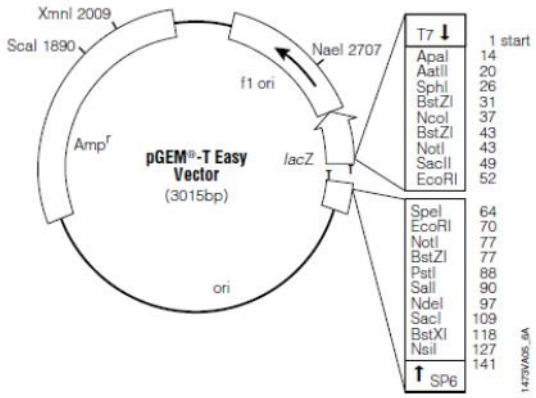

Figure 15: pGMT®-T Easy Vector Map and Sequence Reference Points

Primers were designed to provide a gradual uAUG remoteness from the initiation codon: -5bp, -15bp,-25bp and -38bp (see Table 3). Later, one construct with two uAUG mutations was designed using -5bp and -25bp mutations (Figure 16). The design was careful to make the minimum change on the wt sequence. Smaller mutations were preferred and known targets for transcription factors were avoided (e.g. Kozak sequence [13]).

Table 3: Primers used for mutagenesis via QuikChange® Site-Directed Mutagenesis Kit.

Primer name	F. primer	R.primer
PuAUG-5	5'-catggccgcattctcccgcctagcggcg-3'	5'-cgccgctaggcgggagaatgcggccatg-3'
PuAUG-15	5'-ctctcccgcatagcggcgcgttcc-3'	5'-ggaacgcgccgctatgcgggagag-3'
PuAUG-25	5'-agcggcgcattcctcccgcccagg-3'	5'-cctgggcgggaggaatgcgccgct-3'
PuAUG-38	5'-cctcccgcccatgacggcgccag-3'	5'-ctggcgccgtcatgggcgggagg-3'

Figure 16: a representation of new uAUG sequences generated after directed mutagenesis. The original sequence called wt, and the new sequences are named after the nucleotides between the uAUG and the initiation codon.

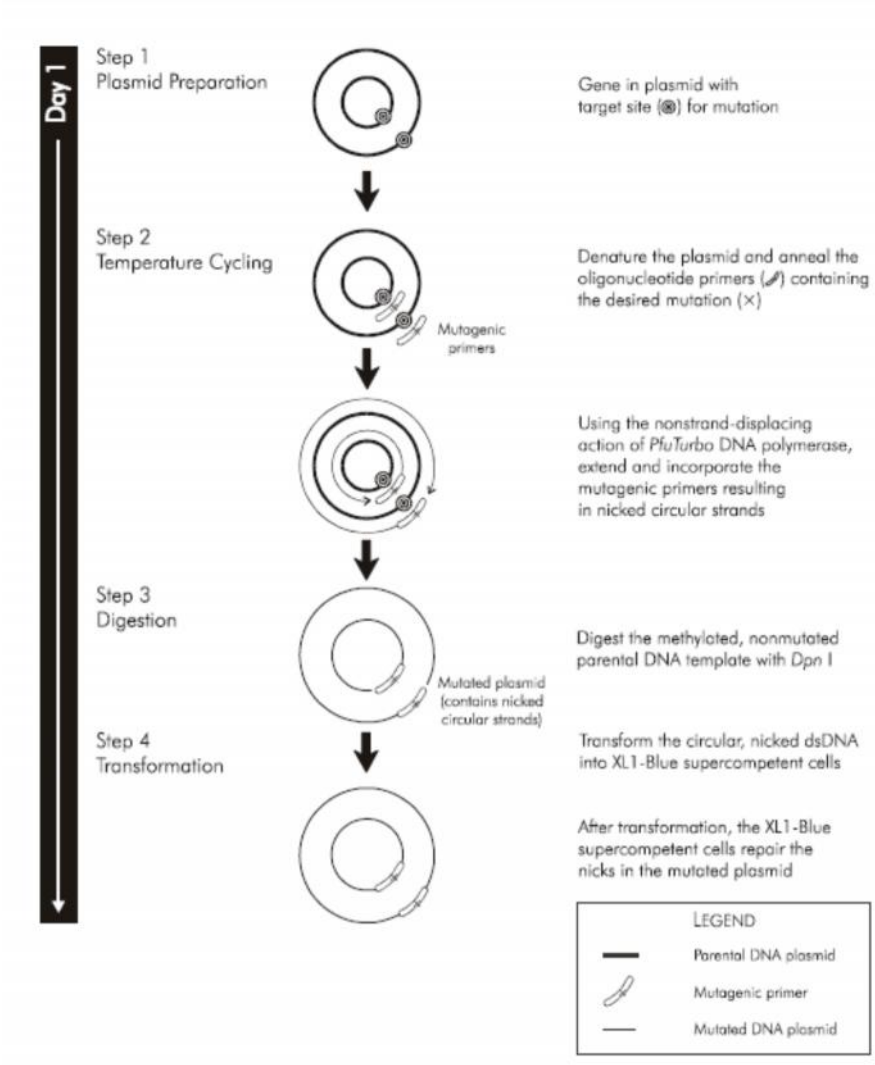

Figure 17: Overview of the QuikChange® site-directed mutagenesis method.

3.4.3. Measurement of protein expression

All five mutated constructs were digested with HindIII and NcoI restriction enzymes and merged with pGL3 Basic plasmid and named after the distance of uAUG from the initiation codon.

All The plasmids were transfected in super competent bacteria (DHα5) and DNA was extracted via Maxi-Prep kit (Genomed), and sequenced to confirm mutagenesis. Finally, COS1 cells were transfected with 1000ng of each plasmid using X-tremeGENE HP DNA Transfection Reagent (Roche). In addition, a control plasmid pRL-SV40 (Renilla) was used at 10ng (1:100 of pGL3) with each experiment. Plasmids were sequenced at each step.

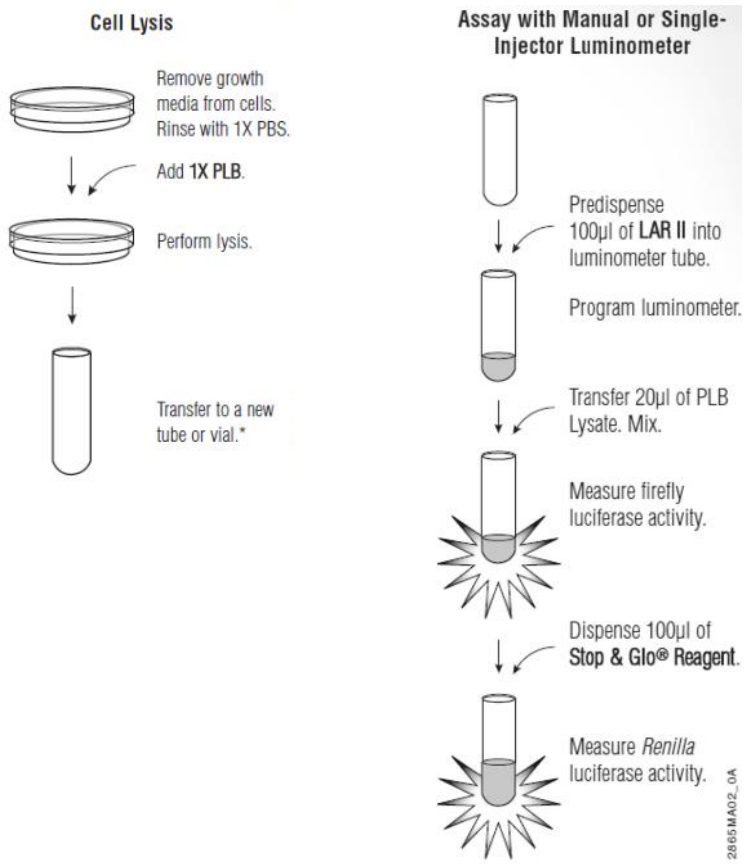

Figure 18: Using Dual luciferase system. Lysis of cells, measuring luciferase then measuring the control Renilla.

After 24 hours, the percentage of pGL3-Luciferase/ Renilla-Luciferase was measured using the Dual-Luciferase® Reporter Assay System (Promega) via FB12 apparatus (TITERTEK).

The experiments were repeated 4 times for each uAUG mutated plasmids and 2 times for the double-uAUG mutated plasmid (uAUG 5-25), the average was calculated and the data was normalized (Percentage of expression relative to wt).

3.5. BIOINFORMATICS AND STATISTICS

Our bioinformatics analysis consisted of searching for "AUG" in 5'UTR in the whole transcriptome, and analyzing RNA expression in published NGS results of lung tissue samples. Statistical analysis was used in genotyping, protein expression and isoform study.

3.5.1. Samples for isoform analysis

We analyzed 87 RNA-Seq samples obtained from European Nucleotide Archive (ENA/EBI); 48 sample from normal lung tissue, 25 sample from lung tissue of COPD patients and 14 samples from NSCLC tumors. Those samples were collected from 7 different studies (see Appendix A).

3.5.2. NGS data analysis

Next generation sequencing are the most common sequencers nowadays. They demand a preparation of a library and produce short reads of the sequences provided. If the original sample was RNAs (mRNA, miRNA and ncRNA), the reads are called RNA-Seq.

The short reads need to be aligned to a template genome. The most common tool to align the reads is Bowtie (http://bowtie-bio.sourceforge.net/index.shtml). Bowtie is not designed to handle big gaps in reads (i.e. introns in RNA reads). Thus many adjustments were developed such as TopHat and HiSat.

The aligned reads then need to be counted and the transcripts and mutations need to be identified. One of the most common transcript assembly programs and estimator is Cufflinks.

Before aligning the reads, their quality needs to be checked. FastQC Version 0.63 was applied to check the quality of the reads (http://www.bioinformatics.babraham.ac.uk /projects/fastqc/). Then FASTQ Quality Trimmer Version 1.0.0 was applied when needed to get at least a quality score of 20. [92]

To align the reads TopHat2 Version 0.9 [93, 94] was used with hg19 as a reference genome. Mean Inner Distance between Mate Pairs were checked via CollectInsertSizeMetrics Version 1.136.0 (Picard tools- http://broadinstitute.github.io/picard/).

To assemble transcripts and estimates their abundances, Cufflinks Version 2.2.1.0 was used [95]. A reference annotation from UCSC Main site was used (hg19/Genes and Gene Predictions/ Ensemble Genes). RNA was evaluated using Fragments Per Kilobase of transcript per Million mapped reads (FPKM).

3.5.3. Scheme of analysis

To avoid using command line and automate the analysis of NGS data, a web-based platform was used. Galaxy platform (galaxy.org) was a simple, fast and free option [96]. A consortium of organizations supports a free cloud server with limited space and capacity under UseGalaxy project (usegalaxy.org).

TRAPLINE is a Galaxy-based published, standardized and automated pipeline for RNA sequencing data analysis [97]. In theory, it requires no bioinformatics skills and decreases the processing time of the analysis and works in the cloud. However, due to the limited resources provided from UseGalaxy project for free users, TRAPLINE is not an applicable workflow. This is due to its inability to apply read correction via duplication reads tool (Picard tools- http://broadinstitute.github.io/picard/).

3.5.4. Program scripting and statistics

Analysis of massive data of transcriptome from Biomart.org (hg19) and tubular data from RNA-Seq were performed using both python 2.7 and RStudio v0.99.447/R v3.2.1.

For statistical analysis, IBM SPSS v23 and MS Excel 2013 were used.

3.5.5. RNA folding

To evaluate the extent of mutagenesis on RNA 3D folding and minimum energy structure RNAFold webserver was used [98]. Minimum free energy (MFE) centroid secondary structure was chosen instead of MFE optimal secondary structure because centroid secondary structure is a better representative for thermodynamics of RNA. [99]

3.5.6. Genotyping data analysis

Data were analysed using statistical software package IBM SPSS version 23.0. For the purposes of our study, we leave the detailed descriptive study and Uni-variant analysis to *de Prado Otero*

and *Jiménez Massa* [89, 90]. Rather we were interested to present the frequencies of allelic variants of genes related to autophagy in both lung cancer patients and controls.

The study analysed the relationship between two factors: the allelic frequency and the state of disease (control or patient). This test is categorized under bi-variant analysis in statistical communities. And we used the main stream confidence interval of 95% to evaluate the hypothesis in our work.

Our work relies on Hardy–Weinberg principle, were the allele and genotype frequencies in a population will remain constant from generation to generation in the absence of other evolutionary influences.

The frequencies were weighted. Using analyse/ descriptive statistics/ cross-tables looking for Person's Chi-Square test (χ^2) between the genotype and state of disease and the risk (odds ratio). The value of Chi-square was reported along with statistical significance (*p* value), and risk for the two allelic variants that drove the most change.

The presence of a disease in epidemiological study are represented with Odds ratio (OR), where if OR is equal to 1 then no association exists, and OR less than 1 mean that there is a protective effect (the allele type is protecting from the disease), and if OR is higher than 1 it means that it is a possible factor in developing the disease (risk factor). In order to accept H_i, the confidence interval should not include OR=1.

3.6. CELLULAR STUDIES

3.6.1. Cell growth (MTT)

The most common assay to assess cell metabolic activity and cell growth is MTT. It is a colorimetric assay based on tetrazolium dye 3-(4,5- dimethylthiazol-2-yl) -2,5-diphenyltetrazolium bromide (MTT). The NAD(P)H-dependent cellular oxidoreductase enzymes can reduce the yellow colored MTT to insoluble purple formazan. The formazan dye can be dissolved in many solvent such as Dimethyl sulfoxide (DMSO). The color is measured with spectrophotometer at 570-590nm.

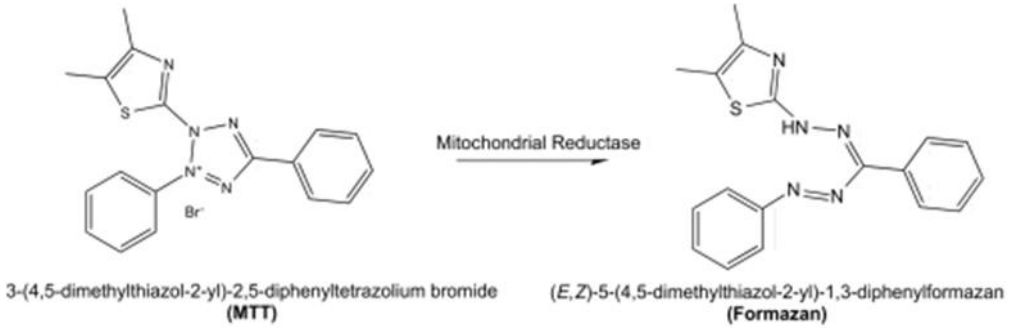

Figure 19: MMT chemical structure, and the reaction to convert it to Formazan

The cells were cultured in 24 well-plate, where 5000-10000 cells were added to each well, and after some time of cell growth the drugs were added. The plate was divided into triplicated wells, three for each concentration, in addition to three for negative control and three for the positive control.

In order to measure the cell activity, 110µl of MTT solution (5 mg/ml) was added to each well. After an hour of incubation at 37°C, the growth medium was removed and 1ml of was added DMSO to each well.

The plate was shacked for a few minutes to homogenate the solution of formazan. Then it was measured by *Infinite F500 / Tecan®*. The readings were analyzed using Microsoft Excel 365™.

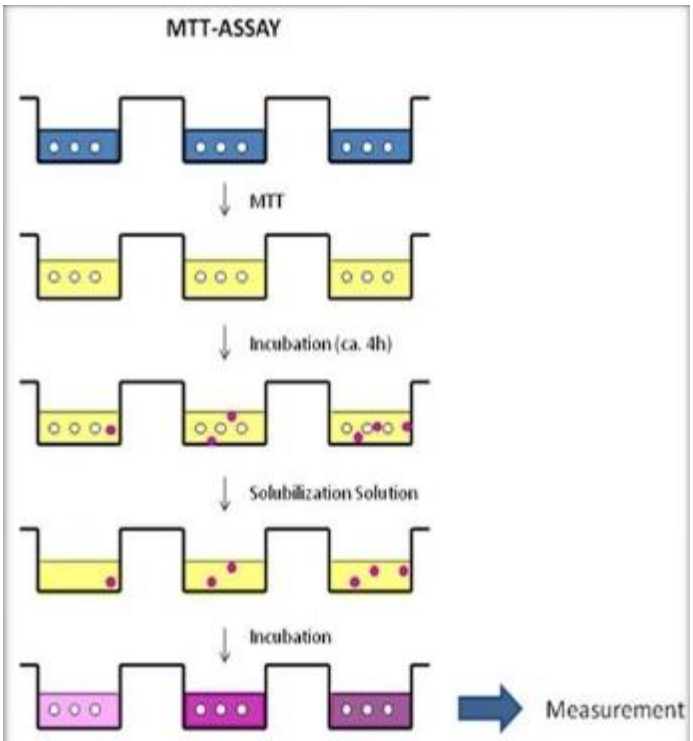

Figure 20: The principle of MTT assay. Adding MTT to the cell culture, incubating 1-4hours, removing the liquid phase then adding dissolvent (DSMO). Finally, measurement)

3.6.2. Cell survivability (FACS)

Flow cytometry is an analytical method to detect individual cells and separate them. One of the earliest applications for this method was identifying the cell-division cycle phase. The method depends on cell contents of DNA which is variable throughout the cycle phases. A dye that is used to bind to DNA is propidium iodide.

The cell normally reside in G0 phase, until a promoting event pushes the cell into division. The first phase G1 of this process is just the increase in size and preparation of raw materials for division, this growth phase is merged with G0 because there is no change in DNA content. We call them G0/G1 or just G1.

The duplication starts in phase S, where the DNA content in the cell is slightly higher than G0/G1 phase. But phase S is only a short transition till the full duplicated DNA. The next phases is G2 and M, where the whole DNA is duplicated and the signal is strongest.

Cells that die by autophagy for example, have fragmented DNA and they appear to have less DNA than G0/G1 cells. On the other hand, multi nuclear cell and unspecific residues show more DNA content than G2. (See Figure 21)

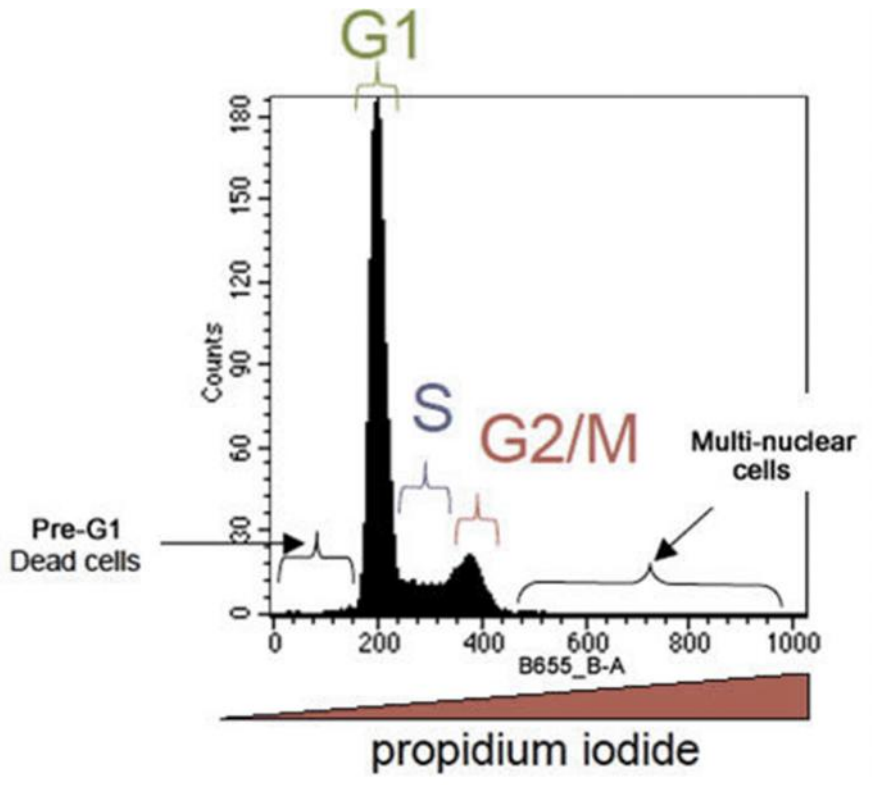

Figure 21: A typical graph demonstrates the different cell-division phases.

Workflow:

- Harvest cells with trypsin. Wash the cells with 5ml phosphate buffered saline (PBS), centrifuge at 1300 rpm for 3 minutes and discard the supernatant.
- Add 1ml of 70% ethanol, then place the solution in -20^{o}C for at least 24 hours.
- Wash the cells with 1 ml PBS twice, centrifuge at 1300rpm for 3 minutes and discard the supernatant.
- Re-suspend the cells in 1 ml PBS, and add 7.5µl RNase and 4µl propidium iodide (1mg/ml). Incubate in dark at room temperature for 1 hour.
- Measure with *BD FACSCalibur*® instrument using *Cell Quest*® software:
    - Close the pressure valve, run the instrument with full tube of FACS solution. Run the *Cell Quest*® software and connect to the device (Acquire /Connect to cytometer).
    - Prepare target folder (Acquire/ Parameter description) and naming profile (e.g. Sample ID).
    - Select number of events to be 30.000 cells (Acquire/Acquisition and storage/ counters), and open counter panel (Cytometer/ Counter).
    - Set up 3 graphs, A) SSC vs FSC dot plot B) B655-W vs B655-A dot plot C) Count vs B655-A histogram.
    - Run a tube for calibration (Setup mode), and change the gate values to make sure that G0/G1 peak is at 200 and G2/M at 400.
    - Measure each sample
- The data is analyzed with WinDMI® ver2.9.

3.6.3. Western-blot

Western-blot is a techniques where proteins are separated by molecular weight and transferred to a solid support. To separate the proteins, a SDS-PAGE method (sodium dodecyl sulphate-polyacrylamide gel electrophoresis) is the most common. The concentration of the gel affect the separation, while light concentrations (e.g. 8%) are used to separate heavy weight proteins, high concentrations (e.g. 12%) are used for light weight protein separation.

Extracting proteins

To eliminate the bias of tertiary structure of proteins, proteins need to be converted into single peptide strands (primary structure). In this part, we only worked with two cell lines so the protocols are listed here for cell-lines only.

- Cells were washed with 5ml Phosphate Buffered Saline (PBS) to remove dead cells.
- 2-4 ml Trypsin was added and incubated in 37^{o}c for 10-30 minutes.
- Cells were washed twice with 5ml PBS, and centrifuged at 1500rpm for 3 minutes.
- The supernatant was discarded and 0.5-1ml of cell lysis is added. The solution was held in ice for 30 minutes, during which it is mixed each 5-10 minutes.
- The mixture was centrifuges for 15 minutes at 4000rpm, in 4^{o}c.
- The clear part of supernatant was separated, divided into two tubes and held at -80^{o}c.

Protein levels were measured using both Nanodrop 2000® and Bradford kit (ThermoFisher: 23200). Diluted solutions of 1:10 were prepared and checked.

Preparing Gels

- The glass plate and its cover were cleaned with ethanol and put in a clamp, on a casting stand.
- The suitable solution was swirled and pored carefully into the cast.
- A 20µl of isopropanol was added to level up the surface.
- The gel solidify in 45 minutes, and the isopropanol was removed.
- The stacking gel was prepared, and cast it using suitable combs.
- The stacking gel solidify in 45 minutes.

Table 4: the composition of separating gel

Separating gel	8%	12%
dH2O	4.6ml	3.2ml
Acrylamide30%	2.6ml	4ml
Lower Tris	2.6ml	2.6ml
TEMED	5µl	5µl
ammonium persulfate 25%	20µl	20µl

Table 5: The composition of stacking gel

Stacking Gel	
dH2O	6ml
Acrylamide30%	1ml
Lower Tris	2.6ml
TEMED	10µl
ammonium persulfate 25%	20µl

The upper tris buffer pH is 6.8, and the lower pH is 8.8. The well is about 1cm in height, so the proteins in the bottom of the sample have about a 1cm head start compared to the proteins on the top of the sample loaded into the well. The upper gel is designed to concentrate all proteins into a narrow band so that they begin migrating through the lower gel at the same time. At pH6.8 glycine has a neutral charge, so it migrates very slowly and all proteins get concentrated in a narrow band between glycine and Cl- (from the Tris-HCl) until they reach the lower gel (pH 8.8), where glycine acquires a net negative charge and greatly accelerates. Since the lower gel has a higher concentration of acrylamide, larger proteins will travel more slowly than smaller ones.

Running Samples:

- Prepare 200µg of total protein for each sample.
- Samples were heated at 95^{o}c with sample buffer 1:4 for 5-10 minutes.
- Gels were loaded in the tank and chambers were filled with running buffer 1x.
- Samples were loaded into the gel, and 5µl of weight marker was used (PageRuler plus)
- The running started at 50v for 10minutes, then at 140v for 45-60 minutes.

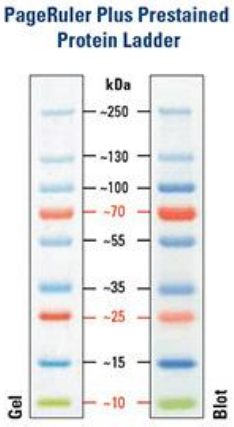

Figure 22: PageRuler plus, the moleculer weight marker.

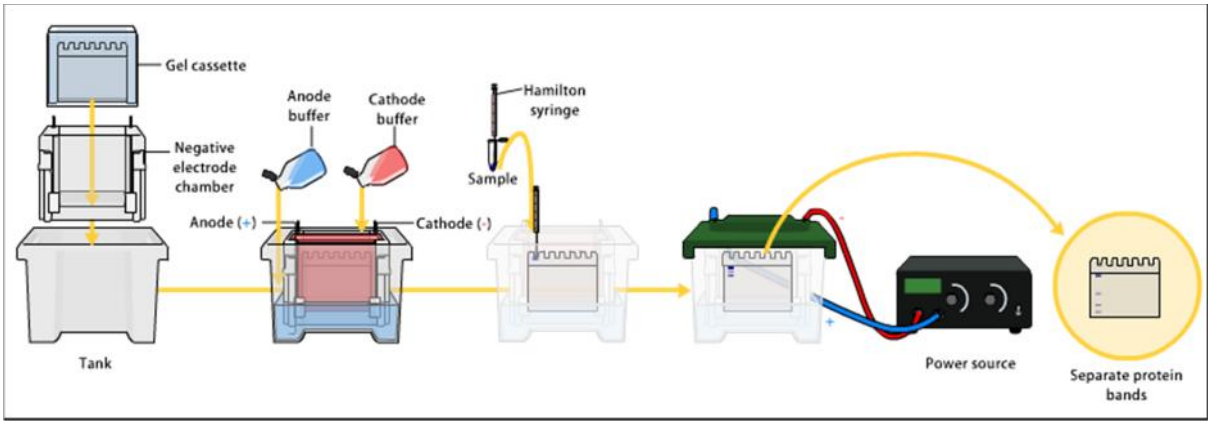

Figure 23: Preparing gel in the tanker, loading samples and running them.

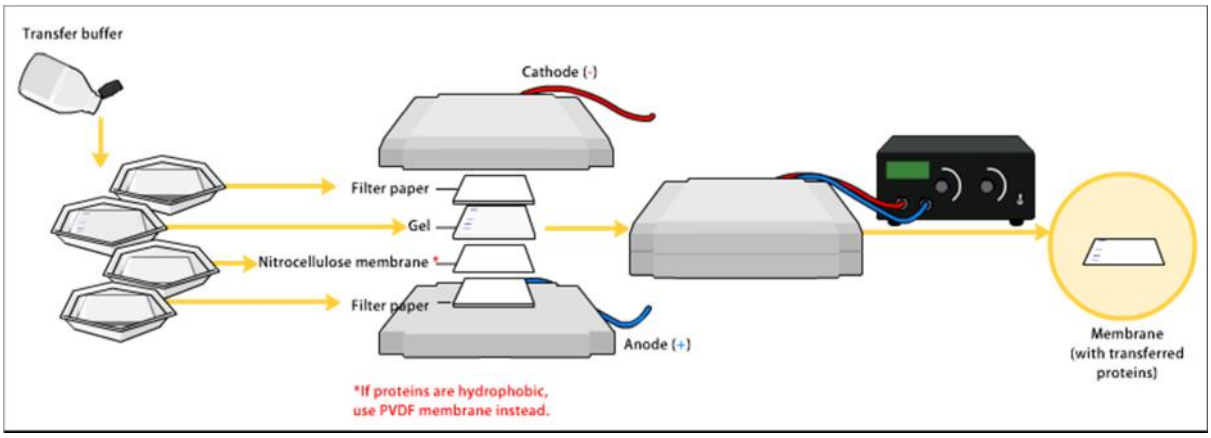

Figure 24: Transferring proteins from gel to a solid membrane.

Transferring to a solid membrane

Several kinds of solid phases were used in Western-blot. For our proteins we prefer to use Polyvinylidene fluoride (PVDF) membranes (GE®).

- Cut the membrane and Whatman's paper to be suitable in size for one gel.
- Wet Whatman's paper in transferring buffer.
- Activate the solid membrane with absolute methanol for 1 minute, and wash it with dH2O for another minute.
- Put one layer of Whatman's, the membrane, the gel, and finally two layers of Whatman's paper. Use a tube to get rid of air bubbles.
- Run the transferring for 45 minutes at 15v.

Antibody reaction and Visualizing

To save expenses, two types of antibodies were used. The primary antibody, was a specific antibody which targets the peptide chain of the protein, each protein has a different antibody. A secondary antibody was directed towards the antibodies of an animal (mouse, goat, rabbit… etc.) that was used to generate the specific primary antibody. In this way, one secondary antibody can tag many proteins. The tagging could be radioactive, fluorescent or a peroxidase enzyme (e.g. HRP).

- Block the membrane using 10ml of blocking solution for 1 hour.
- Wash 10sec with TBST.
- Add 3ml of primary antibody, and incubate 1 hour in room temperature or overnight in +4^{o}c.
- Wash 3 times with TBST (5,7 and 15 minutes)
- Add secondary antibody solution and incubate in room temperature for 45 minutes.
- Wash 3 times with TBST (5,7 and 15 minutes)
- Use peroxidase substrate (Pierce™ ECL Western-blotting Substrate), 250ml of each solution per membrane. Wait for two minutes.
- Reveal using X-ray films.

3.6.4. Immunofluorescence

This technique is based on identifying proteins in cells using florescent antibodies. The location and the quantity of proteins can be observed under confocal florescence microscopy and photographed.

Protocol:

1- Cell growth:
- Place 3-4 glass disks in 6 well-plate.
- Add 1.5ml of growth medium to each well.
- Prepare 30ml of cell suspension from 10ml petri dish.
- Add 0.5ml of cell suspension to each of the 6 wells

2- Cell fixation
- Prepare a dilution of 4% formaldehyde in PBS (The stock of formaldehyde is 37%)
- Wash the wells with PBS twice on ice.
- Incubate with formaldehyde for 10 minutes.

- Wash twice with PBS for 5 minutes each.

3- *Permeability:*

- Incubate for 10 minutes with 0.5% TritonX diluted in PBS.
- Wash three times with PBS for 5 minutes each.

4- *Blocking*

- To reduce background noise, blocking can be done with 1mg/L BSA in PBS for 1:30 hour.

5- *Incubation with primary antibody*

- Put cell in a humid room
- Add 30ul of antibody dilution to each glass disk.
- Incubate for 1:30 hour
- Return the disks to the wells, while keeping the face where the cells are upside.
- Wash three times with PBS for 5 minutes each.

6- *Incubation with secondary antibody*

- Return the disks to the humid room.
- Prepare a dilution of the secondary antibody in PBS + 1mg /mL of BSA. (Alexa flor 488 1:400)
- Add 30ul of antibody dilution to each glass disk
- Incubate for 1 hour in the dark.
- Return the disks to the wells
- Wash three times with PBS for 5 minutes each.

7- Coloring nucleus with DAPI

- Put the disk in the humid room.
- Prepare a dilution 1:200 of DAPI in PBS.
- Add 30ul to each disk for 5 minutes in the darkness
- Return the disks to the wells
- Wash three times with PBS for 5 minutes each.

8- *Revealing*

- Warm mowiol (Sigma) at 50^{o}c to decrease its viscosity
- Draw the target on the slides and add 15ul of mowiol for each disk.
- Flip the disk over the drop of mowiol.
- Leave the slide to dry for a few hours in darkness
- Do your photos at normal or confocal florescence microscopy

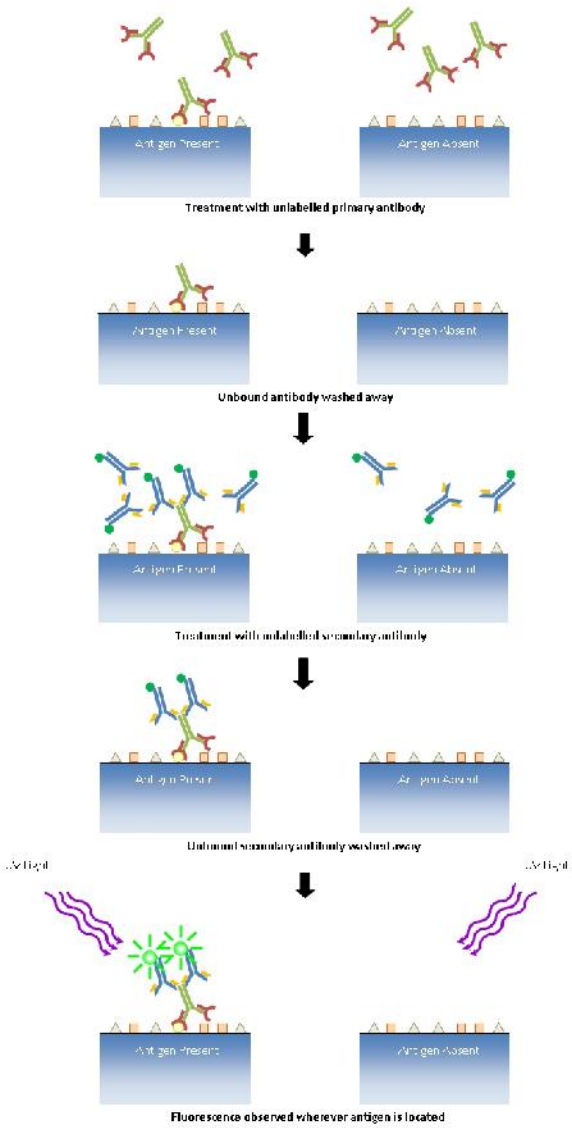

Figure 25: The principle of immunofluorescence. Fixing the cells or tissue of a solid phase, adding primary antibodies, adding secondary antibodies then washing and measuring the signal.

3.6.5. 3D cell culture

"Hanging drop" method is a simple method to produce 3D spheroids of cells in culture and study the effects of drugs in a more realistic models. While many other 3D culture methods are available, this methods remains the simplest and cheapest among them all.

The idea behind the "hanging drop" is using gravity to allow cell to merge in the bottom of the drop. The cells will form a spheroid that resembles the tumor in a living organism, where only few cells are in contact with the notorious medium while the cells in the middle lack direct access to nutrients and are under stress (hypoxia).

Protocol: [100]

1- Add trypsin to the cell culture, and incubate in 37^{o}c for a few minutes. Then wash with 5 ml PBS and centrifuge at 1500rpm for 3 minutes twice.
2- Prepare 2.0 x 10^{6} cells/ml in culture medium (RPMI, FBS 10% and antibiotic 1%). Any drugs are applied at this stage.
3- Open a 10 Petri dish and add 5 ml of PBS to the bottom of the dish to maintain humidity.
4- Use 30µl of the culture medium with the cells to form drops on the inner side of the top of the palte of and invert the top.
5- Incubate at 37°C/5% CO_2/95%.
6- Monitor cells daily, and usually after 2-4 days the spheroids will form in the control.

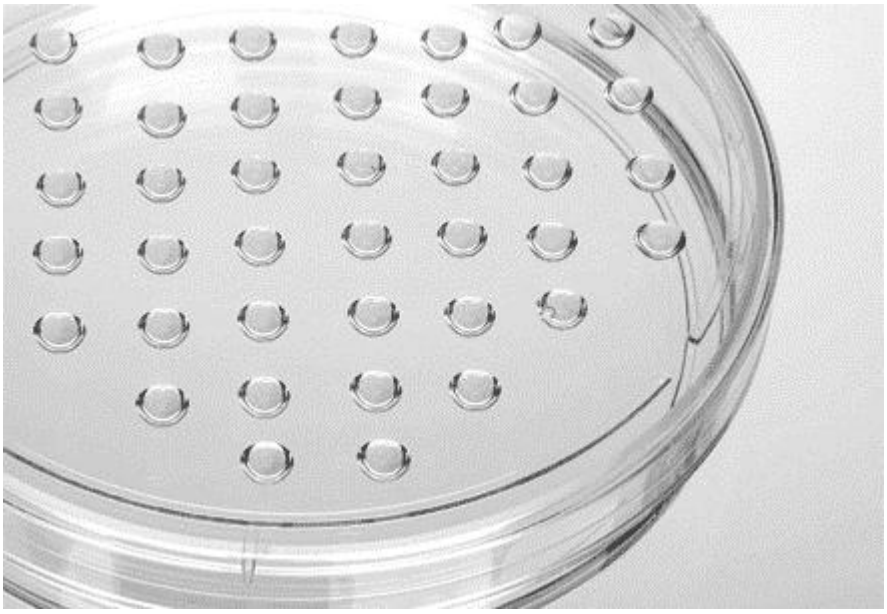

Figure 26: A plat with hanging drops to produce 3D cell culture

3.6.6. Composition of solutions:

Lower Buffer (for the separating gel)
1.5M Tris 36.4g pH to 8.8 with 6M HCl until nearing desired pH, 0.4% SDS 8mL of 10% SDS.
Up to 200mL with water
Upper buffer (Stacking)
0.5M Tris 6.06g pH to 6.8 with 6M HCl until nearing desired pH, 0.4% SDS 0.4g.
Up to 100mL with water
30% Acrylamide
Acrylamide 30g, Bis-acrylamide 0.8g. Up to 100mL with water.
Sample buffer
10% w/v SDS
10 mM Dithiothreitol, or beta-mercapto-ethanol
20 % v/v Glycerol
0.2 M Tris-HCl, pH 6.8
0.05% w/v Bromophenolblue
Running buffer 10x
SDS 10g, up to 100ml with water. Running buffer is diluted and used 1x when running the gel.
Transferring Buffer (Semi-dry)
100ml of stock transfer buffer (250mM Tris, 1.9M glycine)
200ml of methanol
Up to 1 liter with dH2O
TBST
Tris-Buffered Saline 250ml (1M Tris and 3M NaCl, pH 7.6), Tween 20% 5ml, up to 5 liters with dH2O.
Blocking buffer
Fat-free milk 0.5 g, TBST 10ml
Primary antibody solution
100.000ui of antibody in 3ml antibody solution (3% bovine serum protein in TBST)
Secondary antibody solution
3ml of TBST, 0.2mg of fat-free milk, and 0.3µl secondary body.
Lysis buffer (Triton buffer)
2.5ml Tris HCl 1M
1.5ml NaCl 5M
100µl EDTA 0.5M
0.5ml Triton
One tablet Complete® (Roche)-Protease inhibitor
dH2O up to 50ml

3.7.6. Cell lines

3.7.6.1 Cell line NCI-H1299

The cell line was established from a lymph node metastasis of the lung from a 43 years Caucasian male patient who had received prior radiation therapy. These cells lack P53 expression and the cell line is considered a common example to study p53 effects in tumors. These cells stain for keratin and vimentin but are negative for neurofilament triplet protein. The cells produce neuromedin B.

This cells are morphologically epithelial and they grow in both RPMI-1640 and DMEM mediums (10% fetal bovine serum, 1% antibiotic). The cells grow in 95% air with 5% carbon dioxide (CO2), at 37°C. The cells should be frozen in complete growth medium supplemented with 5% (v/v) DMSO.

H1299 is also reported to have a mutatrion on NRAS (G12C), a GTPase related to KRAS. RAS GTPases regulate cell growth, proliferation and differentiation. [101]

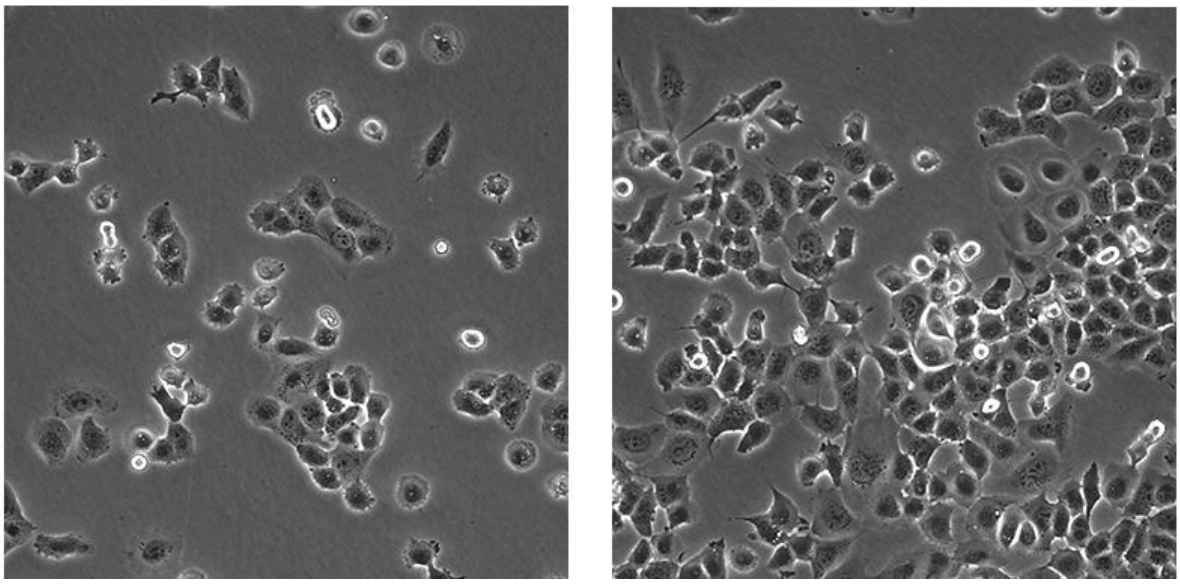

Figure 27: NCI-H1299 cell line (Left) 50% = one day of growth. (Right) 90% full = three days of growth.

3.7.6.1. COR-L23 cell line

This cell line is derived from the pleural effusion of a 62-year-old Caucasian male and classified as large cell carcinoma (NSCLC). They are adherent and grow in RPMI1640 medium with 2mM glutamine and 10% fetal bovine serum (FBS).

These cell are tumorigenic in nude mice. Though no much is known about its mutations due to a very complex karyotype. The cells have a huge number of changes: mTOR (Missense Mutation: E1921V, Splice Site SNP: V808_splice), ARID1A (Silent: G1740G), KRAS (Missense Mutation: G12V) and HIF1A (insertion in 3'UTR). [102]

This cell line is also referred to as L23/p (for parent), to distinguish it from COR-L23/R. The latter is a multi-drug resistant (MDR) sub-line derived from the parent line after treatment with doxorubicin. COR-L23/R contains reduced levels of glutathione and glutathione-S-transferase activity compared to the parent line. MDR seems to be connected with overexpression of multi-drug resistance-associated protein (MRP) which is discussed as a drug transporter.

Our work is limited to the parent cell line, as we only studied autophagy and the effects of treatments.

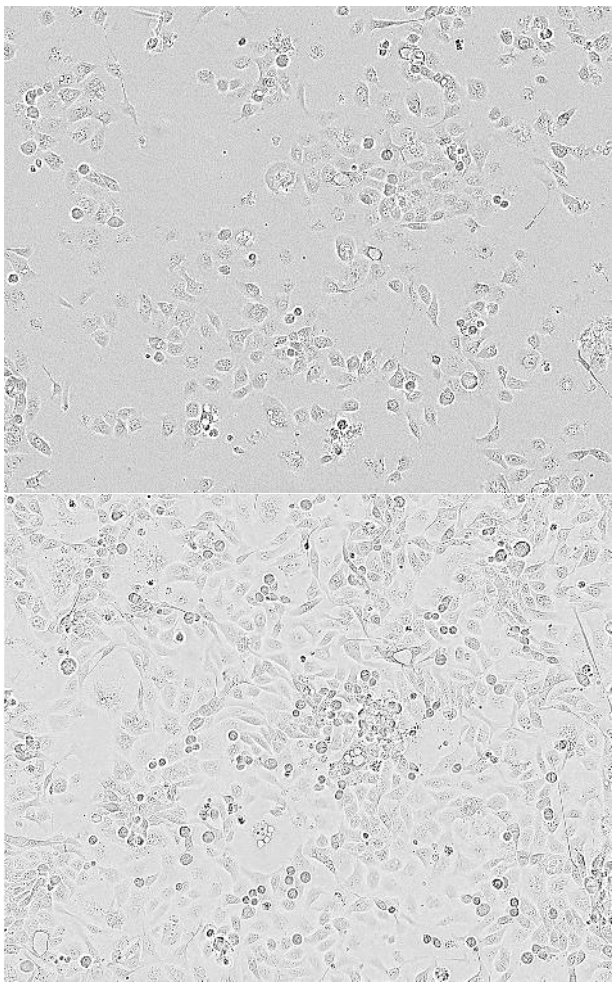

Figure 28: COR-L23 cells after 24h (up) and 48h (down) from growth.

4. RESULTS

4.1. uAUG CONTROLS GENE EXPRESSION

A bioinformatic analysis of the whole transcriptome using a copy of BioMart.org database (GRCh37.p1) showed that the existence of "AUG" sequence is less likely to be found in the 5' untranslated region (5' UTR) of genes than in random sequences, especially within the 100 base pairs closer to the initiation codon (Figure 29). We call "AUG" sequence upstream the start codon: "uAUG".

Our results show that the inclusion of novel uAUG sequences induces a reduction in protein expression (Figure 30). Moreover, the inhibition is clearly related to the distance of the single d*e novo* uAUG from the initiation codon. The closest uAUG to the canonical AUG the highest repressor effect. (1 tailed Person´s correlation for mediums of expression/distance was r=0.934, p=0.033). Moreover, double uAUG mutations induce higher repression than a single mutation.

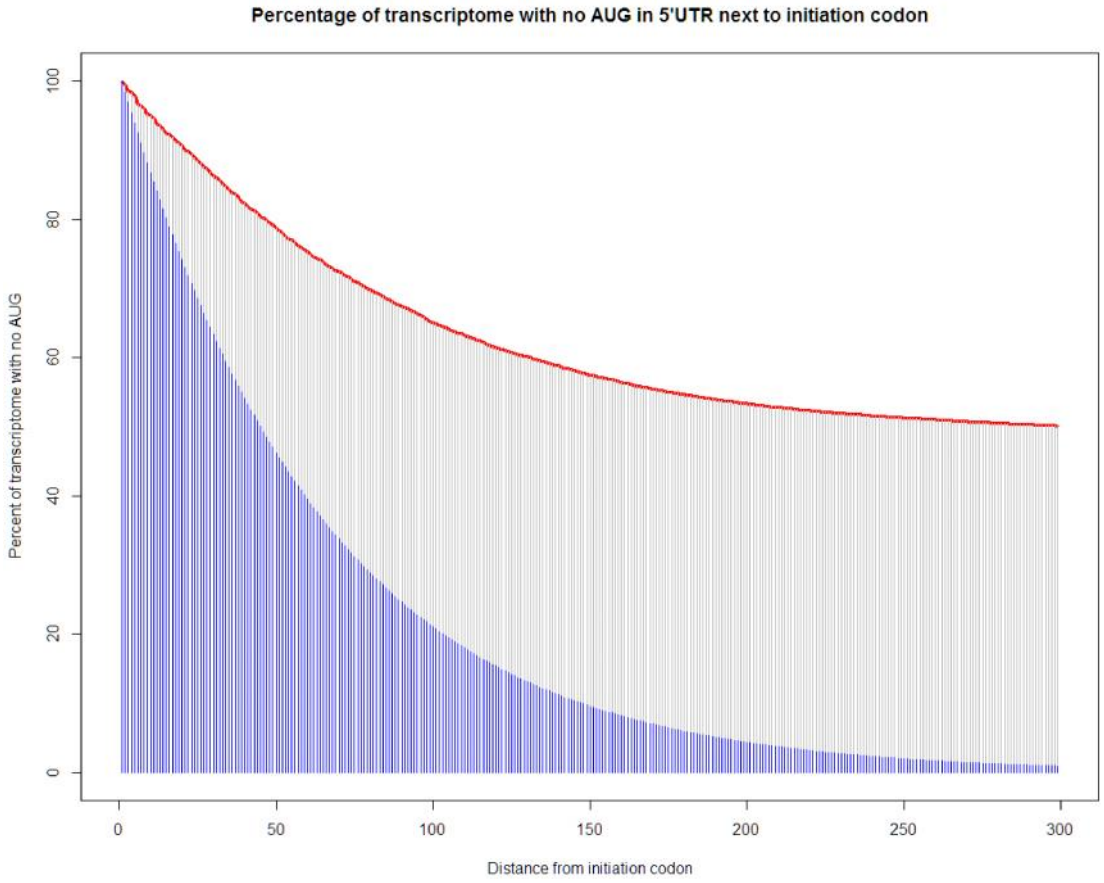

Figure 29: The percentage of transcriptomes that does not contain AUG sequence in 5' UTR in relation to the distance from the initiation codon (distance in bp). Transcripts that don't have 5' UTR were ignored. Data from BioMart-GRCh37.p11 database. (Total number analyzed is 90273 transcripts). The Figure shows that there is a huge percentage of transcription forms that lack uAUG sequence in proximity to the initiation codon. Blue space is the expected existence of random triplet sequence (p=1:64)

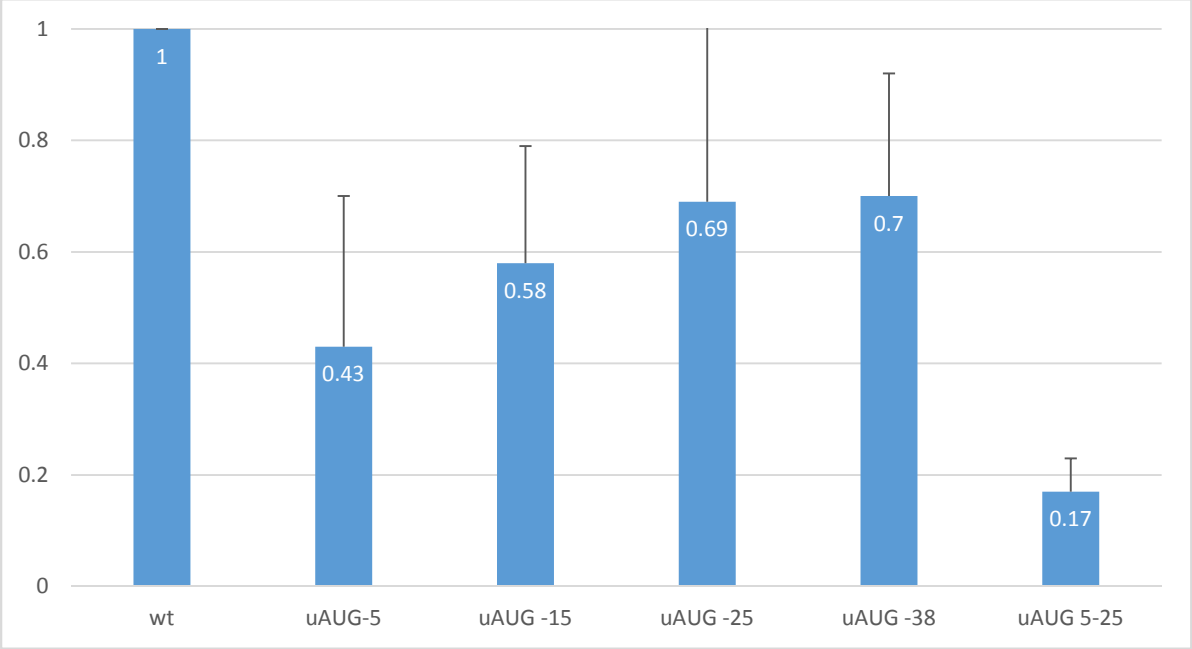

Figure 30: Expression of luciferase with mutated plasmids containing uAUG in the 5'UTR compared to the wt (normalized).

When studying RNA folding (RNAfold webserver [98]), changes in MFE centroid secondary structure had no correlation with changes in protein expression (r=0.300, p=0.567) (Table 6).

Table 6: Comparison between levels of protein expression with centroid minimum free energy (MFE) that represent optimal RNA folding structure. (Measured by RNAfold webserver)

Protein expression	1	0.43	0.58	0.69	0.7	0.17
Centroid secondary structure minimum free energy	-456.01	-422.41	-381.46	-449.21	-392.96	-425.21

4.2. BIOINFORMATIC ANALYSIS OF ISOFORM EXPRESSION IN LUNG DISEASES

4.2.1. Definitions:

- In our study, we calculate the total gene expression (TGE) as the simple sum of all different transcripts.
- The main isoform is the highest expressed isoform in a normal tissue. (e.g. CASP6-001 in Table 8).
- Mean of isoform expression (MIE) is the mean of each positive sample expression. Isoforms were taken from transcript expression file, and any value over 0.1 FPKM was considered as a positive read.
- Isoform prevalence is the percentage of positive isoforms in each group (normal, cancer and COPD).
- Distinct isoforms change (DIC) is a change in isoform pattern of expression or prevalence that produces undeniable biological change with $p<0.05$ (e.g. In Table 8: mTOR in Cancer and Caspase3 in COPD). This means that:

- Changes in isoforms that produce the same protein sequence are not considered distinct change.
- A change in the main isoform that is not accompanied by another isoform is considered a change in gene expression not isoform change.
- "Retired" isoforms from the next version of annotation (hg38) are merged with the main isoform.

However, most isoform changes are accompanied by a respective change in TGE (e.g. Caspase3 in COPD- see Table 8).

Place of gene expression on a graph makes a perfect sense and reveals a consistent activation or deactivation of different pathways. It also indicted that a single key point in each pathway controls the flow of signal, and each key point has a distinct isoform change.

In autophagy we found an important isoform change in mTOR in both COPD and lung cancer, while in apoptosis caspase3 expressed a new isoform in COPD.

4.2.2. Isoform changes in Lung Cancer

- Over-expression was detected in ULK1, ATG13, ATG16L1, Beclin1, P62/SQSTM, ATG7, ATG4B, ATG9A and ATG2A. Most proteins in autophagy pathway starting ULK1/ATG1 have been elevated pro-autophagy effect (Figure 65).

  Upstream mTOR, we observed an anti-autophagy effect with a decrease in AMPK and an increase in Erk1 and Raptor.

mTOR has been elevated TGE, and it could mean an increase in its inhibitory effect on ULK1-ATG13-FIP200, and a decrease in autophagy. The flowchart shows exactly the opposite effect, the autophagy pathway is down below has high expression of most genes.

We notice that MTOR-001 have no significant change, while MTOR-002 had an elevated MIE (*p=0.015*). Total mTOR expression was raised due to MTOR-002 change.

- Analysis of apoptosis in lung cancer showed an increase in Caspase2, Bid, Bax, Bak and Caspase9, which are pro-apoptotic. We also found a decrease in later stages of apoptosis pathway (Caspase8, Caspase4 and Caspase7).

  The change of genes expression seems to be built around Caspase10 which had no change its total expression. Isoforms of Caspase10 suffered a decrease in isoform 001, and an increase in isoform 003.

4.3.3. Isoform change in COPD lung tissue

- We observed a decrease in expression of the pro-autophagy genes: ULK1, ATG16L1, ATG12, ATG7, ATG4B and P62.

  On the other hand, there is no significate change in total mRNA expression of mTOR. Nevertheless, pro-autophagy genes decreased upstream of mTOR (ERK1 and AMPK).

  In theory, mTOR should be overexpressed due to ULK1 inhibitions, however its total expression levels were not changed. Analyzing mTOR isoforms we found that MTOR-001 increased comparing to samples from healthy lung-tissue (*p=0.0006*). While MTOR-002 prevalence was decreased (52% compared to 94% in normal). The levels of MTOR-002 expressed has no statistically significant change (*p=0.19*).

- We observed some overexpression in pro-apoptotic genes in COPD: Caspase8, Caspase10 and Caspase4. However, most of the apoptotic pathway is unchanged.

  Total expression of Caspase3 was elevated, but that was due to a newly expressed isoform (Caspase3-005) related to resistance to anti-apoptotic drugs [103]. Caspase3-005 was expressed in 41% of COPD samples compared to 0% in normal and tumors. Genes that come after Caspase3 in apoptosis pathway were under expressed.

Table 7: Significant total gene expression (TGE) in some autophagy genes. The full list is in Appendix B.

Gene	Ave. Normal	Ave. COPD	P	Ave. Cancer	P
AMPK α1	22.9	30.6	0.005	13.0	0.000
ATG101	21.4	19.6	0.379	37.7	0.029
ATG16L1	7.3	6.7	0.039	13.0	0.007
ATG2A	5.0	4.9	0.690	8.6	0.000
ATG4B	27.7	16.6	0.000	53.4	0.134
ATG5	10.0	9.9	0.987	10.2	0.882
ATG7	7.0	6.7	0.915	9.3	0.241
ATG9A	15.1	13.8	0.121	24.1	0.007
Beclin1	27.2	23.9	0.152	31.4	0.054
LC3B	21.9	19.9	0.137	20.7	0.743
mTOR	8.5	8.1	0.239	12.9	0.010
PTEN	11.2	14.0	0.003	5.8	0.000
P62	171.1	140.9	0.010	327.5	0.033
PIK3CA	4.4	5.3	0.014	2.3	0.000
ULK1	11.1	9.6	0.147	23.0	0.006
PRAS40	7.01	8.39	0.194	57.17	0.015
Raptor	5.01	5.36	0.539	8.04	0.004
ERK1	30.38	21.76	0.000	41.21	0.010
ERK2	12.80	11.72	0.256	10.07	0.103
TSC1	6.70	7.02	0.453	5.50	0.123
TSC2	18.36	13.26	0.009	43.47	0.019

Table 8: Some Distinct isoform Change (DIC).

Isoform	Normal Count	Normal Average	COPD Count	Average	P	Cancer Count	Cancer Average	p
MTOR-001	47	4.0	25	5.89	0.0006	12	5.88	0.1588
MTOR-002	45	4.85	13	4.18	0.1897	11	10.05	0.0151
Total mTOR	48	8.47	25	8.07	0.239	14	12.94	0.0100
CASP3-001	46	4.51	25	4.44	0.9214	12	4.89	0.6328
CASP3-003	44	8.86	25	8.02	0.4501	14	8.70	0.9364
CASP3-005	0		11	13.49		0		
Total Caspase3	48	12.48	25	18.44	0.0089	14	12.90	0.8491
CASP6-002	6	2.21	0			6	7.48	0.0268
CASP6-001	46	6.33	24	5.65	0.1233	14	6.76	0.6239
CASP6-009	1	0.28	0			0		
CASP6-008	1	2.05	0			0		
CASP6-006	4	3.45	0			1	2.32	
CASP6-007	2	4.18	0			0		
CASP6-003	1	2.17	0			0		
Total Caspase6	48	6.89	24	5.65	0.0016	14	10.13	0.0681
CASP8-007	42	5.48	23	7.38	0.0128	6	3.39	0.0102
CASP8-012	46	7.64	25	9.95	0.0160	14	5.78	0.0313
Total Caspase8	48	15.40	25	19.16	0.0177	14	12.38	0.0411
CASP10-001	46	4.11	24	5.16	0.0032	12	2.87	0.0053
CASP10-201	17	1.65	4	2.58	0.4161	7	2.42	0.3358
CASP10-003	26	1.73	17	2.05	0.2299	12	2.94	0.0160
Total Caspase10	48	5.48	25	6.76	0.0003	14	6.20	0.2703

4.3.4. Correlation with splicing factors and proteins

We studied the correlation between mTOR isoforms and some proteins factors in normal and COPD samples. Reports indicated that the splicing factor Sam68 in mice is related to mTOR splicing [104], the gene Sam68 in humans is called KHDRBS1.

We also studied the correlation between AMPK and mTOR isoforms. AMPK inhibit mTOR and activated autophagy. Drugs such as metformin use AMPK pathway to modulate autophagy, which could explains their anti-tumor effects. AMPK has three subunits and seven genes, we used PRKAA1 and PRKAA2 as representatives of AMPK expression.

Table 9: correlation between mTOR isoforms and some proteins (IBM-SPSS v23)

		MTOR1	MTOR2
TSC1	Pearson Correlation	.208	.099
	Sig. (2-tailed)	.080	.461
TSC2	Pearson Correlation	-.224	.465**
	Sig. (2-tailed)	.059	.000
Raptor	Pearson Correlation	.741**	-.428**
	Sig. (2-tailed)	.000	.001
PRAS40	Pearson Correlation	-.015	-.063
	Sig. (2-tailed)	.900	.639
ERK1	Pearson Correlation	-.132	.246
	Sig. (2-tailed)	.270	.063
ERK2	Pearson Correlation	.600**	-.332*
	Sig. (2-tailed)	.000	.011
AMPK1a	Pearson Correlation	.417**	-.504**
	Sig. (2-tailed)	.000	.000
AMPK2a	Pearson Correlation	.264*	-.367**
	Sig. (2-tailed)	.025	.005
Sam68	Pearson Correlation	.481**	-.461**
	Sig. (2-tailed)	.001	.003

RAPTOR, PRAS40, TSC1/2 and ERK1/2 also affect mTOR expression. The mechanism could be a change in isoform expression patterns.

mRNA expression of Sam68, AMPK, Raptor and ERK1 correlate to a different degree with both isoforms of mTOR (see Table 9). Raptor and ERK1 correlation can be explained by affecting MTOR001 expression as their correlation is much higher with this isoform. On the other hand, AMPK seems to affect levels MTOR002 more than the main isoform.

4.3. GENOTYPING OF AUTOPHAGY-RELATED SNPS

We have studied 165 men with lung cancer. The average age was 65.4 years old (S.D. 10.6), with a range [32-85 years old]. A group of 145 healthy control subjects with similar characteristics and life style was studied.

All participants had prolonged tobacco contact in some point of their lives, with the majority smoking over than 20 daily cigarettes over 20 years.

In our study, 87.7% of the patients were diagnosed with Non-Small Cell Lung Cancer (NSCLC) (Figure 31). That agrees with the epidemiological data on lung cancer subtypes [105]. All samples were in Hardy-Weinberg Equilibrium.

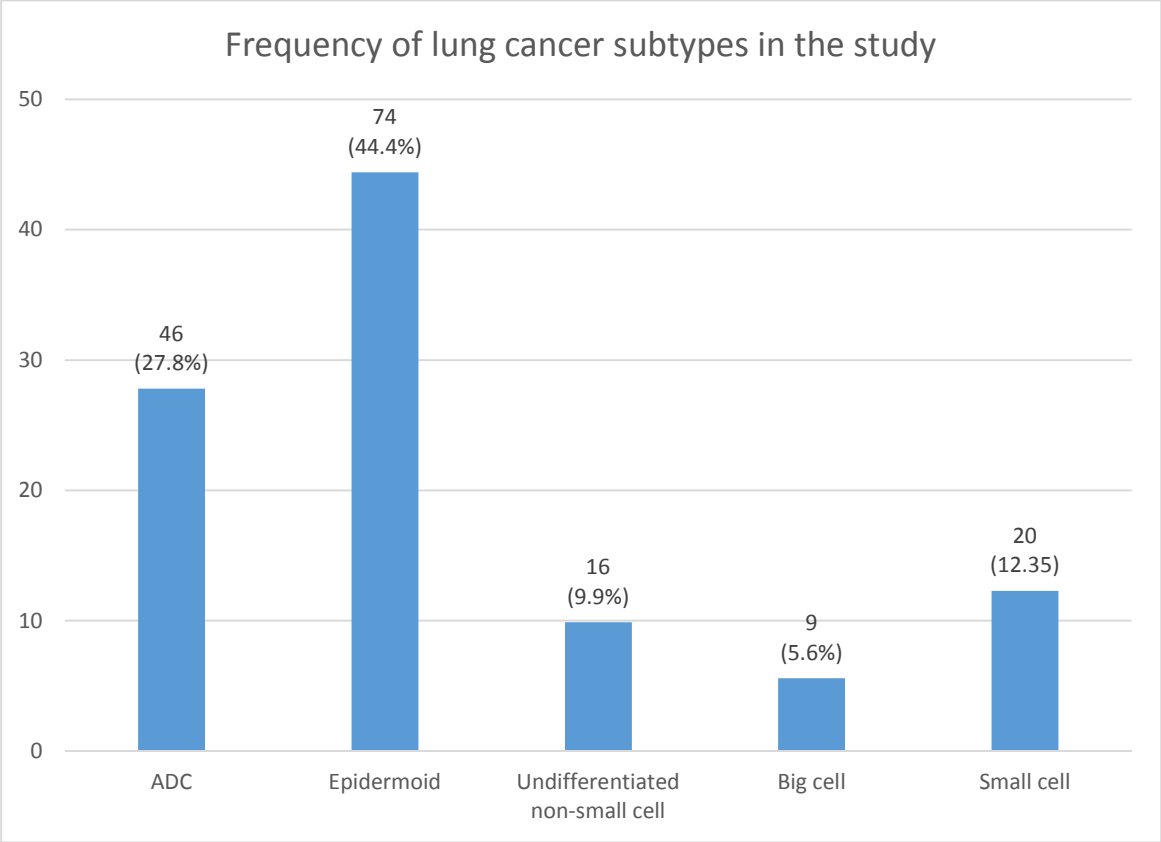

Figure 31: Distribution of lung cancer types in our sample

In our study, 30% of lung cancer patients had COPD (54 patient). 71 patients had first degree relatives (parents and siblings) with some form of cancer (lung and other cancers) (Figure 32 and 33).

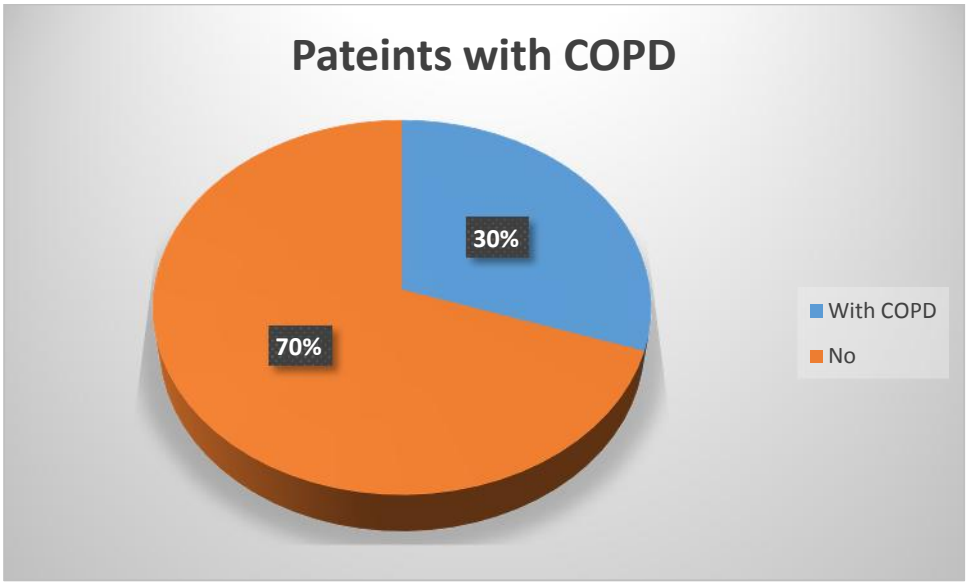

Figure 32: patients with COPD

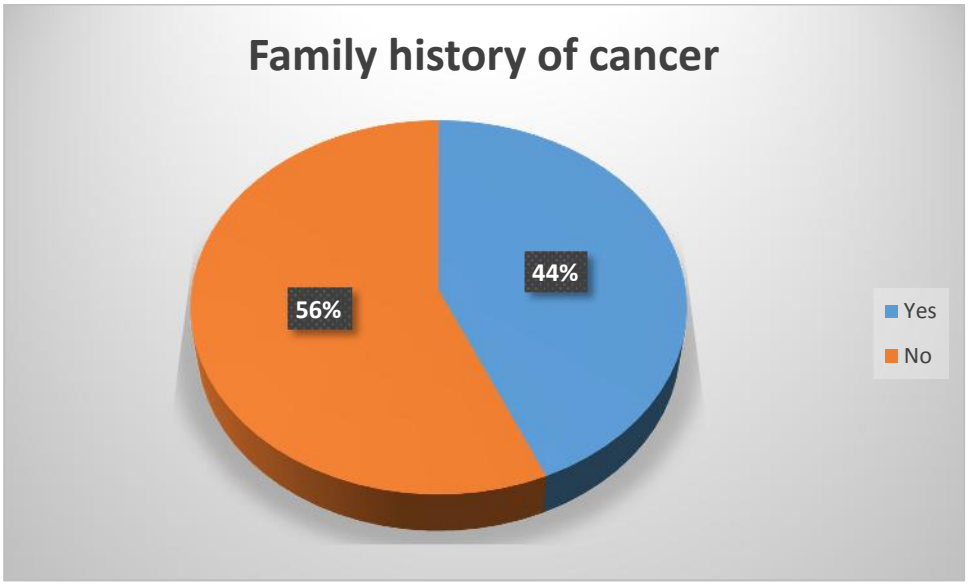

Figure 33: Family history in patients with cancer

Both *de Prado Otero* and *Jiménez Massa* [90, 89] presented a detailed data about correlation between tobacco consumption, life style, work and age from one hand and risk of lung cancer from the other, and thus we refer to those studies for more details and in Figure34 we show the correlation of years of tobacco consumption and age of diagnosis.

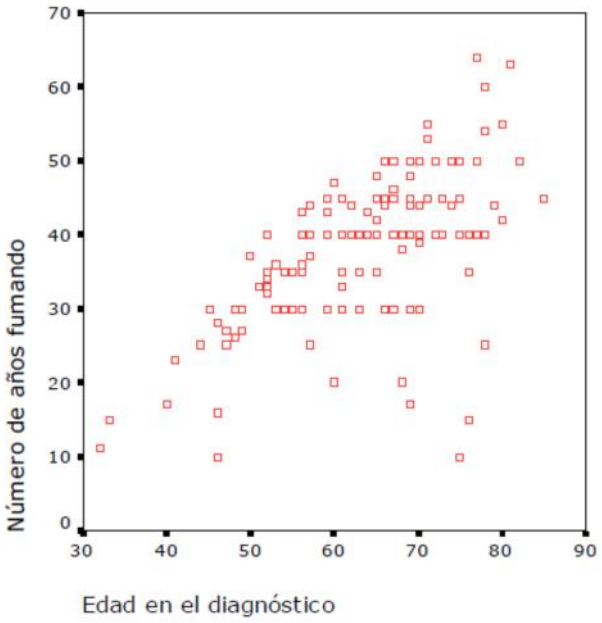

Figure 34: years of tobacco consumption vs age of diagnosis [90]

4.3.1. COPD, lung cancer and autophagy

COPD is one factor that modify susceptibility to lung cancer; it is also related to tobacco consumption. So we expected that patients with COPD had different genotype than those without. Indeed, our results show that lung cancer patients without COPD are protected by allele G in ATG16L1 (rs2241880), while no significant statistical change can be observed in the other three SNPs (Table 11). There was no significant differences in patients with COPD (Table 10)

Table 10: distribution of SNPs in autophagy gene in patients of lung cancer with COPD

ATG2B		Controls	%	Patients	%	
	GG	62	42.2	24	44.4	Chi=0.399
	CG	64	43.5	21	38.9	p=0.819
	CC	21	14.3	9	16.7	
		147		54		
ATG5		Control	%	Patients	%	
	CC	51	34.5	22	40.7	Chi=3.284
	CG	80	54.1	22	40.7	p=0.194
	GG	17	11.5	10	18.5	
		148		54		
ATG10		Controls	%	Patients	%	
	CC	49	33.3	15	27.8	
	CT	68	46.3	30	55.6	Chi=1.368
	TT	30	20.4	9	16.7	p=0.505
		147		54		
ATG16L1		Controls	%	Patients	%	
	AA	35	24.3	15	27.8	Chi=0.982
	AG	67	46.5	27	50	p=0.612
	GG	42	29.2	12	22.2	
		144		54		

Table 11: distribution of SNPs in autophagy gene in patients of lung cancer without COPD

ATG2B		Controls	%	Patients	%	
	GG	62	42.2	51	45.9	Chi=0.861
	CG	64	43.5	42	37.8	p=0.65
	CC	21	14.3	18	16.2	
		147		111		
ATG5		Control	%	Patients	%	
	CC	51	34.5	46	41.4	Chi=1.475
	CG	80	54.1	52	46.8	p=0.478
	GG	17	11.5	13	11.7	
		148		111		
ATG10		Controls	%	Patients	%	
	CC	49	33.3	30	27.3	Chi=1.72
	CT	68	46.3	51	46.4	p=0.44
	TT	30	20.4	29	26.4	
		147		110		
ATG16L1		Controls	%	Patients	%	
	AA	35	24.3	23	20.7	Chi=6.129
	AG	67	46.5	68	61.3	p=0.047
	GG	42	29.2	20	18	
		144		111		
	AA+AG	102	70.8	91	82	Chi=4.234
	GG	42	29.2	20	18	p=0.040
		144		111		OR=0.534 (0.292-0.975)

4.3.2. Lung cancer types and autophagy

One classification of lung cancer is being histologically small cell or non-small cell. The two types differ in development and resistance to therapies and radiation. So we explored the relation between lung cancer histology and autophagy.

We had 145 patients with NSCLC, and 20 patients with SCLC. We were not able to use them in a reasonable statistical comparison with SCLC due to the small sample size.

Patients with NSCLC had no significant statistical relationship with the genotypes of autophagy genes. (Table 12)

Table 12: distribution of SNPs in autophagy gene in patients of non-small cell lung cancer (NSCLC)

ATG2B	Controls	%	Patients	%	
GG	62	42.2	65	44.8	Chi=0.553
CG	64	43.5	57	39.3	p=0.758
CC	21	14.3	23	15.9	
	147		145		
ATG5	Control	%	Patients	%	
CC	51	34.5	56	38.6	
CG	80	54.1	67	46.2	Chi=1.994
GG	17	11.5	22	15.2	p=0.369
	148		145		
ATG10	Controls	%	Patients	%	
CC	49	33.3	38	26.2	
CT	68	46.3	74	51	Chi=1.774
TT	30	20.4	33	22.8	p=0.412
	147		145		
ATG16L1	Controls	%	Patients	%	
AA	35	24.3	33	22.8	Chi=4.142
AG	67	46.5	83	57.2	p=0.126
GG	42	29.2	29	20	
	147		145		
AA+AG	102	70.8	116	80	Chi= 3.276
GG	42	29.2	29	20	P=0.070
	144		145		

4.3.3. Total sample of lung cancer and autophagy

When we compare all patients with lung cancer, we found no statistical significant differences between the disease and genotype in general. Studying allele G in ATG16L1 (rs2241880), show that genotype GG could have a protector effect on from lung cancer. (Table13)

Table 13: distribution of SNPs in autophagy gene in patients of lung cancer (total)

ATG2B		Controls	%	Patients	%	
	GG	62	42.2	75	45.5	Chi=0.956
	CG	64	43.5	63	38.2	p=0.62
	CC	21	14.3	27	16.4	
		147		165		
ATG5		Control	%	Patients	%	
	CC	51	34.5	68	41.2	Chi=2.647
	CG	80	54.1	74	44.8	p=0.266
	GG	17	11.5	23	13.9	
		148		165		
ATG10		Controls	%	Patients	%	
	CC	49	33.3	45	27.4	Chi=1.32
	CT	68	46.3	81	49.4	p=0.517
	TT	30	20.4	38	23.2	
		147		164		
ATG16L1		Controls	%	Patients	%	
	AA	35	24.3	38	23	Chi=4.91
	AG	67	46.5	95	57.6	p=0.086
	GG	42	29.2	32	19.4	
		144		165		
	AA+AG	102	70.8	133	80.6	Chi=4.032
	GG	42	29.2	32	19.4	p=0.045
		144		165		OR=0.584
						(0.345-0.990)

4.4. DRUGS ASSAYS ON LUNG CANCER CELL LINES

4.4.1. H1299 CELL LINE AND AUTOPHAGY-RELATED DRUGS

After transferring H1299 cells to a new culture dish, the cells grow at a slow pace and most proteins are expressed at low levels including beta-actin and alpha-tubulin. The growth increases radically after the third day (confluence of 60-70%). The results of protein analysis with and without treatment are not consistent, and it heavily depends on the day the treatment starts. One problem we faced in this cell-line is the enlarged S phase in cell cycle (>50% of cells) during the first two days before the confluence rate reaches over 60%. Later, the cells in S phase are at stable rate (7-9%).

Adding 4 ml of trypsin to cell culture required around 20 minutes at 37^{o}c to suspend the cells. This time increased with metformin to more than 30 minutes, did not change with LBH and decreased with chloroquine to 5-10 minutes. For that reason, we studied the effects of these drugs of the formation of 3D spheroids to see possible effect upon cell to cell interactions.

To standardize the procedure for all samples, trypsiniztion lasted for 20 minutes for all samples, and any remaining cells are washed off the plat with PBS.

In order to get a consistent results and get a steady levels of autophagy, we have chosen “0 hour” when the cells cover 70-90% of the dish, then the treatment starts and samples were taken each 24h. Proteins were extracted immediately and saved at -80^{o}c.

To check consistency, we always used a series of daily control samples for one week. Each protein was measured and checked to be consistently expressed throughout the whole week. We also used flow cytometer to check the cell cycle. (Appendix A)

A possible isoform of mTOR (MTOR-005) was recorded in H1299 cell line at 18KD. The antibody used (cell signaling) could in theory detect this isoform. We did not investigate this isoform using other techniques, as we left this task to future studies. The images of western-blot is added here for future reference.

We used Paclitaxel (Taxol®) to study the effects of anti-cancer treatments on this cell-line (Figure 35). Taxol® is a common treatment for lung cancer, as it stops the cell line from growing causing cell death with even the smallest amounts of therapeutic doses (0.6ug/l)

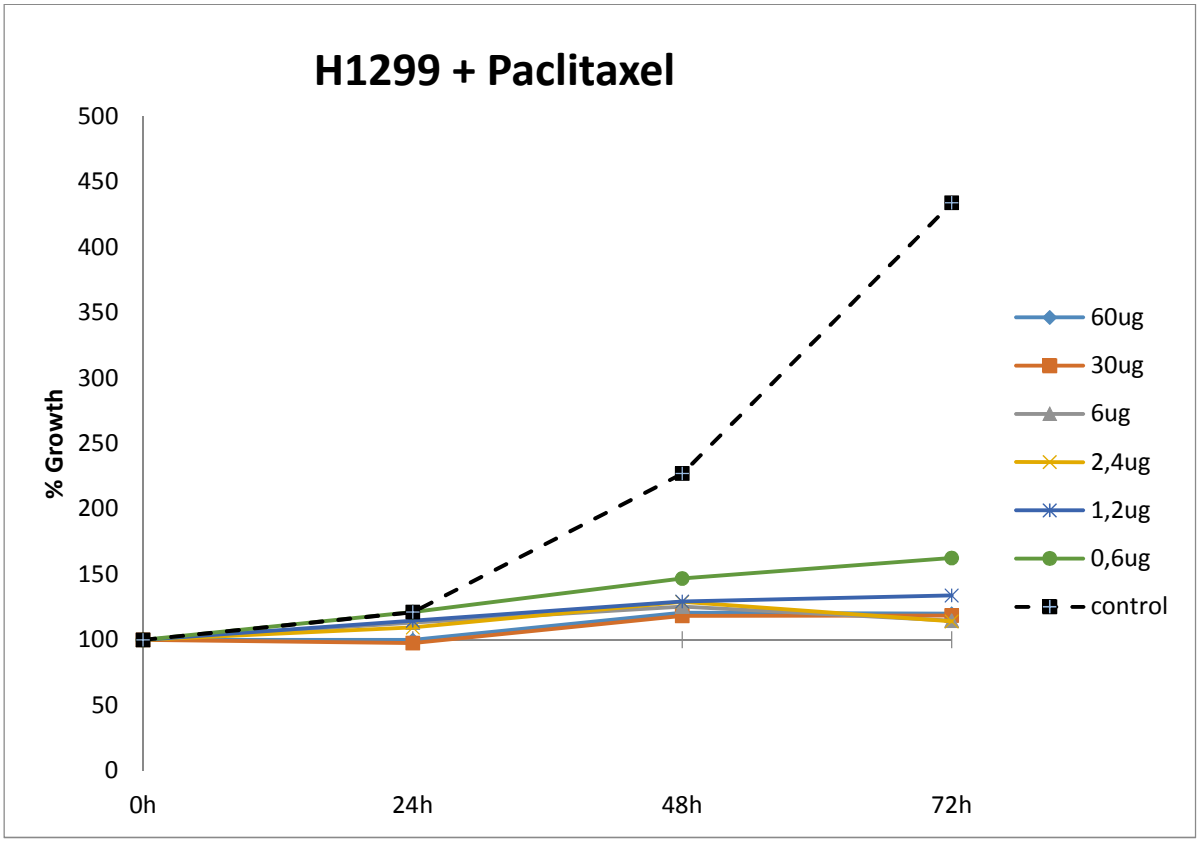

Figure 35: H1299 growth when treated different doses of paclitaxel.

4.4.1.1. Metformin and H1299

Previous studies focused on apoptosis in H1299 and metformin with little attention to autophagy. It has been reported that cells treated with metformin (10mM) had a decreased G2/M stage. They suffered from high levels of apoptosis, increased AMPK phosphorylation and a decreased phosphorylation of mTOR [106]. Some studies reported an inhibitory effect of metformin on H1299 mediated by activation of JNK/p38 and AMPK pathway and GADD153 inducing apoptosis [107, 108].

Metformin had no measurable effects on cell cycle of H1299 in long-term treatment and its effect on cell growth is limited. Cell growth decreased to 50% of control at maximum therapeutic dose used (8mM) (Figure 36).

A)

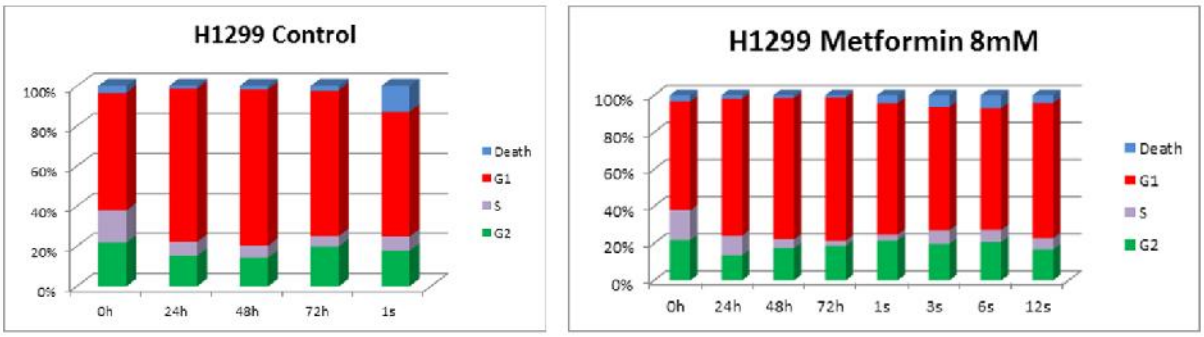

B)

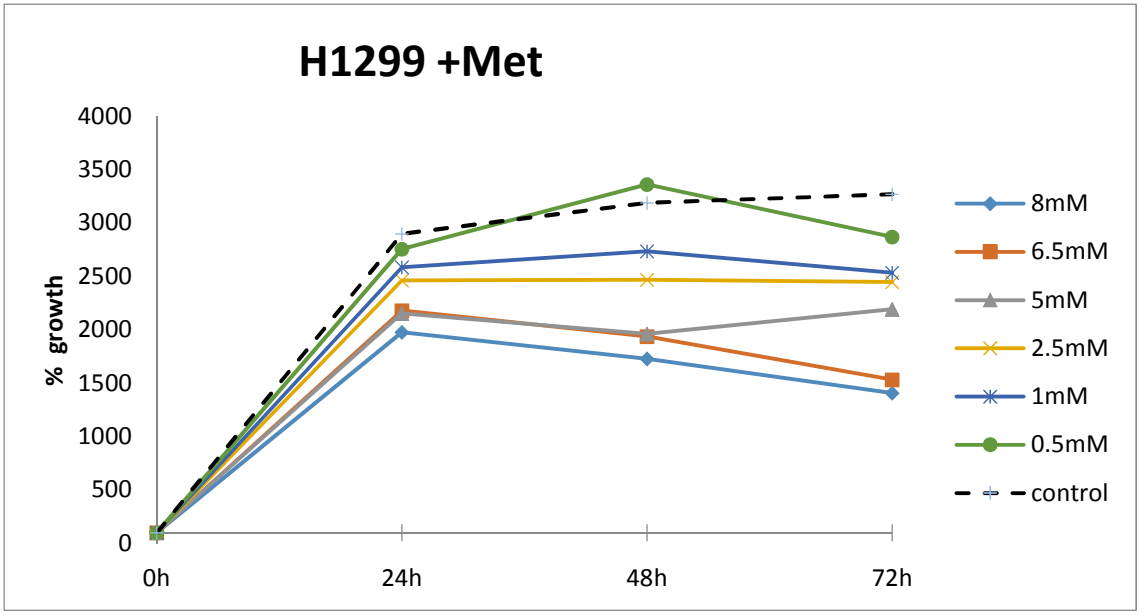

Figure 36: (A) Metformin has no significant change of cell cycle in long-term treatment compared with control cells at upper-left, (B) Metformin effects on cell growth is a decrease 10-50% in growth comparing to control.

When proteins were studied from H1299 cells treated with 8mM metformin. P62/SQSTM1 showed a moderate decrease in quantity starting 48h, and reaching a peak of decrease at 4 weeks and maintaining it till 10 weeks, and the same happens to Beclin1. LC3B had a total decrease in quantity, and a huge decrease in LC3B-I and an increase in LC3B-II after week 4.

Total amounts of mTOR decreases starting 48h and continues till they became undetectable.

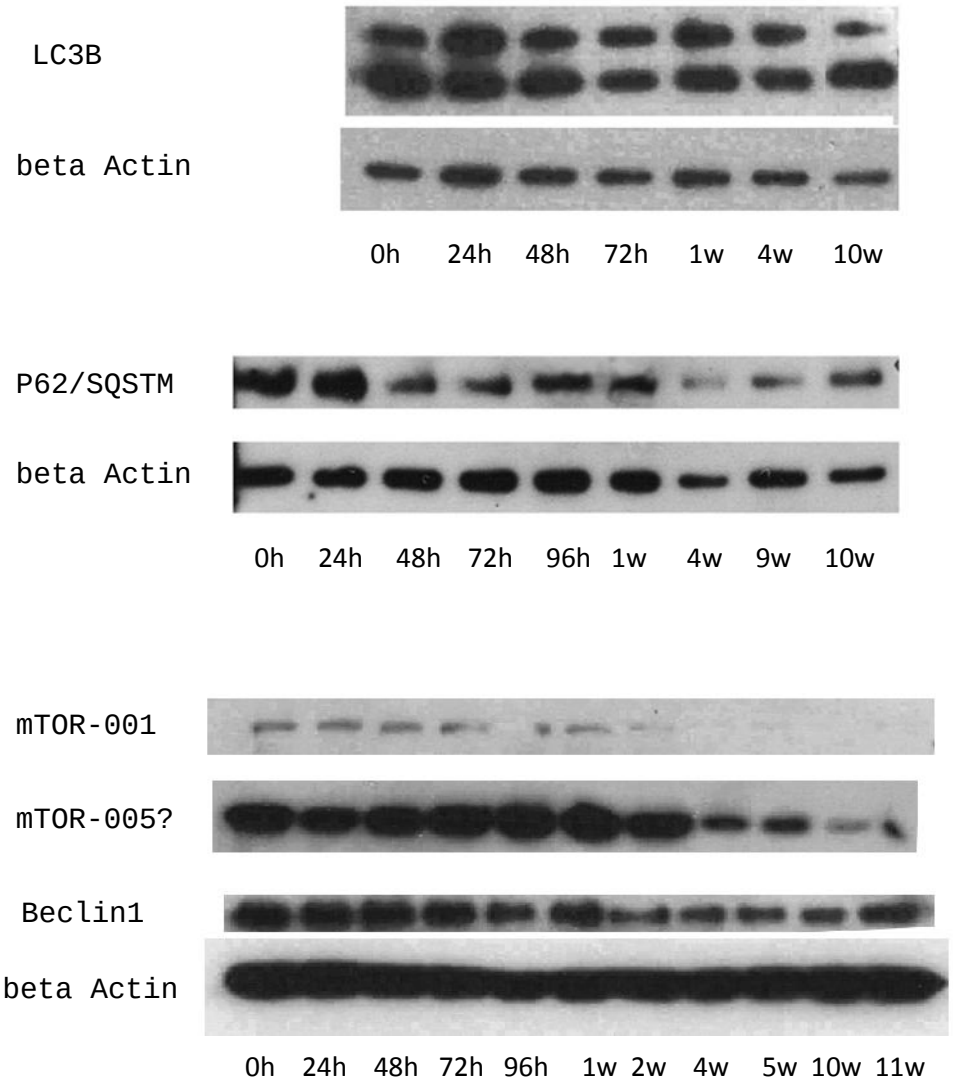

Figure 37: Long term treatment with metformin (8mM) causes a decrease in P62 that starts at 48h and reaches a peak after 4 week. LC3BII increases after week 4, and LC3BI decreases. mTOR and Beclin1 levels decreased starting 48-72h.

Under normal microscope, cells treated with metformin for over 4 weeks were not able to reach confluency of more than 60-70%. In addition to that, cell shape was elongated and bigger than control (Figure 38). 3D cell culture exhibited a decrease in tumor size up to 50% compared to control spheroids, but no changes in spherical shape was detected (Figure 39).

Figure 38: Cell morphology change after 10 weeks of treatment with metformin, a longer and less active kind of cells.

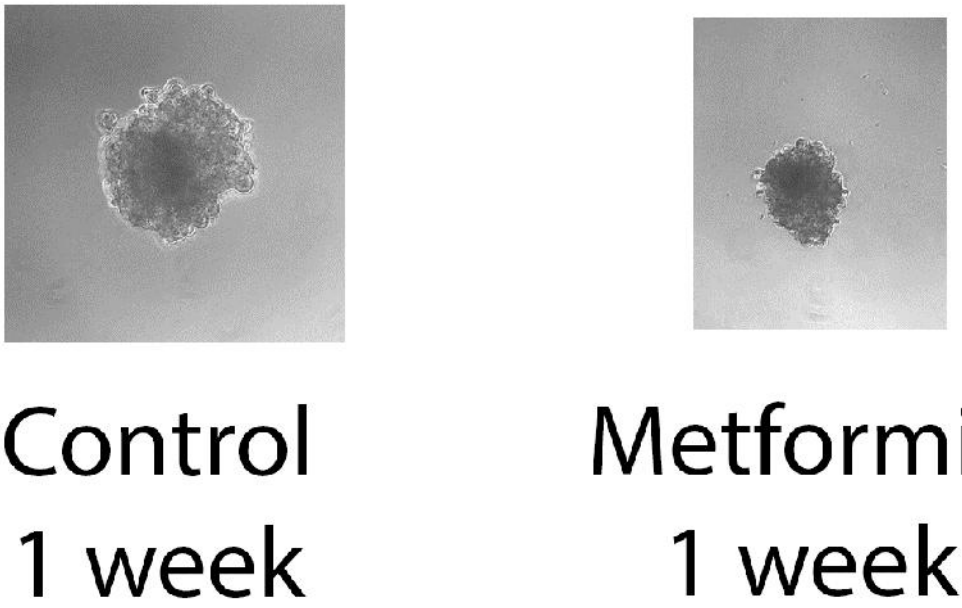

Figure 39: A 3D cell culture of H1299 after 1 week, the metformin has a significant suppressing effect on 3D cell growth up to 75%.

We confirmed our results with immunofluorescence assay using confocal microscopy. In control cells, P62 was evenly distributed in the cytoplasm. Metformin did not change this pattern much. (Figure 40)

H1299 present little if any LC3B, after metformin 8mM treatment for 48 hours we did not observe any change. Similar to Western-blot results, metformin take very long time to affect autophagy on H1299 cells. (Figure 41)

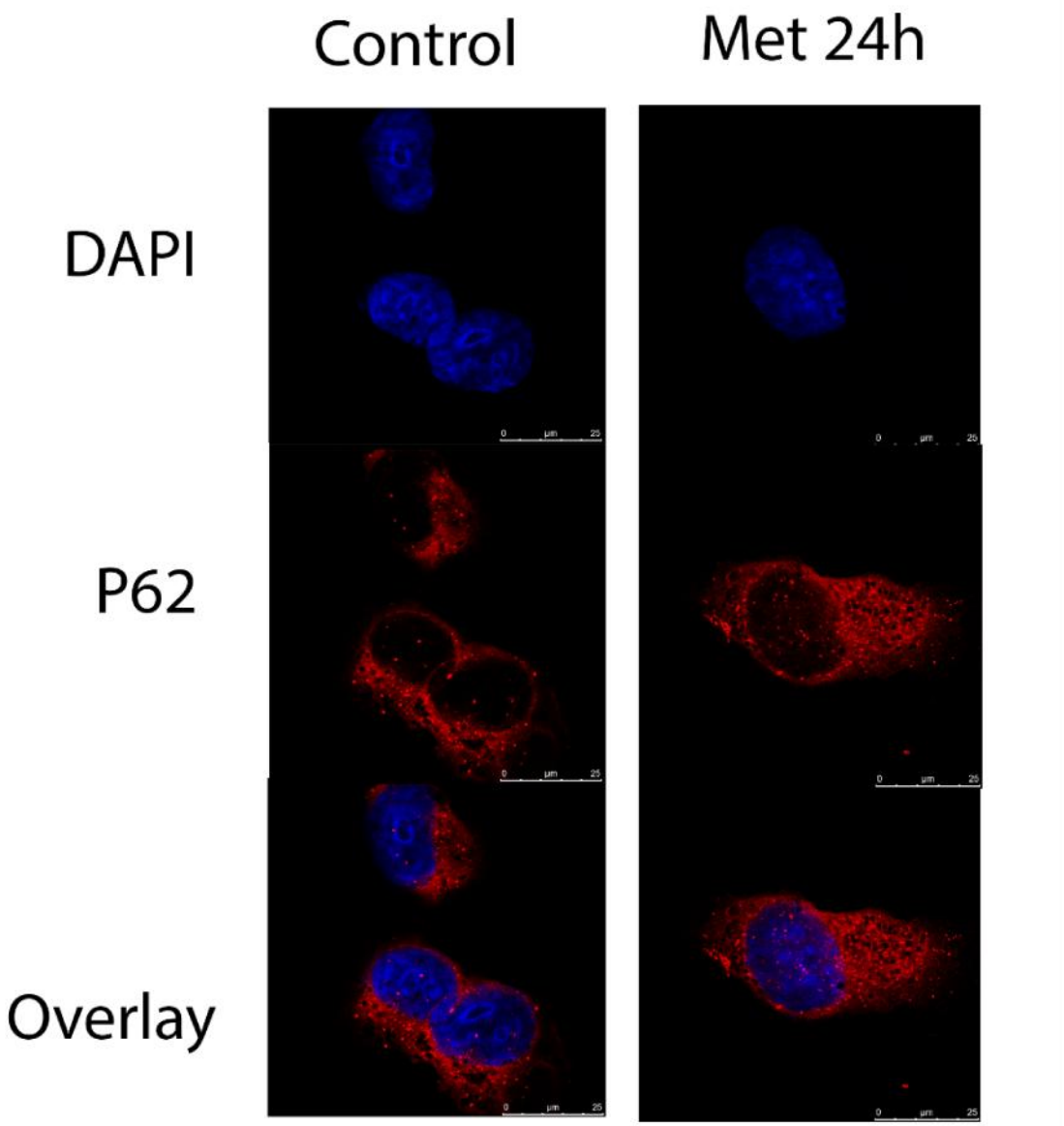

Figure 40: P62 in H1299 after 24 hours of treatment. With metformin, p62 remains uniformly distributed in cytoplasm.

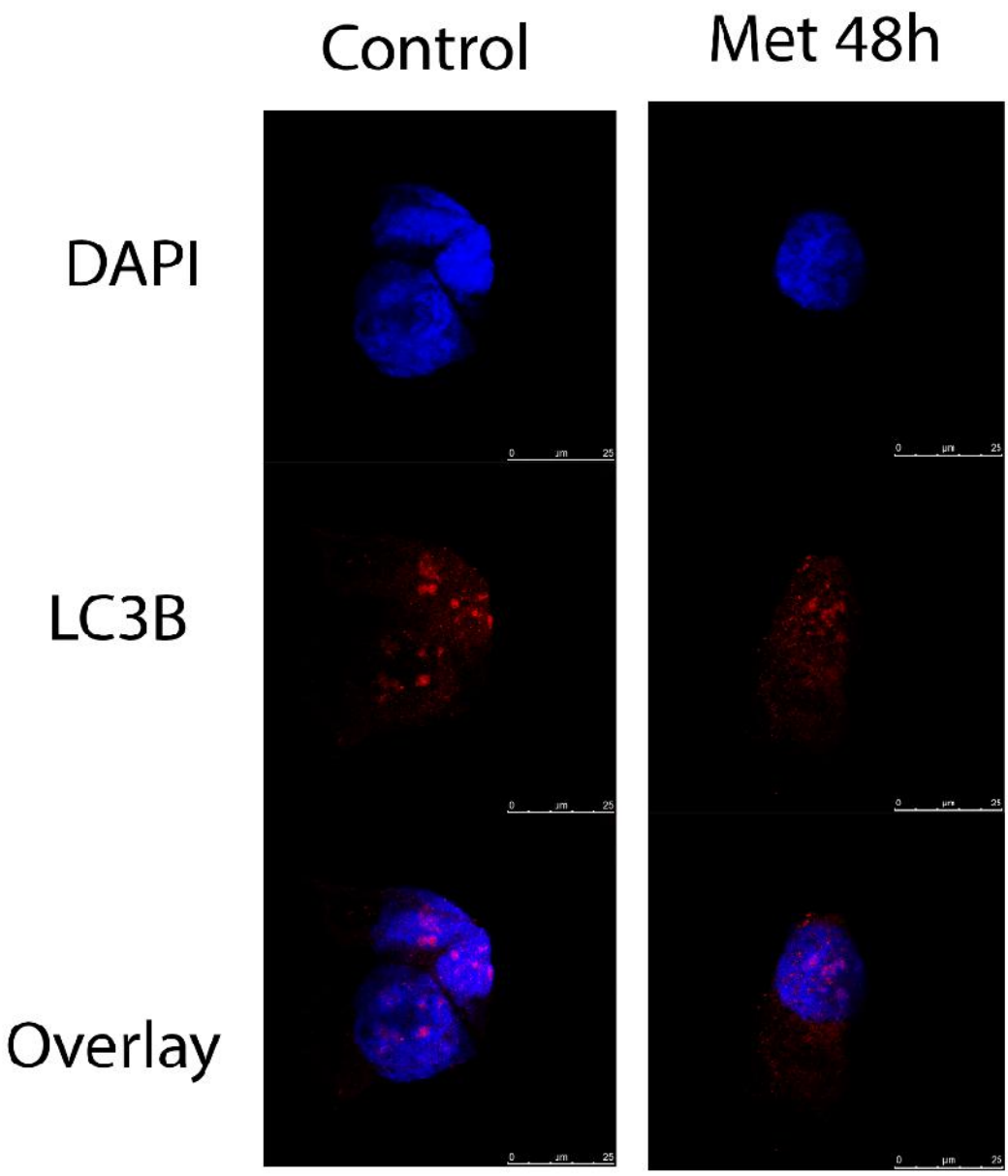

Figure 41: LC3B in H1299. Cells that are treated with chloroquine 25uM show and accumulation of LC3B in autolysosomes. Metformin 8mM presents no visual change after 48h of treatment.

4.4.1.2. LBH-589 and H1299

LBH produced no significant change in cell cycle nor did it increase cell death when used in therapeutic doses (50nM). However, the drug was able to stop cell growth in dose-dependent form. (Figure 42)

A)

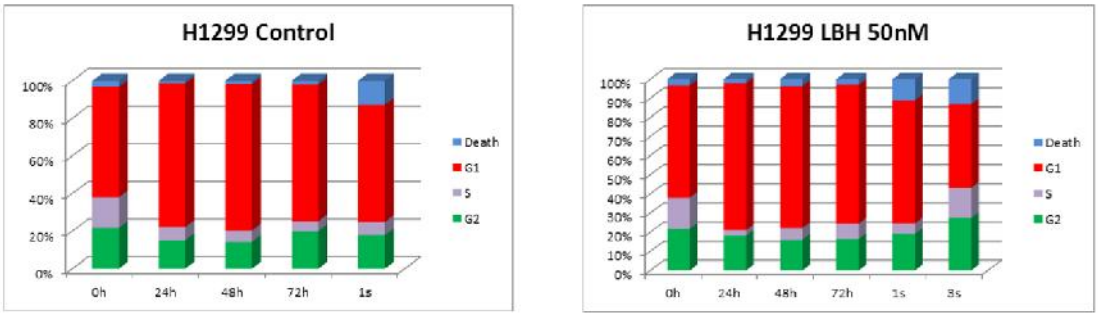

B)

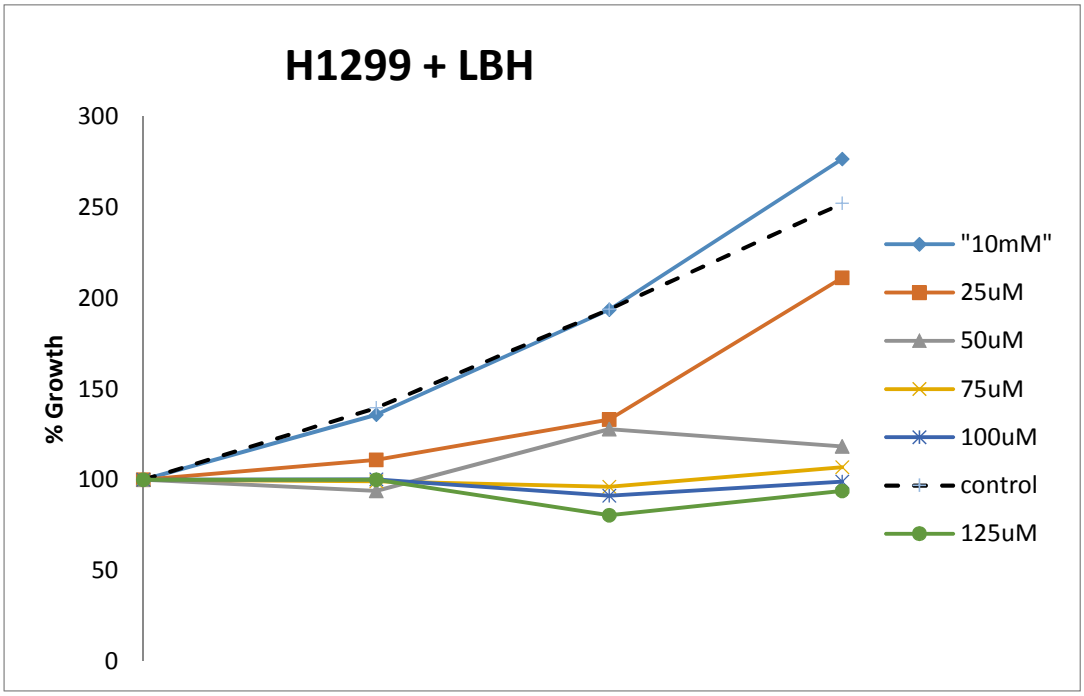

Figure 42: (A) No change in cell cycle compared to control, but an increase in G2/M phase at week 3. (B) LBH causes a dose-dependent decrease in cell growth, but no cell death.

mTOR levels increase the first 24h. After a long treatment with LBH (50nM), mTOR levels decrease starting 2nd week. The concentration of LC3B does not change. However, levels of p62/SQSTM1 decrease gradually starting from 24h with undetectable amounts at 4 weeks. Beclin1 rapidly losses detectable concentration after the first week. (Figure 43)

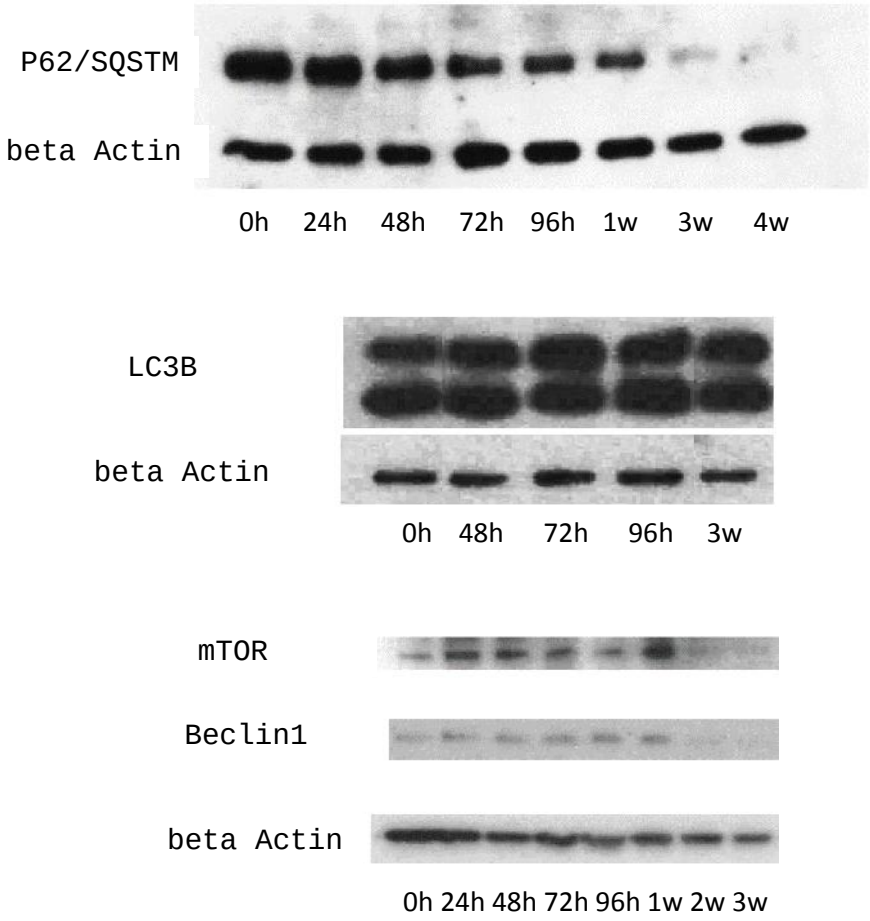

Figure 43: After long term treatment with LBH: a decrease in P62, mTOR and Beclin1 especially starting week 2. No change is detected in LC3B.

4.4.1.3.. Chloroquine and H1299

After one week of chloroquine treatment, cell death reaches 70% with therapeutic dose (25uM). The inhibitory effect of chloroquine is dose-related as it is observed in MTT study. (Figure 44)

Cells struggle to stay on the dish after one week of chloroquine treatment. In 3D cell culture, cells in the center of the spheroid dye rapidly causing and explosion after day 4. (Figure 45 and 46)

In normal 2D culture, cells treated with chloroquine and transferred to a new plat were not able to survive and adhere. Chloroquine affect their ability to adhere to the dish causing them to die eventually.

A)

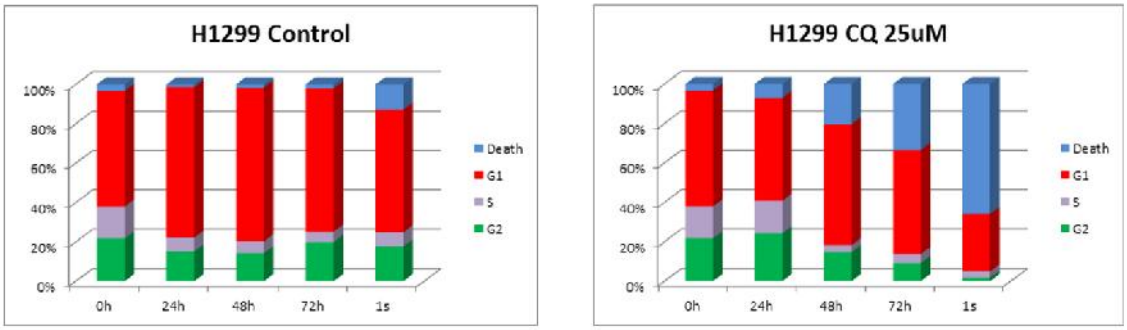

B)

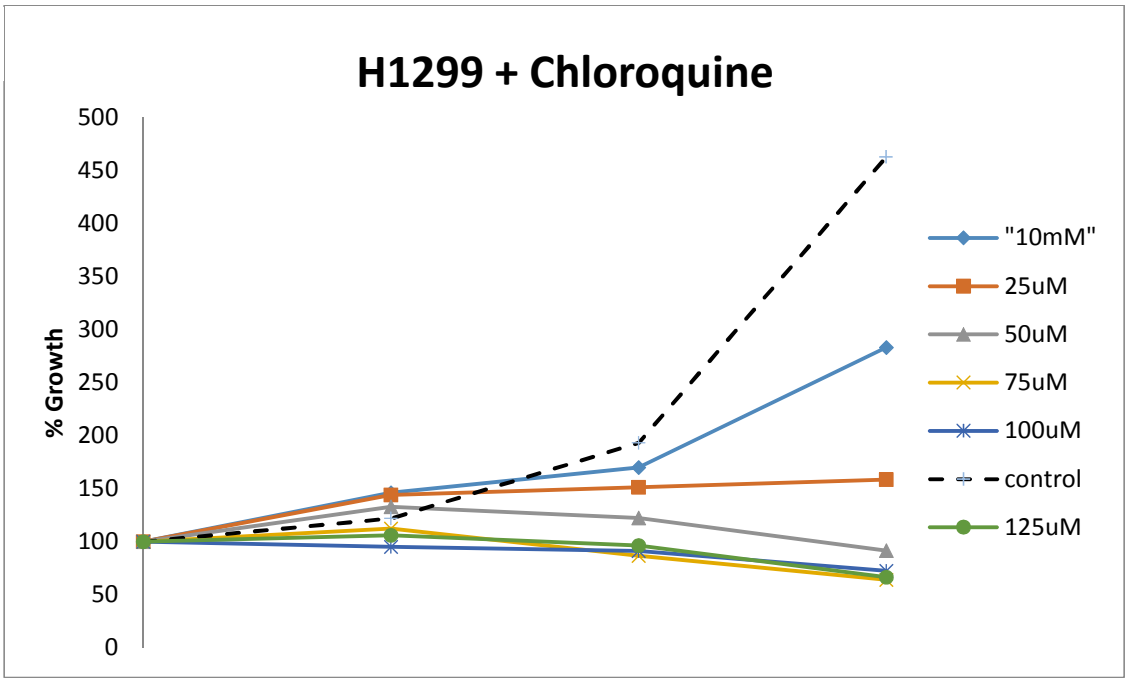

Figure 44: A) Cell death of H1299 when treated with chloroquine 25uM. The percentage of dead cells are 70% at day 7. (B) Cell growth are related to the dosage of chloroquine.

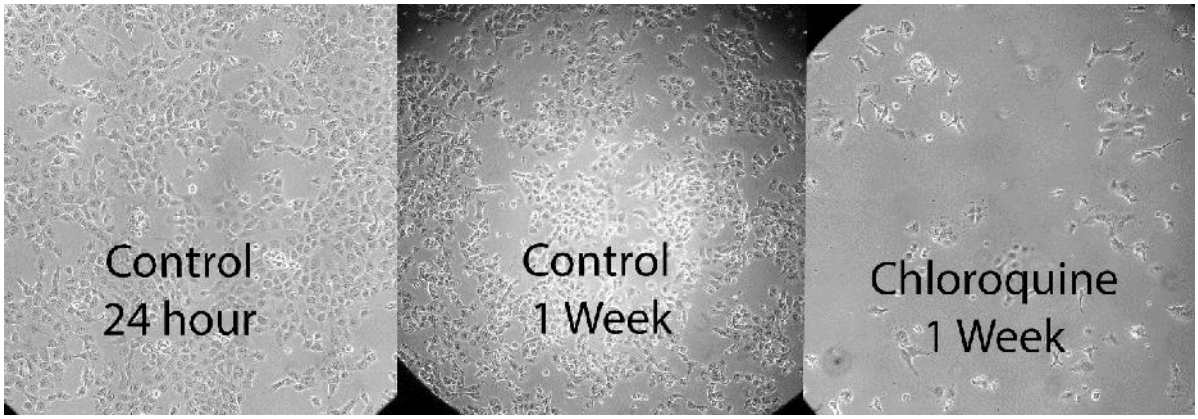

Figure 45: Cell death with chloroquine treatment 25uM for 1 week. A high cell death rate can be seen comparing to the control at 24h time and after a week.

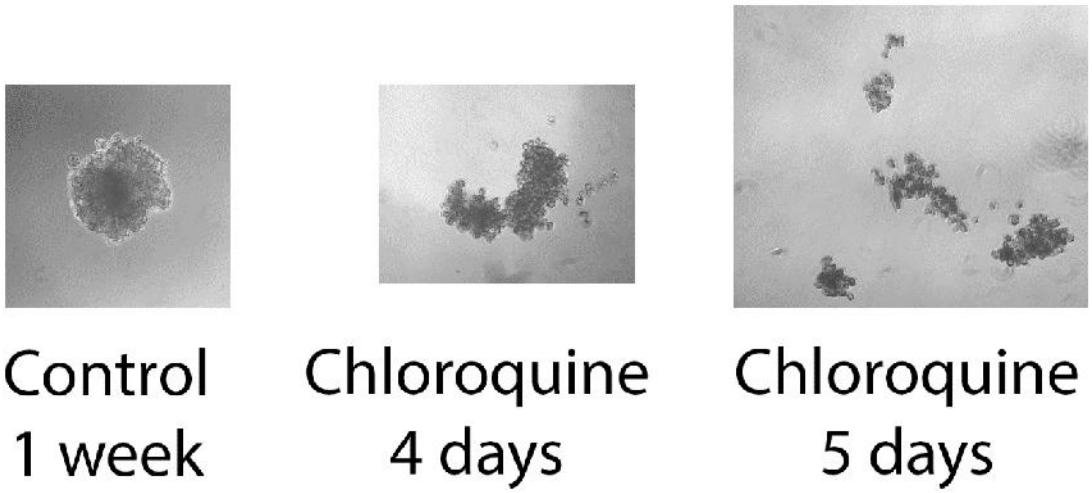

Figure 46: Using 3D cell culture, the spheroid explodes at day 4 and turns into uncoherent pieces at day 5. While control cells continue to form a spheroid after 1 week.

It has been reported that H1299 is one of the least sensitive cell-lines to 48hours chloroquine therapy (30uM) [109]. Long-term treatment with chloroquine for a week revealed a significant impact on those cells.

The effects of chloroquine causes a clear arrest in autophagy. Both p62 and LC3B increase, which indicates the stop at autophagosome level, which agrees with previously published results in other studies [110]. Beclin1 had no change in its levels. On the other hand, mTOR suffers a small decrease in expression probably due to a negative feedback. The levels of 18KD protein increases that could be isoform005.

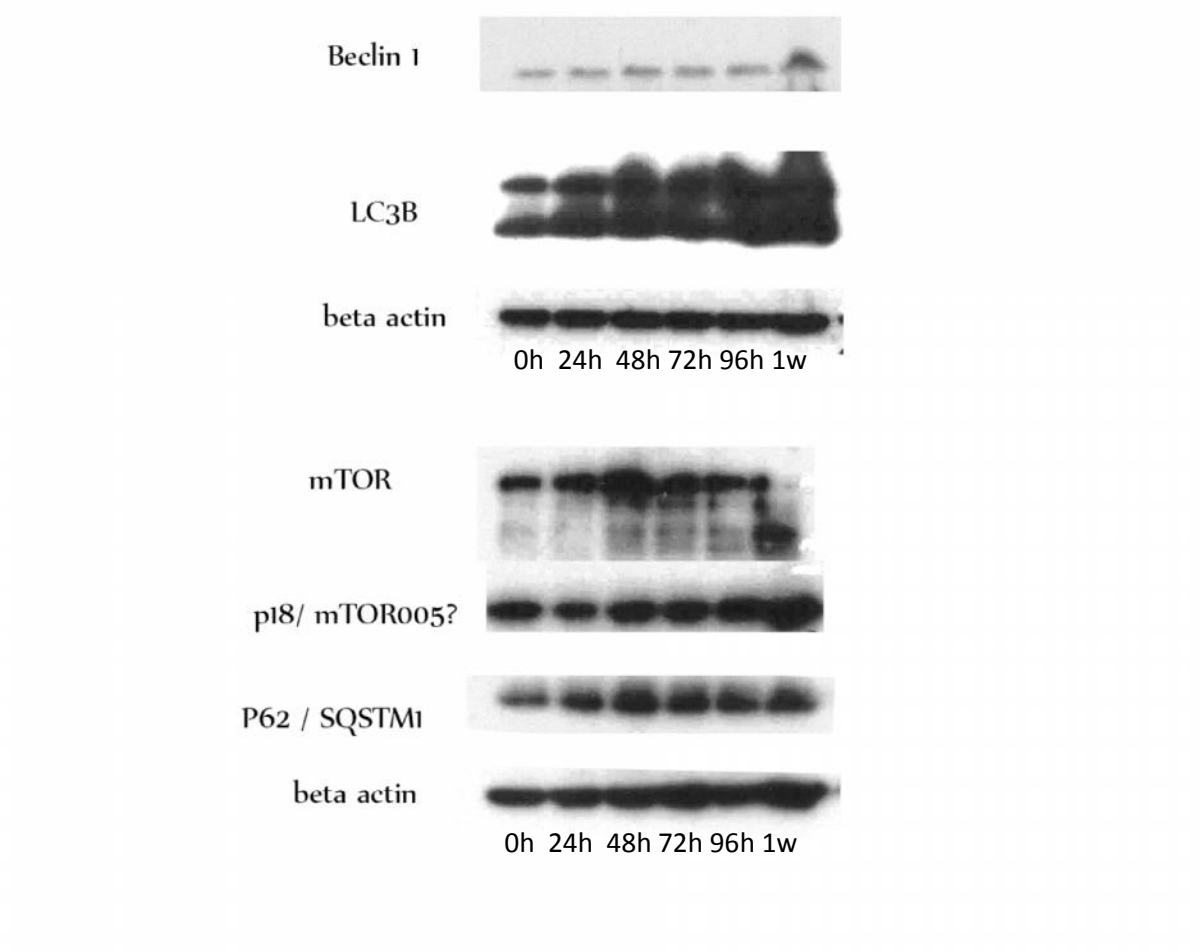

Figure 47: Chloroquine changes autophagy in H1299, Increased levels of LC3B and p62. Levels of Beclin1 is not changes, while mTOR increases for 48h then decreases.

We confirmed our previous results with immunofluorescence using confocal microscopy. We studied both p62/SQSTM1 and LC3B.

H1299 is affected severely with chloroquine treatment. Protein pattern showed an accumulation of pro-autophagy proteins P62 and LC3B in autolysosomes.

In control cells, p62 was evenly distributed in the cytoplasm. Chloroquine Caused P62 to accumulate in autolysosomes compared to control. (Figure 48)

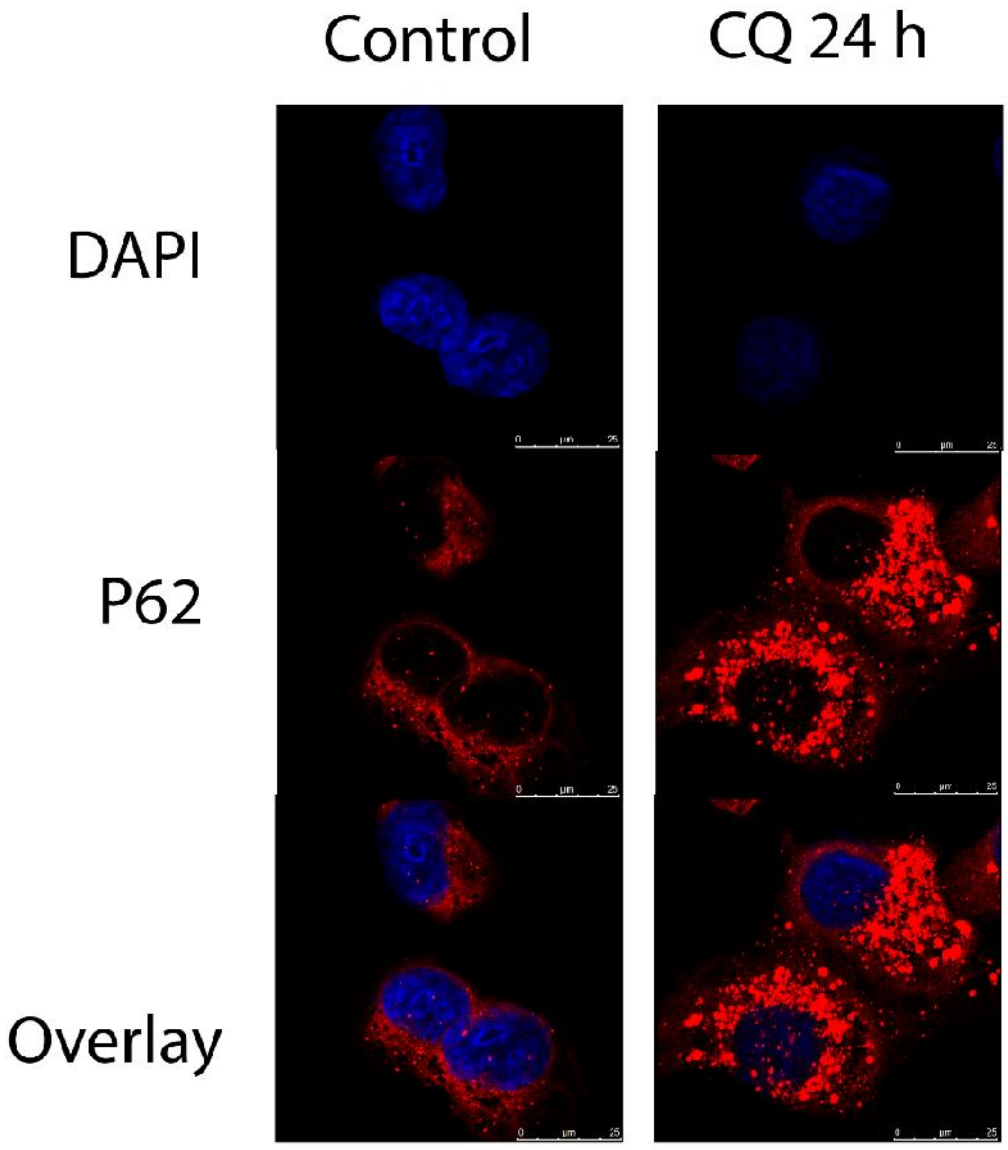

Figure 48: P62 in H1299 after 24 hours of treatment. With chloroquine, p62 accumulated in autolysosomes.

Untreated H1299 cells presented little if any LC3B. Chloroquine 25uM was caused LC3B to accumulate in autolysosomes after 48 hours of treatment. This correlates with Western-blot results as chloroquine is able to stop autophagy and produce protein change rapidly.

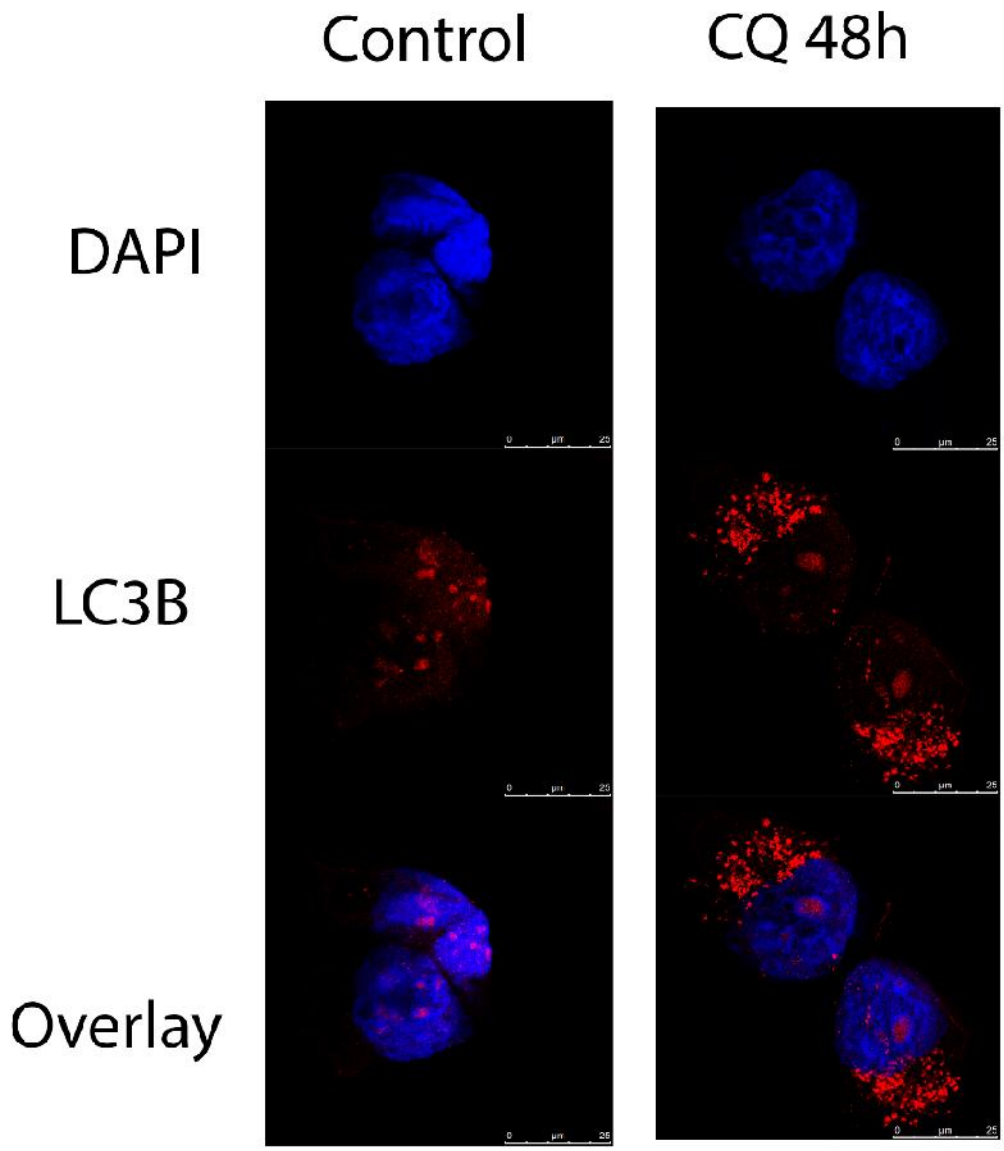

Figure 49: LC3B in H1299. Cells that are treated with chloroquine 25uM show and accumulation of LC3B in autolysosomes.

4.4.1.4. Combination of chloroquine and LBH

A combination of both chloroquine 25uM and LBH 50nM was used to evaluate its therapeutic effect. The treatment did not improve the chloroquine therapy. A combination of chloroquine and LBH was less effective in general compared to chloroquine alone. Cell death was lower than chloroquine therapy by itself, and no evidence were found of changes in cell cycle. (Figure 50)

A)

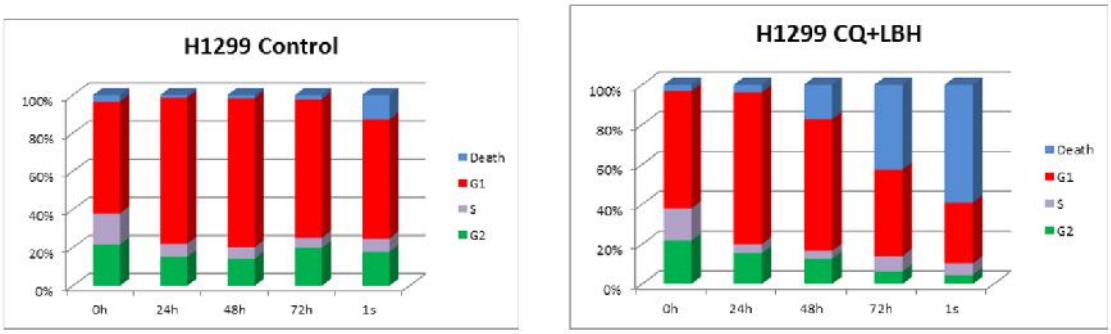

B)

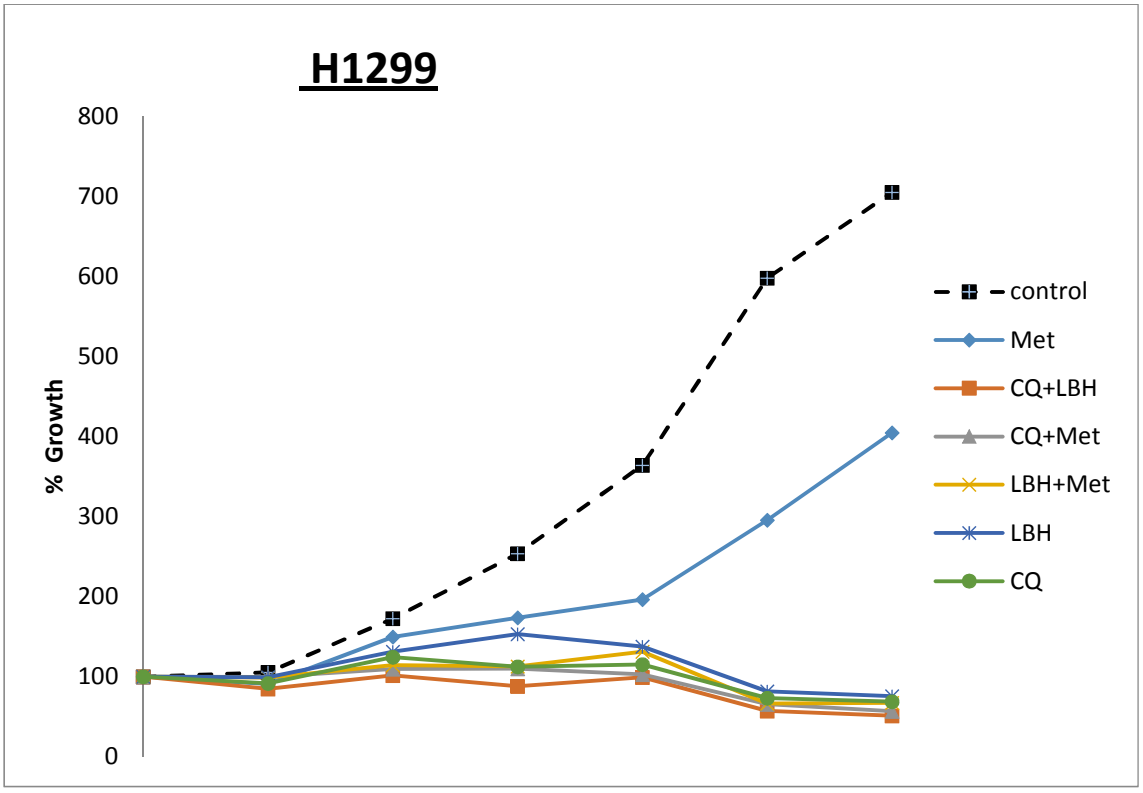

Figure 50: (A) Combination of chloroquine and LBH caused a cell death up to 65% after one week. (B) A comparison of cell growth, using MTT, shows no significant gain in combining CQ and LBH.

LC3B levels increase with combined therapy. P62/SQSTM1 did not change significantly. mTOR decreased rapidly, while Beclin1 stays consistent (similar to chloroquine).

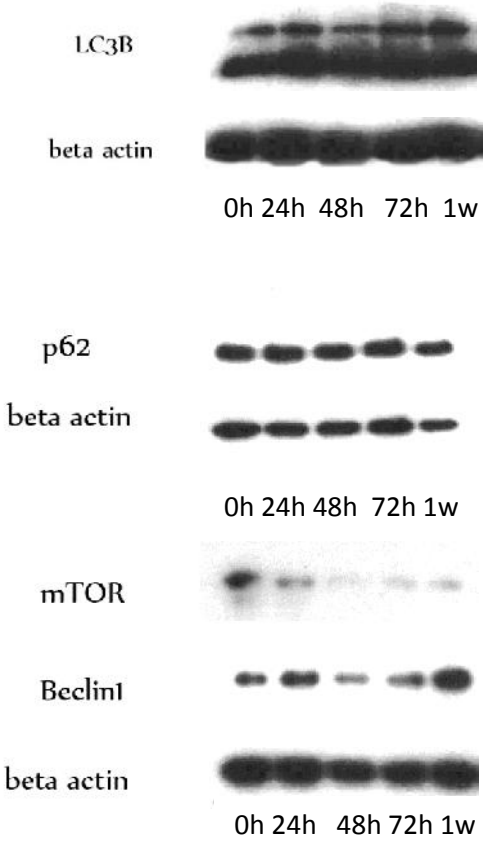

Figure 51: No significant change in p62, and a limit increase in LC3B. An important decrease in mTOR expression. Beclin1 levels are roughly without a change.

4.4.2. COR-L23 AND AUTOPHAGY-RELATED DRUGS

COR-L23p is a typical cell line derived from large cell lung cancer. Cell growth is relatively slow but constant. Treatment with LBH and metformin could not be continued beyond week 1, while with treatment chloroquine for more than 2 weeks presents no significant changes.

4.4.2.1. Metformin with COR-L23

Almost no change in cell cycle is detected in cells treated with metformin, nor was the death increased. With the highest concentrations of metformin, the cells were 50% slower in growth. (Figure 52)

A)

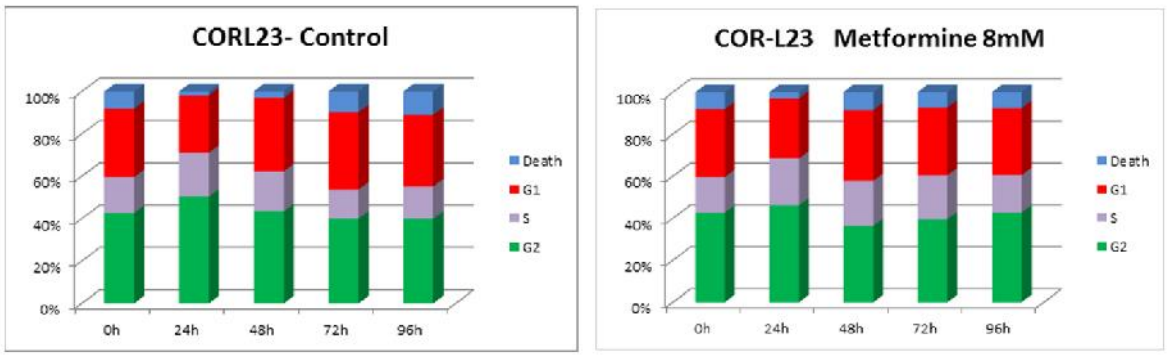

B)

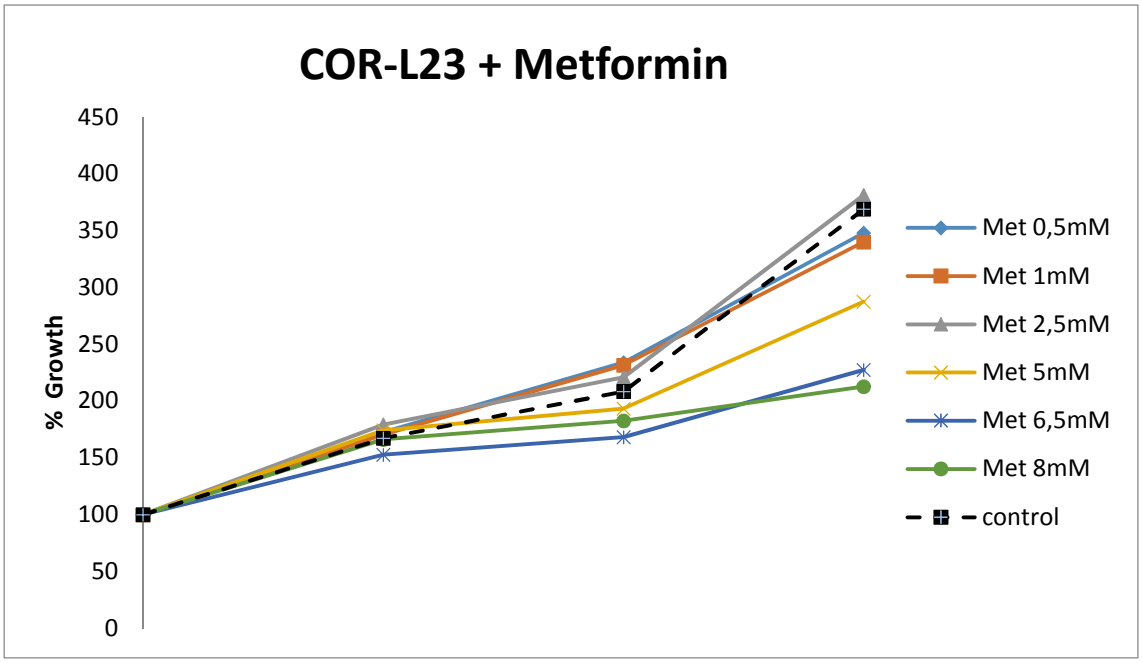

Figure 52: (A) Cell survivability did not change hugely with metformin. At 8mM dose, cell growth decreased 50% compared to the control. (B) No change in cell death and changes in cell cycle are too minute to report.

LC3B, mTOR and P62 were not detectable in the control, they increased briefly for 48h then returned to decrease. LC3B-II expressed high levels while LC3B-I decreased.

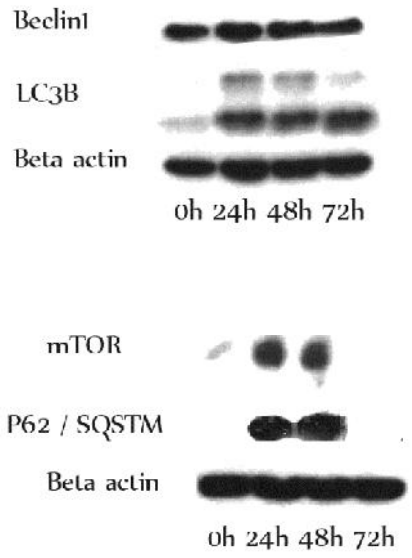

Figure 53: LC3B, P62 and mTOR are not detected normally in the cell line. A temporary increase in mTOR and P62 starting 24h of treatment with metformin, followed by a huge decrease. LC3B increased at 24-48h, but it LC3BI was decreased at 72h. Beclin1 did not suffer any change.

4.4.2.2. LBH treatment and COR-L23

LBH toxicity was dose related and it could kill up to 75% of cells after 48h using a therapeutic dose (50nM). Cell growth was negative (-50%) with the highest doses (125nM). (Figure 54-B)

Measuring cell death at 72h and 96h reveals that cellular death stops and decreases, but the percentage of phases of cell cycle had not sufered much of a change. (Figure 54-A)

A)

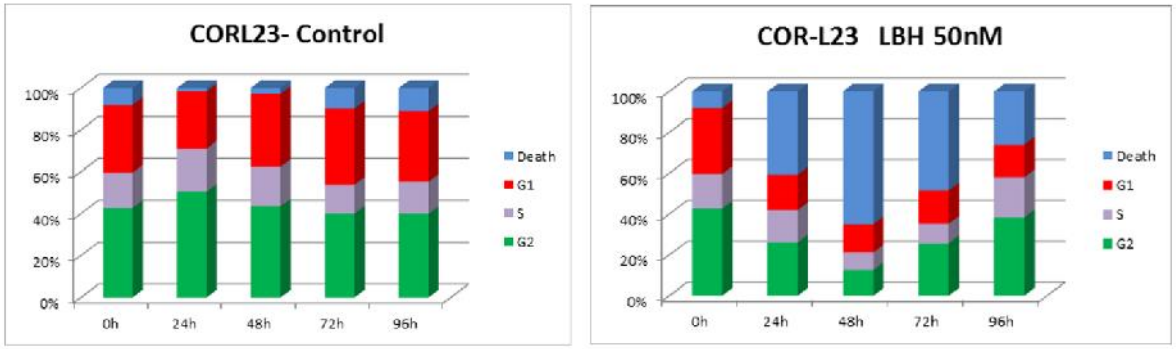

B)

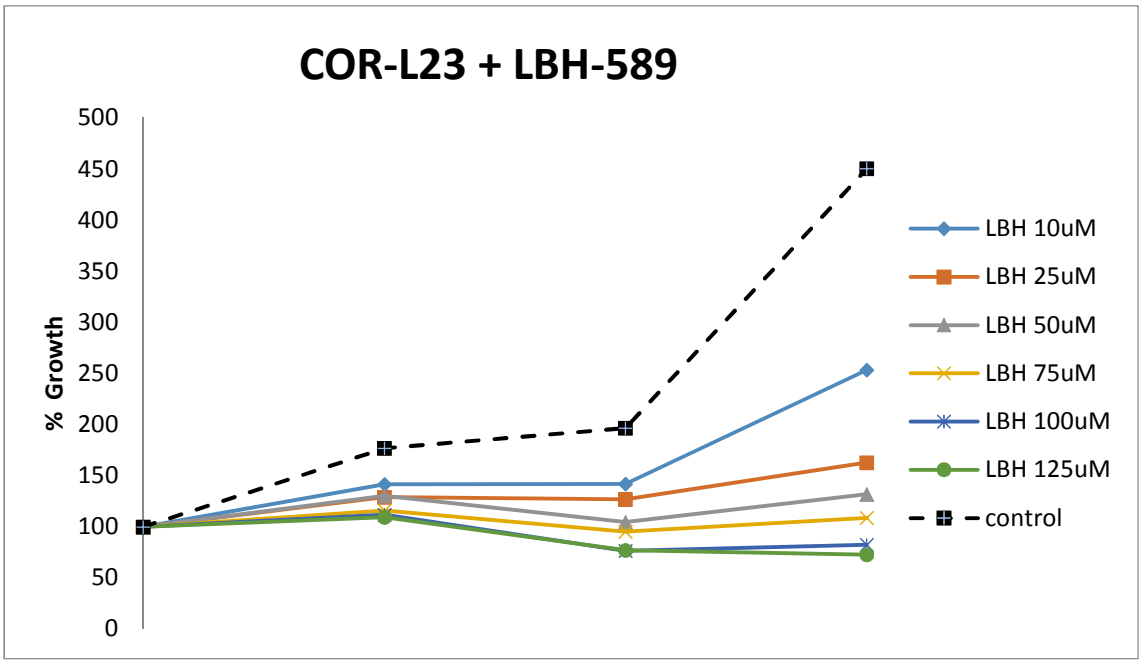

Figure 54: (A) a decrease in cell survivability related to dose. (B) At 50nM, cell death is high for the first 48 hours. The cells that survive continue dividing slowly, the G2 phase composes over 50% of life cells compared to less than 35% in control.

LBH effect on the proteins of autophagy (P62, LC3B and Beclin1) was limited to the first 24h, a slight increase was observed. Later, those proteins decreased. LBH had no detectable effect on mTOR.

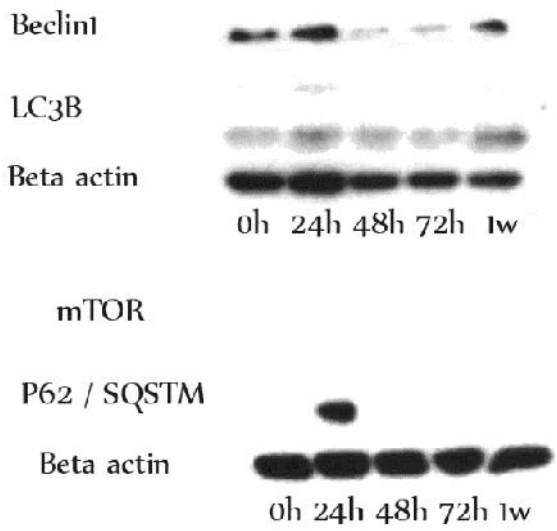

Figure 55: no change in mTOR is detected, a temporary increase at 24h in Beclin1, P62 and LC3B.

A compatible results can be observed with immunofluorescence assays. The control cells do not present P62/SQSTM1 in the untreated cells, while it showed a small increase and accumulation in autophagosomes after 24h of treatment. (Figure 56)

LC3B was present in small quantities in control cells, and its concentration seems to return to normal after 48h of the treatment. (Figure 57)

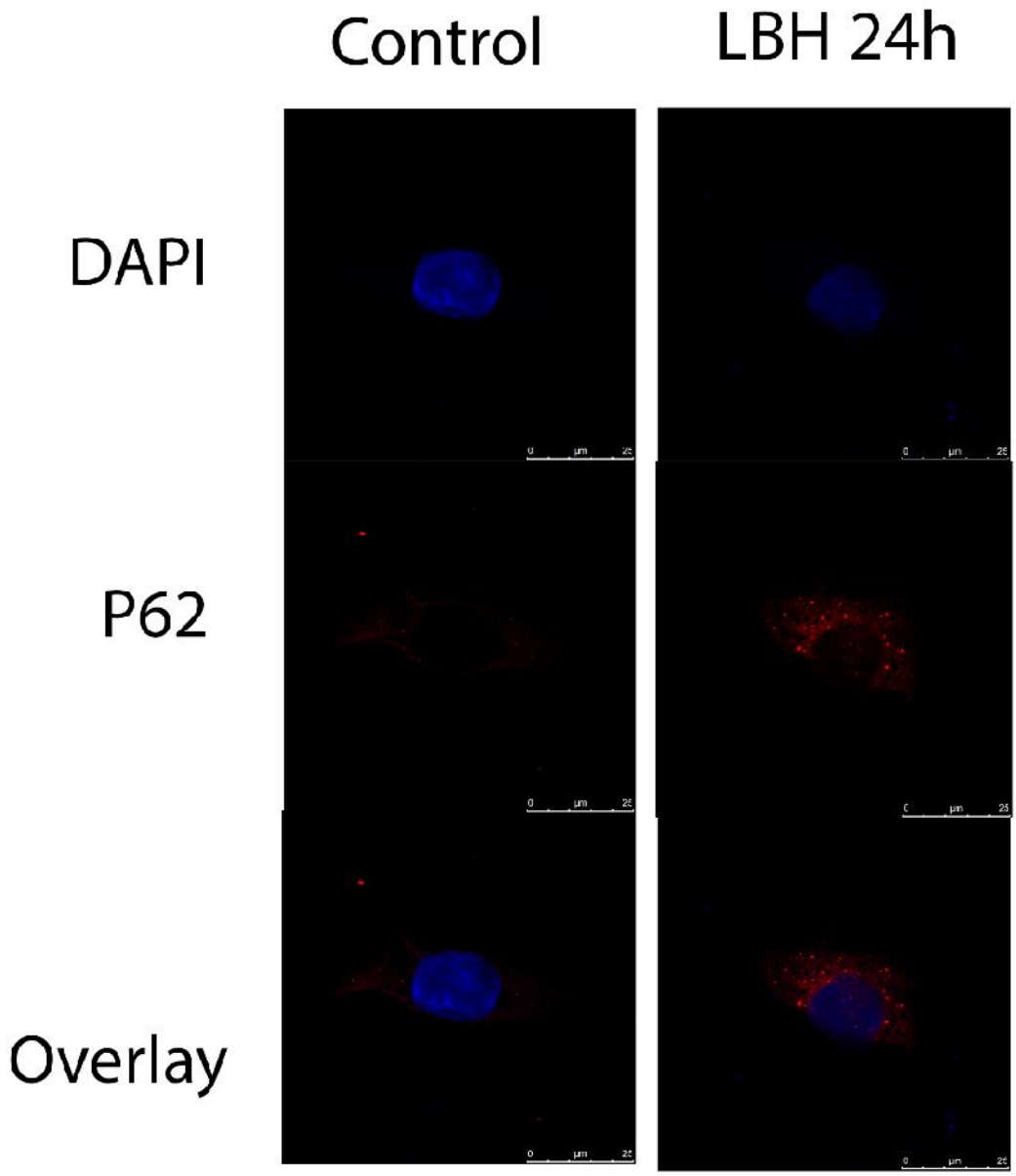

Figure 56: After 24h of treatment, a moderate increase with LBH.

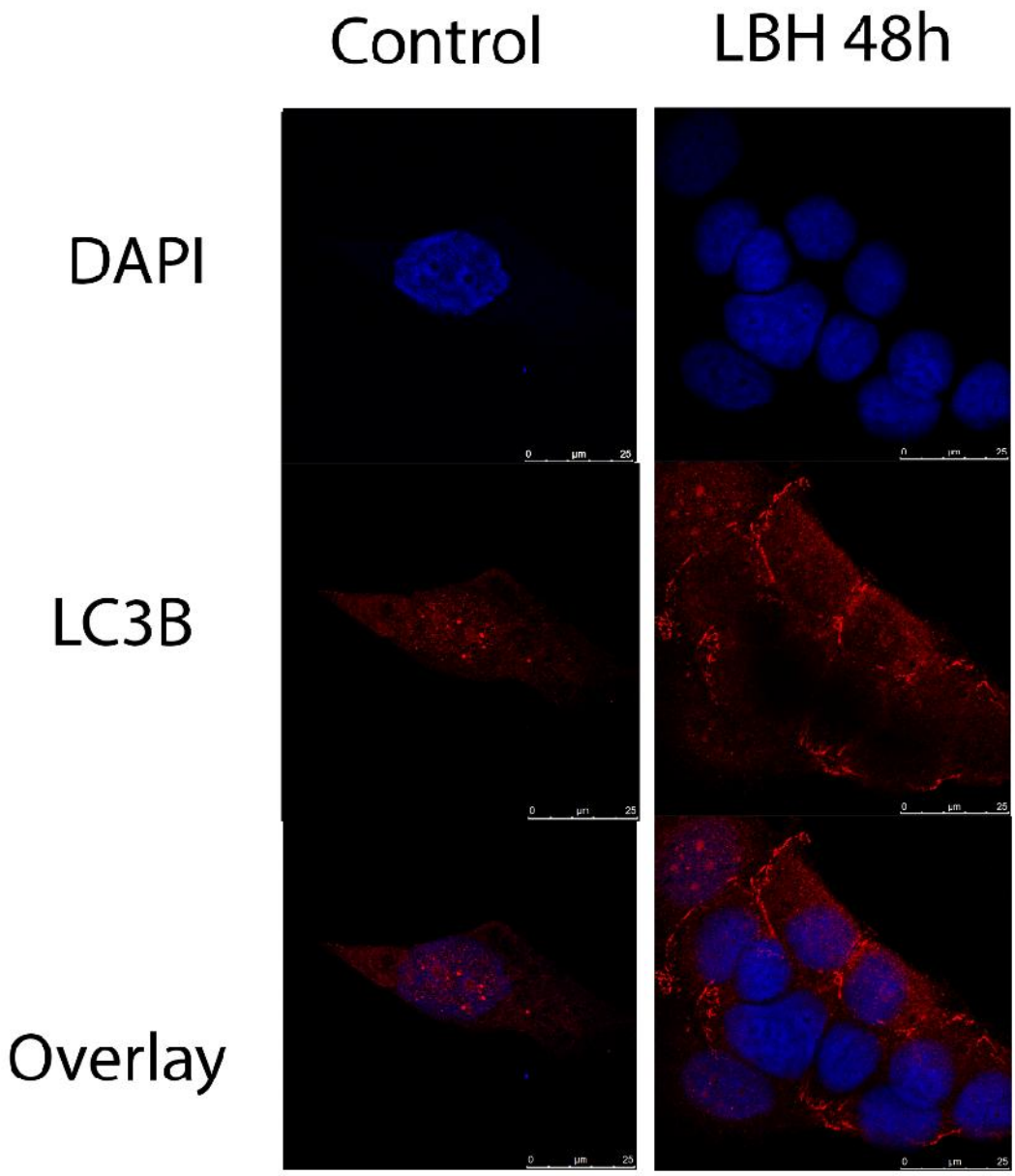

Figure 57: After 48h treatment, no detectable change in LC3B with LBH comparing to control.

4.4.2.3. Chloroquine and COR-L23

This cell line showed no cell death or change in cell-cycle. Cells continued to growth at fast rate, and continued the growth beyond two weeks. Cells treated with the highest concentrations of chloroquine had a decreased speed of growth down to 60% of the untreated cells after one week. (Figure 58)

A)

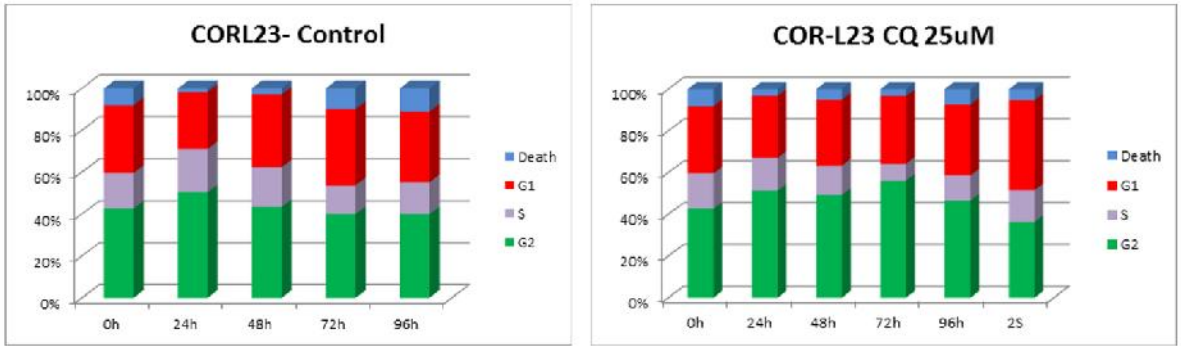

B)

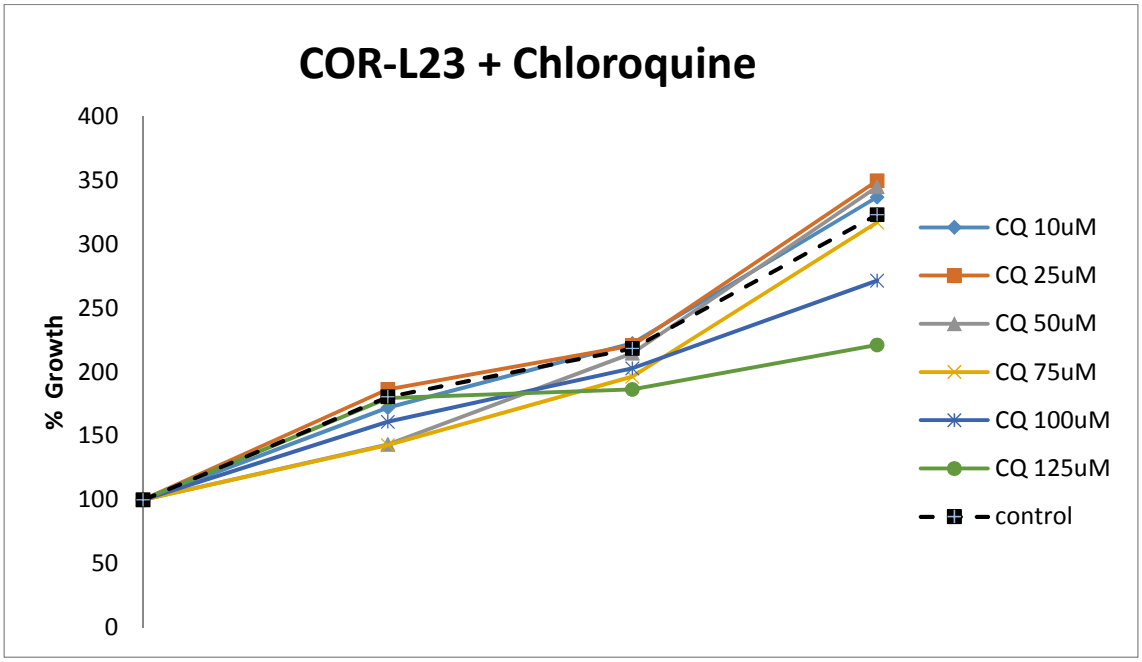

Figure 58: (B) Chloroquine barely changes cell growth. (A) No change detectable in cell life cycle at 25uM of chloroquine.

mTOR increases after 24h then decreases gradually. The same can be seen with Beclin1 and P62. LC3B increases continuesely till 72h, then LC3BI decreases starting week 1.

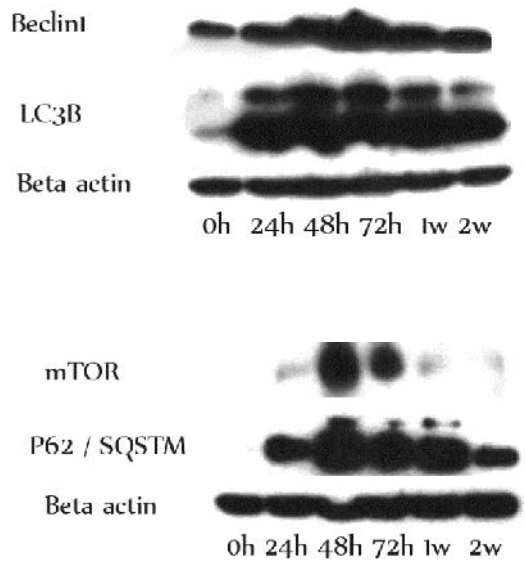

Figure 59: An increase in all autophagy proteins (mTOR, P62, LC3B and Beclin1) for 24h, then a steady decrease (except LC3BII).

Images from immunofluorescence show a high accumulation of P62 and LC3B in autolysosomes at 24h and 48h respectively of treatment with chloroquine. (Figure 60 and 61) This data correlated with the results obtained from Western-blot.

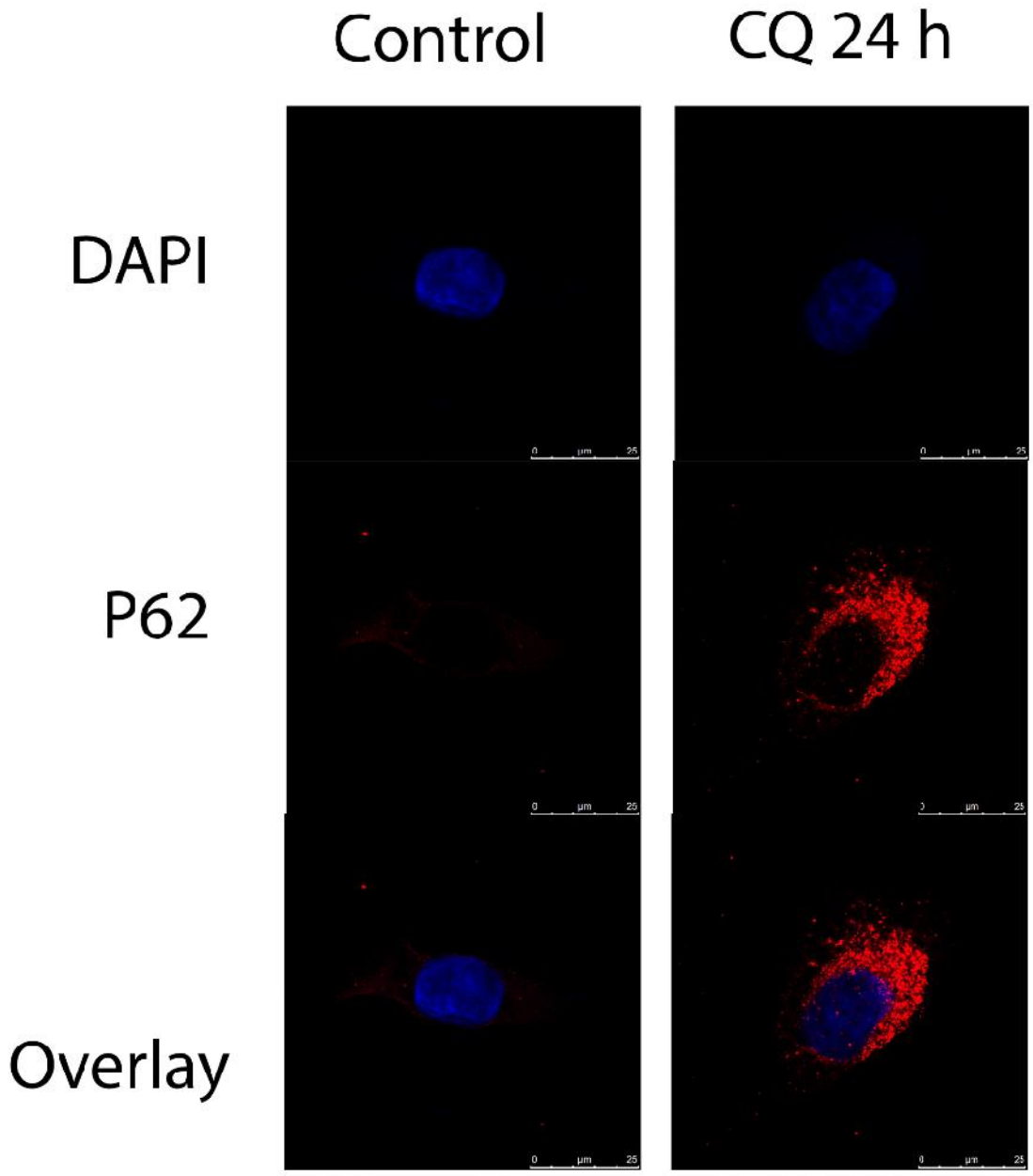

Figure 60: After 24h of treatment, high accumulation of P62 with chloroquine comparing to the control.

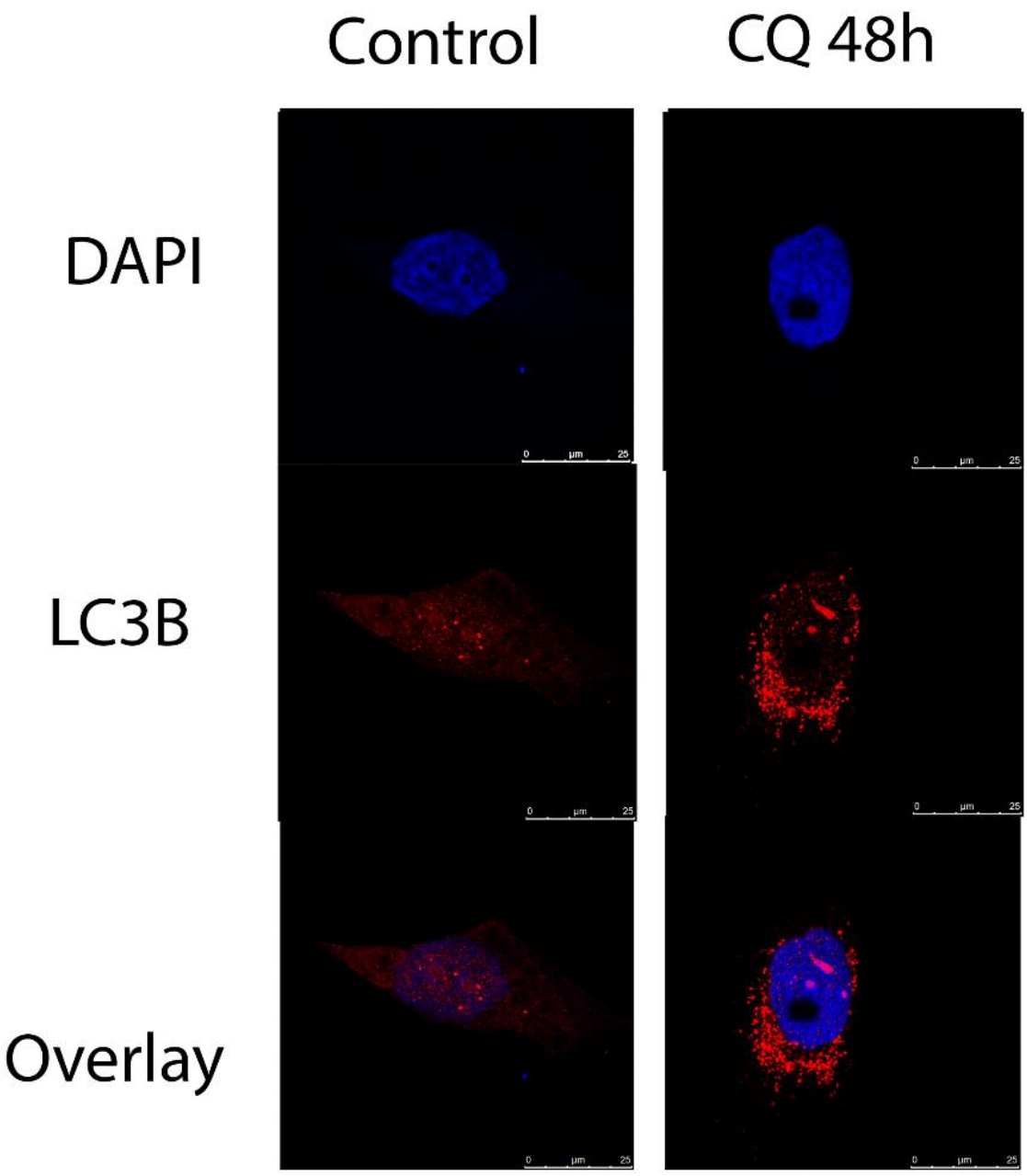

Figure 61: After 48h treatment, LC3B accumulation with chloroquine treatment.

4.4.2.4. Chloroquine and LBH treatment and COR-L23

Cell growth levels detected via MTT are similar to LBH treatment alone. Cell death reaches up to 75% of cell population. However, the peak of cell death is reached 24h later compared to LBH. No change in the percentages of cell cycle phases compared to untreated cells. (Figure 62)

A)

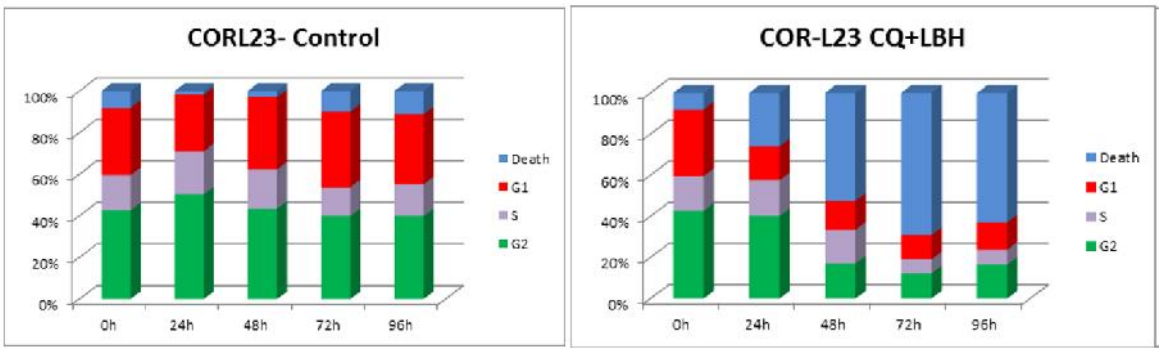

B)

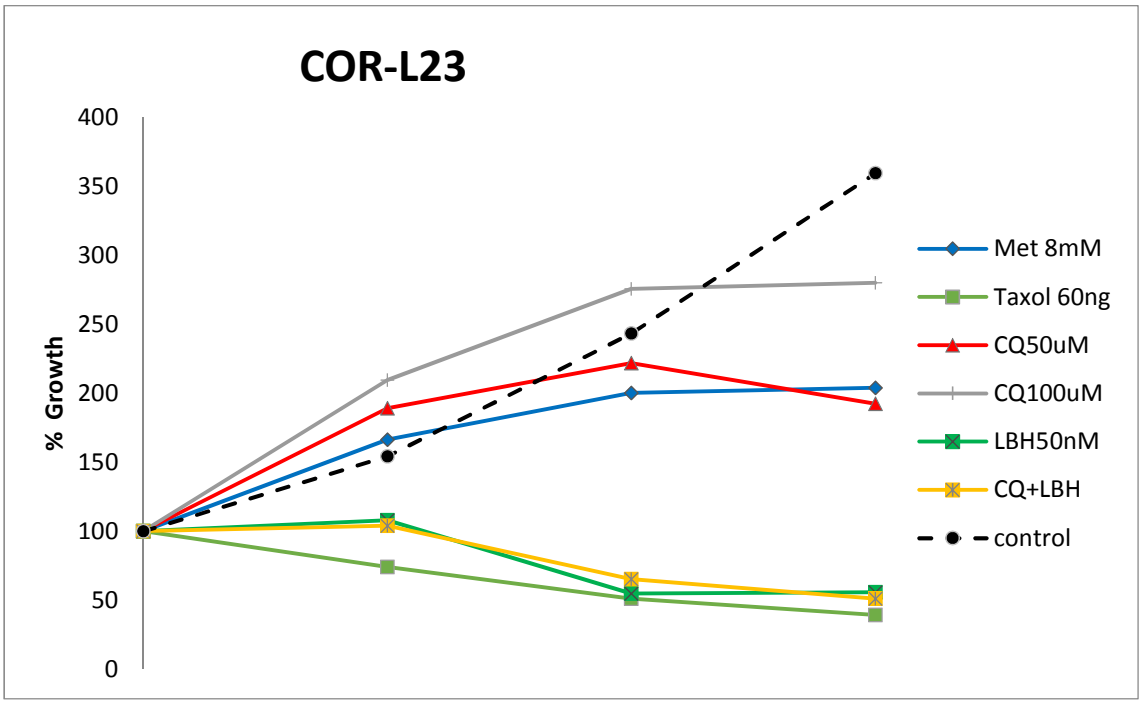

Figure 62: (A) COR-L23p compared with several compenations of treatment. Combining chloroquine and LBH do not provide any change comparing to using LBH individually. (B) cell death in combination of chloroquine and LBH is a little slower than LBH alone. Yet the same level of lethality and reverse growth is seen.

A decrease in Beclin1 levels is observed in combination of chloroquine with LBH treatment. Levels of P62 increases breifly then decreases after 48h. Levels of both LC3B I&II increases in the first 24h then a steady decrease in LC3B-I is detected. Levels of mTOR was not detectable. (Figure 63)

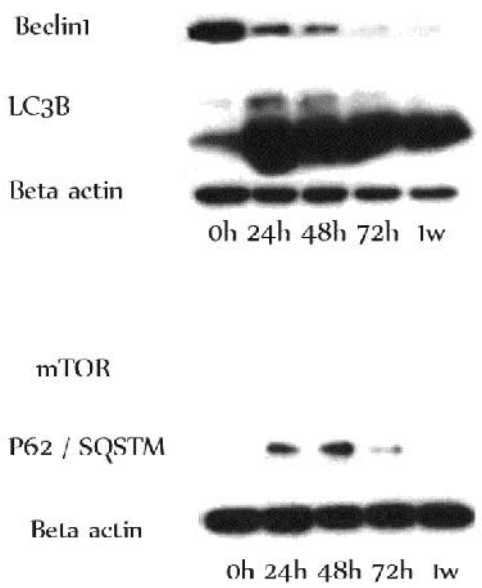

Figure 63: An increase in LC3B and P62 in the first 24h, followed by a gradual decrease in P62 and LC3B-I. Beclin1 decreases with the treatment. mTOR levels are not detectable.

5. DISCUSSION

5.1. GENOTYPING

Lung cancer can be produced by a variety of mechanisms. It has been suggested that alterations in autophagy may play a role in disease development, especially as autophagy is responsible for eliminating damaged proteins due to smoking, radiation and reactive oxidative stress [41, 111].

We have evaluated the relationship between lung cancer and four autophagy-related SNPs. Three of the SNPs were missense changes: ATG2B (rs3759601), ATG10 (rs1864183) and ATG16L1 (rs2241880), the fourth ATG5 (rs2245214) was an intronic mutation. No previous studies were published about lung cancer and those SNPs. Our study found an association between lung cancer and ATG16L1 (rs2241880) SNP.

Other studies had revealed a correlation of the minor allele of ATG2B (rs3759601) with progression and recurrence of bladder cancer after BCG intravesical instillation therapy [112].

ATG5 (rs2245214) has been associated with higher probability to develop thyroid carcinoma [113], and that G allele has been associated with an increased risk of developing Paget disease of bone [114].

Allele T of ATG10 (rs1864183) has been associated with a decreased risk of suffering Paget disease of bone [114]. A recent study showed that ATG10 (rs1864183) was associated with an elevated ATG10 mRNA expression and poor lung cancer survival. The change in mRNA expression might be due to ATG10 (rs1864183) is located at the region containing enhancer histone marks and possible motifs that alter transcription factor binding (GR, DMRT1 and Myc) [115].

With these results, we can reject the alternative hypothesis for ATG2B (rs3759601), ATG5 (rs2245214) and ATG10 (rs1864183), and accept the null hypothesis. We conclude that previously mentioned polymorphisms in genes of autophagy have no relation with lung cancer predisposition.

Recent studies have shown that patients with the minor allele G of ATG16L1 (rs2241880) had lower likelihood of bacterial sepsis [116]. Also allele G has been associated with a minor risk to develop pericarditis [117]. The ATG16L1 gene variants rs2241880 has been strongly associated with susceptibility to Crohn's disease [49], and it is associated with an increased risk of developing Paget disease of bone [114]. But it was found to protect patients from Buruli ulcer [118].

Thus, for ATG16L1 (rs2241880) we accept H_{a2} hypothesis OR=0.584 (0.345-0.990). Genotype GG of ATG16L1 (rs2241880) protect from lung cancer. Furthermore, we accept the null hypothesis for ATG16L1 (rs2241880) in NSCLC and in COPD patients. We conclude that this polymorphism has no statistically significant relation with non-small cell lung cancer subtype or lung cancer in COPD patients.

Finally, we accept H_{a2} hypothesis for ATG16L1 (rs2241880) and conclude a relation with lung cancer in patients without COPD. The GG genotype is a protection factor against lung cancer in patients without COPD (OR=0.534: 0.292-0.975).

The mechanism of protection against lung cancer is not clear. ATG16L1 (rs2241880) correlates with lower autophagy levels due to enhanced degradation via Caspase3 [53] reduced engagement with WDD-binding molecules needed for ATG16L1 function [54].

The pathological role of this SNP in other diseases could be explained by a decreased immune activation [119] and increased inflammation due to high levels of IL-1β [120]. On the contrary, this SNP have a protective role in our study.

Elevated autophagy levels are common in many types of cancers [121, 122, 123]. Both patients and healthy individuals studied here were smokers. Studies have shown that autophagy might promote tumor cell survival especially in conditions of hypoxia [124]. Smoking could be the key to explain why a decreased autophagy via allele G of rs2241880 have a protective role. The conditions of high toxin levels and hypoxia make development of lung cancer cells dependent on autophagy in smokers.

5.2. UPSTREAM AUG REGULATES GENE EXPRESSION

The sequence of the genome affect protein expression and this is restricted not only to the coding sequence (CDS) but also to introns, promoters, enhancers and inhibitors. In our study, we focused on sequences located in the 5'UTR.

I has been reported that the existence of "AUG" upstream the start codon (also called uAUG) decrease protein expression. uAUG creates upstream open reading frame (uORF) which competes with the original ORF thus inhibiting protein expression. It also explains why other alternative start codon sequences (i.e. "CUG") have an inhibitory effect [125].

Several studies have reported cases of hereditary diseases due to *de novo* uAUG. Hereditary thrombocythaemia due to "uAUG" at -31bp in THPO gene [62], hereditary hemorrhagic telangiectasia in ENG at -9bp and -127bp [63], severe hemochromatosis at -14bp in HAMP gene [64], osteogenesis imperfecta at -14bp in *IFITM5* gene [65], familial melanoma at -34bp in $p16^{INK4a}$ caused cases of [126], and probably much more cases to come.

Less than 10% of eukaryotic mRNAs contain AUG codons within their 5'UTR, but this percentage is much higher in certain classes of genes such as oncogenes and genes that control cellular growth and differentiation (up to 75%) [127]. Our bioinformatic study revealed that uAUG in transcriptome exist 66% less than expected in random sequences. This difference is related to distance from start codon.

In autophagy, many genes had no uAUG such as mTOR, ULK1, P62/SQSTM1, ATG7, ATG10, ATG16L2 and ATG2A. While most of genes had one uAUG at various distance from start codon: ATG13 has a single uAUG at -50bp, ATG101 at -118bp, Beclin1 at -93bp, ATG5 at -23bp, ATG12 at -140bp, ATG16L1 at -66bp, ATG2B at -150bp, ATG3 at -98bp, ATG4A at -11bp and ATG4B at -151bp. The only main gene with multiple uAUG LC3B at -193bp,-286bp,-496bp and -513bp [128].

Recruiting ribosomal small unit to 5'UTR is coordinated by eukaryotic initiation factors (eIFs) called eIF4F. It is compose of eIF4G (interaction between ribosomal small unit and other proteins), eIF4E (recognizes 5'UTR cap), eIF4A (inhibits secondary mRNA structure) and PABP (Binding poly A tail to eIF4B/ G). Ternary complex (eIF2, GTP and methionyl-tRNA) is recruited. The ribosome with these factors scan mRNA till reaching "AUG" sequence, then M-tRNA is uncoupled from GTP and translation begins (Figure 64) [129].

In normal conditions, uAUGs significantly decrease protein expression, and this decrease correlates with the number of uAUG [60]. However, in stress conditions the presence of uAUG can promote the increased expression of certain stress-related mRNAs [129]. Studies reported that mTORC1 is involved in this process. Hypophosphorylated 4E-BP binds tightly to eIF4E, thereby preventing its interaction with eIF4G and thus inhibiting translation (Figure 64), and mTORC1 is responsible of phosphorylating 4E-BP, and allowing translation process to start.

Following nutrient depletion, mTORC1 is inhibited which causes a general inhibition of translation initiation and elongation. [130]

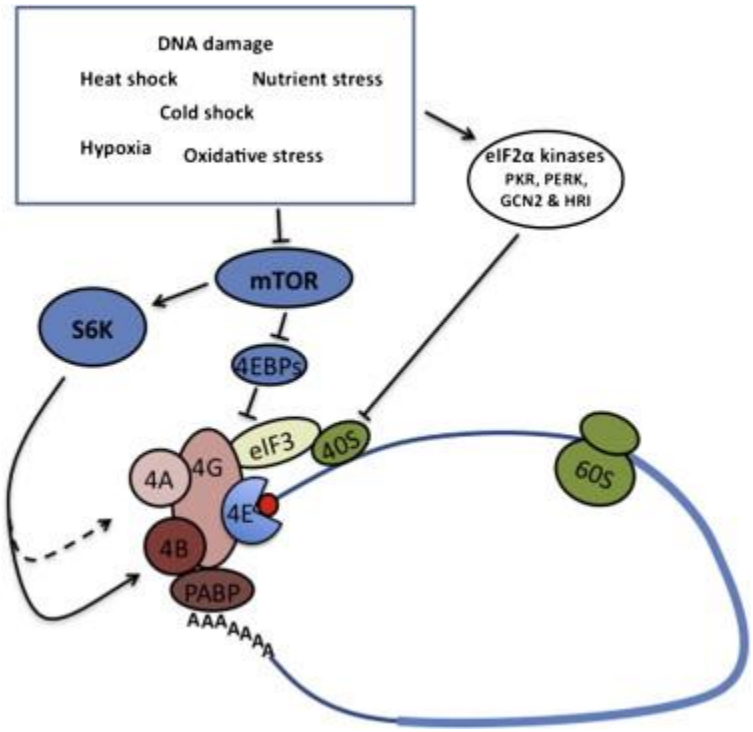

Figure 64: eIF4F complex initiating translation via forming a circular mRNA and binding the small ribosomal unit. mTOR helps initiating translation by phosphorylating the inhibitor protein 4E-BP and the activator protein S6K.

Attached ribosomes to uAUG might face different fates depending on the uAUG and sequence context; the ribosome could continue scanning and reinitiate downstream with high efficiency, such uAUG do not affect gene expression. Another possibility is that ribosomes stall creating a blockade to additional ribosome scanning [127]. Any inhibitory effect of gene expression will decrease with distance. The hypothesis of our work comes from here.

As secondary mRNA structure and folding is considered an important factor in protein expression, we tried to avoid big changes in the sequence. And we checked for the minimum free energy of mRNA to verify that it is not involved (Table 6).

Our study focused on the distance from start codon. Our results indicate clearly that uAUG distance from start codon is an effective single factor in controlling protein expression.

uAUG-5 and uAUG-38 have the same stop codon (+19bp in CDS), uAUG-15 is in-frame and uAUG-25 faces a stop codon after 9bp in 5'UTR. Protein expression was uniformly related to

distance form start codon, so we can deduce that regardless of differences in ORFs distances produce relatively constant effect upon protein expression and ORFs seem to be secondary.

uAUG-38 is a change from the non-AUG alternative initiation codon “CUG”. Non-AUG alternative codons are supposed to suppress protein expression and deleting them enhances the expression which could explain that effect is similar to 25uAUG. [125, 131]

We have noticed that the mutation at -127bp in the ENG gene was more potent than the one at -9bp [63], contradicting with our results. Nevertheless, this could be due to interference with some promoter or enhancer in that region, and our experiments were designed to avoid this possibility.

Many bioinformatic and biological studies reported that two uAUGs have an increased inhibitory effect compared to a single uAUG [56, 61, 55]. Our results confirm that the nearest uAUG do not mask the inhibitory effect of further uAUG. Multiple uAUGs are superior to the distance factor in their inhibitory effect.

These results suggest that mutations in the promotor region of tumor repressor genes that generate uAUG could decrease their expression and could be involved in tumor development, among others in lung cancer.

5.3. DIFFERENTIAL mRNA ISOFORM PATTERNS IN COPD AND LUNG CANCER

New generation sequencing (NGS) is highly computationally demanding technology. Dealing with its data is not usual among biologists although many attempts were made to facilitate the process. In RNA-Seq, the main obstacle seems to be the high error rate in discovering and quantifying new transcripts. The wholistic approach gives a better view of the process and presents a good picture of what interactions happen in cells. We studied the whole biological pathways of autophagy and apoptosis and used *t*-test on each gene and isoform.

Studies have shown that there are general changes in gene expression and isoform pattern in these pathways in diseases such as cancer and COPD [132] and in subjects with risk factors such as smoking [66]. Isoform changes in serum have been suggested to be biomarkers for cancer [133].

We hypothesize that a single isoform change may be involved in activating/blocking a pathway, and that change could be the key for the pathological effects. To prove that, we have studied isoform changes that affects those pathways.

As a result of our analysis the most relevant change in autophagy is in mTOR isoforms in both NSCLC and COPD patients. mTOR is a kinase that has two main isoforms (mTOR001: ENST00000361445, mTOR002: ENST00000376838) [128]. The longest (mTOR001) is responsible for the expression of the active form of mTOR (UniProt: P42345). The shorter isoform lacks the majority of HEAT regions that are responsible of interacting with RAPTOR, an essential activator of mTOR. In theory, MTOR002 is not as active kinase as the main isoform, it may even suppress MTOR001.

Bioinformatics analysis reinforce the suppressive nature of MTOR002. An increase in MTOR002 is correlated with an over-expression of downstream autophagy genes (i.e. lung cancer) (Figure 65). A decrease in MTOR002 leads to active suppression of autophagy gene (i.e. COPD) (Figure 66). In both cases, changes in AMPK and other proteins upstream mTOR do not correlate with the status of mRNA expression downstream mTOR.

MTOR002 isoform dominates autophagy pathway in both non-small lung cancer and COPD, thus we suspect that it could be a key isoform in this pathway.

In COPD lung tissue samples, Caspase3-S (005: ENST00000393588) was present in 11 samples (41%). This splicing variant causes a decrease in apoptosis during chemotherapy [103]. Caspase3-005 was not present in any control sample. This suggests that Caspase3-005 isoform is a possible inhibitor of apoptosis in lung tissue of COPD patients (but not in airway basal cells), which could be a mechanism of defense against elevated apoptosis.

On the other hand, , an increase in Caspase10-003 isoform (ENST00000346817) and a decrease in Caspase10-001 (ENST00000286186) are detected in cancer patients, and apoptosis is inhibited downstream. Caspase10-003 (Caspase10B) is reported to have pro-apoptotic effects [134], it could be worth to investigate this isoforms in the wet-lab.

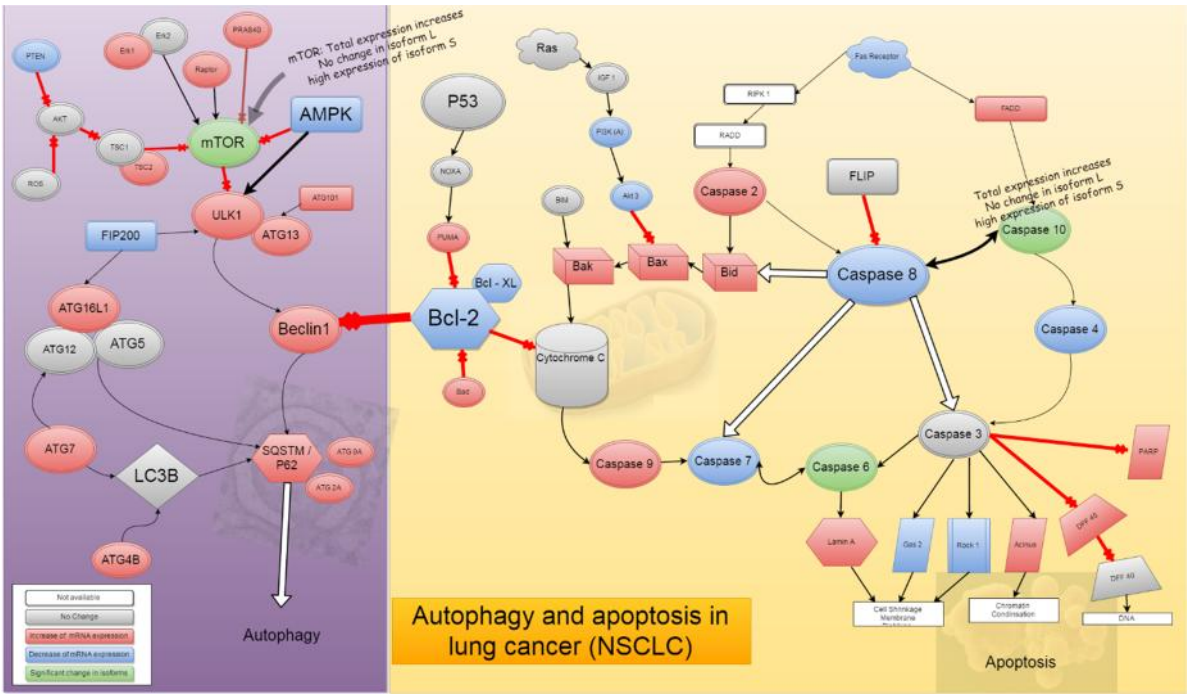

Figure 65: Autophagy and apoptosis in cancer. (Left) mTOR gene expression is increased, but no inhibitory effect on autophagy where most genes are over-expressed. MOTR002 is elevated and probably interfering in inhibition of autophagy. (Right) A change in isoform expression in Caspase10 is correlated with a decrease in Caspase4, 7 and 8. A possible effect of an inhibitory isoform.

Isoform changes should be more carefully studied and observed. With NGS data, total gene expression and isoform expression is not error-free procedure as the algorithms used today fail to conclude biologically useful results. A lot of functional biology need to be applied before going to the wet-lab with NGS summary. However, NGS is way much cheaper and wholistic approach to disease analysis than individual analysis.

Isoform changes occur in key points on the pathways, thus they could be involved in the pathology of the diseases. If such key changes can be identified in other pathways, a panel of isoforms can be designed and used as possible biomarkers (if they can be detected in serum). We also suggest that those key isoform changes maybe a good target for possible therapies.

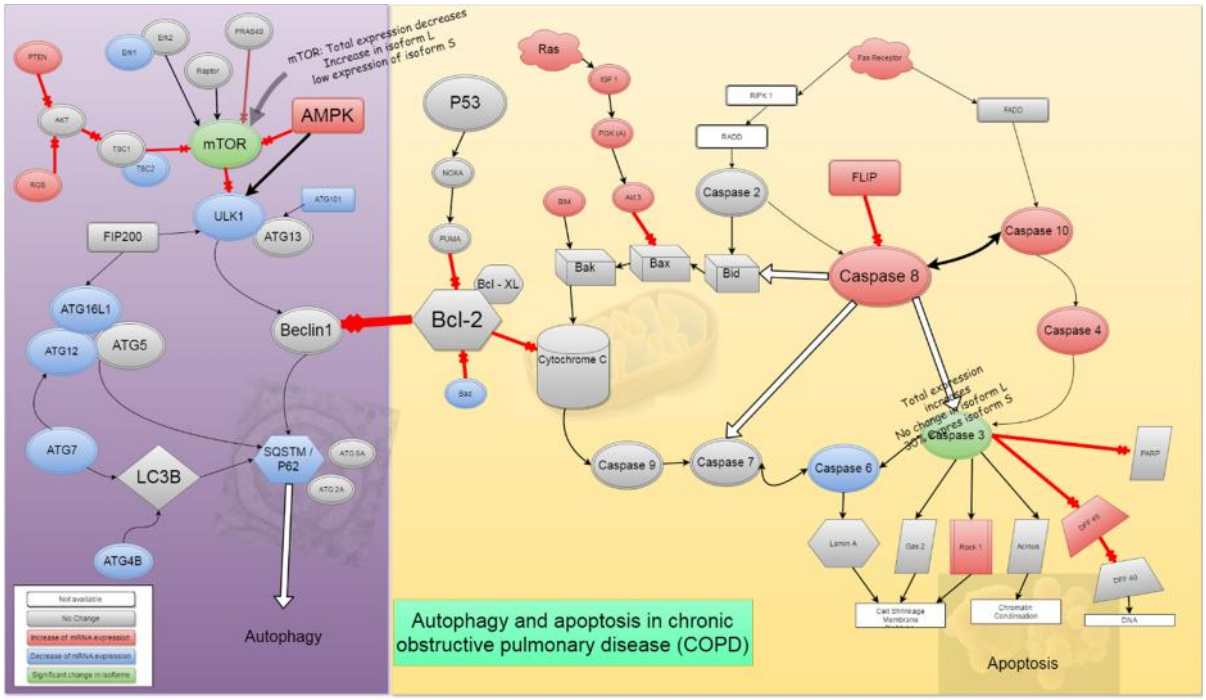

Figure 66: (Left) mTOR have a big inhibitory effect with the increase of the main isoform MTOR001 and the decrease of MTOR002. (Right) New isoform of Caspase3 is present in 40% of the samples, and almost total inhibition of apoptosis after that.

5.4. EFFECTS OF DRUGS THAT MODULATE AUTOPHAGY IN LUNG CANCER CELL LINES

We studied two NSCLC cell lines with three different treatments that affect autophagy. The response differ between these cell lines which could be due to the different molecular abnormalities. For example, oncogenic RAS mutations can induce a cytotoxic level of autophagy and depletion of several genes essential for autophagy [135].

5.4.1. Chloroquine

Chloroquine blocks autophagy in its final stages, this results in protein accumulation in the autophagy pathway. The accumulation includes P62 and LC3B-II, and might include mTOR. On the contrary, Beclin1 is a phosphorylating kinase and is not involved in the physical composition of autophagosomes, so a rapid change in its levels probably happens due to controlling factors of its transcription/translation.

Chloroquine has been studied on several cell-lines for 28 hours. H1299 was the least susceptible cell-line to its effects [109]. P62 and LC3B were measured during chloroquine treatment of H1299 for 4 days. LC3B-I and II levels raise consistently, while P62 levels increase for the first 24h and stays steady [110]. Our results confirm those studies, they show that LC3B levels continue to raise up to one week, and P62 decreases after the third day. Levels of Beclin1 are practically not changed. mTOR levels increase for 3 days and then decrease. Cell growth of this cell-line after 4 days was reported to be 50% when treated with 30uM of chloroquine compared to control [110]. Our study showed a similar result using 25uM of chloroquine and a higher dose-related effect.

H1299 seems to be dependent on autophagy for survival. Stopping autophagy using chloroquine causes the cells to die, especially in the centre of the tumour where autophagy is mostly active as we show in our cell culture experiments. The absence of P53 in H1299 did not affect cell death as chloroquine induces p53-independent death [136]. The cell-line could not be studied with long term treatment of chloroquine due to very high levels of death and inability of treated cells to adhere to the surface.

Chloroquine arrests the autophagy in COR-L23. Our results show an accumulation of P62 and LC3B. This effect does not correlate with cell death or big changes in growth levels. A small increase in G2/M phase that occurs in the first 48 hours is lost and cells continue to grow normally at therapeutic concentrations. The increase in mTOR levels can be explained by a decrease in its catabolism via autophagy [74]. Blocking autophagy in this cell-line does not affect survival, and autophagy seems not to be essential in cell survival and the cells overcome it. In some lung cancers depending on the molecular abnormalities.

Chloroquine is proved to influence autophagy in both cell lines, and accumulation of P62 and LC3B can be observed in autolysosomes via immunofluorescence. But the differences in response indicate that blocking autophagy may not be sufficient as a sole treatment.

Chloroquine was evaluated for a long time as a standalone intervention and as a booster for antineoplastic activity of conventional or targeted chemotherapeutics [137]. Several studies suggested chloroquine might overcome resistance and potentiate when combined with other therapies such as apoptotic-inducing drugs [138], 5-fluorouracil [139], mTOR Inhibitors [140], PI3K inhibitors [141] and dual PI3K/mTOR inhibitors [142].

5.4.2. LBH589

LBH589 was reported to increase autophagy, the increase in autophagy can be toxic in tumours with high levels of basal autophagy [143, 144]. LBH589 is already in use to treat lung cancer [145]. LBH has been reported to have a deadly effect in colorectal cancer cells, where it induces apoptosis and autophagy via DAPK protein [143]. On H1299, IC50 is reported to be 5 nmol/L while LD50 is reported to be 120 nmol/L. [145]

Treatment with histone deacytylase inhibitors (HDACi) do not change LC3B levels in H1299. P62/SQSTM1 decreases steadily till weak 4, at which P62 becomes undetectable. mTOR and Beclin1 levels increase during the first week, but after transferring to another culture dish for the following weeks, they become undetectable too. Cell death is not changed, while high levels of LBH stop cell growth.

COR-L23 has elevated levels of basal autophagy and P62 and LC3B are not detectable in untreated cells. Using LBH raises LC3B and P62/SQSTM1 expression temporary for 24 hours but does not increase mTOR. It also decreases levels of Beclin1 and LC3B-I expression after 48 hours. In immunofluorescence, LBH increased P62 and LC3B in limited quantities. Hyper-active autophagy might be the reason of cellular death in these cells.

The effects of LBH can be observed with most of the proteins. H1299 present the changes in proteins after long-term therapy and cell growth slows down without increase in death. On the other hand, autophagy proteins in COR-L23 increase and return to undetectable levels rapidly. After treatment, cell death in COR-L23 that are treated with LBH is high, and the cell line fail to continue growing after a week.

LBH has a wide range of effects as HDACi and over-activating autophagy is only one of them. Cell death can be induced via apoptosis pathway [146] and autophagy changes might be a side effect of the therapy and not the principal cause of death. One evidence to support that is the brief peak in the levels of autophagy-related proteins, while no change on cell death levels. On the other hand, the sudden decrease in Beclin1 might indicate a collapse in cellular ability to

recycle and produce proteins which may contribute to its death. Further studies might be needed to measure the levels of mRNA expression to identify whether those changes in protein levels are due expression levels or consumption of the proteins.

This result suggests effectiveness of histone deacytylase inhibitors treatment for NSCLC with depleted proteins of autophagy. LBH might also be useful in combination with chemotherapy agents such as Cispatin [147] or bortezomib [148].

5.4.3. Metformin

Metformin activates autophagy via activating AMPK and repressing Bcl-2 expression [82]. Studies reported that metformin has anti-proliferative effects and induces apoptosis in autophagy-dependent way [149].

Both H1299 and COR-L23 had no big changes in cell cycle or cell survival, and both of them presented a limited decrease in growth. In our study, metformin accelerated H1299 growth to reach a stable stage in early hours of cell culture (Appendix A). This explains why some reports describe an arrest of the cells in G0/G1 stage [150]. H1299 presented changes in cell shape and protein expression after 4 weeks of metformin treatment. Levels of Beclin1, P62 and LC3B decreased over time and stabilize after week 4. mTOR levels decreased rapidly after 48h, and this is probably to AMPK activation. H1299 respond slowly to metformin, but after 4 weeks of treatment cells are less active in division and have unique shape (Figure 38). Beyond of short-term effects of metformin in other studies, lower levels of autophagy proteins after the 4^{th} week may indicate a decrease in autophagy and it explains the slow growth and strange cytoskeleton shape.

We observed an increase in autophagy proteins (P62, mTOR and LC3B) in COR-L23 cell-line treated with metformin. Levels of Beclin1 decrease with long treatment. Metformin promoted autophagy mildly, which had some effect on cell growth, but it was not enough to cause detectable cell death.

COR-L23 cells treated with metformin were not able to survive beyond the first week after transfer to a new dish. A phenomena that can be seen in LBH with COR-L23 and chloroquine with H1299, drugs that modify autophagy seem to affect cells ability to adhere to surfaces. It could be explained by a relationship between autophagy and cytoskeleton proteins [151].

Any combination that include metformin that we tried in our lab did not produce a better result than single therapy. Although studies suggested the use of metformin with autophagy inducers such as mTOR inhibitors [152].

5.4.4. Therapy combinations

The most promising combination of therapies related to autophagy was using chloroquine with LBH589. Many studies reported an increase in therapeutic value and the possibility to reduce doses and side-effects [153]. However, this combination proved to be ineffective and provided no gain over single drug therapy. Adding LBH589 to chloroquine in H1299 reduce the cell death and decreased levels of mTOR. Combining LBH589 with chloroquine in COR-L23 reduced the effectiveness of LBH and required longer time to reach to the maximum of cell death.

6. CONCLUSIONS

1- In our series, the allele G in ATG16L1 rs2241880 plays a protective role in lung cancer development, especially in non COPD patients.

2- The existence of uAUG sequences in 5' untranslated region inhibit protein expression, and this inhibition related to the distance from start codon and the number of uAUGs.

3- Differential expression of mTOR isoforms may play a role in pathogenesis of lung cancer and COPD.

4- NSCLC cell lines differ in response to autophagy-modifying treatments. Cells that have hyper-active autophagy will be vulnerable to autophagy toxicity when treated with histone deacytylase inhibitors such as Panobinostat (LBH-589). Cells with normal levels of autophagy can be treated with autophagy blockers such as chloroquine. In NSCLC, using metformin or a combination of autophagy modulators does not provide any improvement in the outcome.

APPENDIX A: H1299 BEFORE CELLS STABILIZE

H1299 take on average 3 days to stabilize. If they were treated before this period the results are unreproducible, partly because the rapid change that may happen in these cell.

After transferring the cells to a new plat, cell grow very slow and have a big S-phase for a couple of days or more. This S-Phase decreases from over 30% of the cells after 24h of growth to the stable 7-8% after 72h of cellular growth. As we study autophagy, this change will not keep the same pace with our different treatments. In particular, metformin increase the speed of reaching the stable face. Practically what it means, if metformin used on under-grown H1299, it will make a transit significant difference between normal and treated cells. This change can affect cell growth phases in addition to proteins related to cytoskeleton, autophagy and possibly many other proteins as well.

Proteins that were measured via NanoDrop® and Bradford kit did not produce a constant house-keeping proteins (beta actin and alpha tubulin). It caused unreproducible results with western-blot. The experiments were redone after cell stability was reached, and the results were constant and reproducible in each step and with each technique.

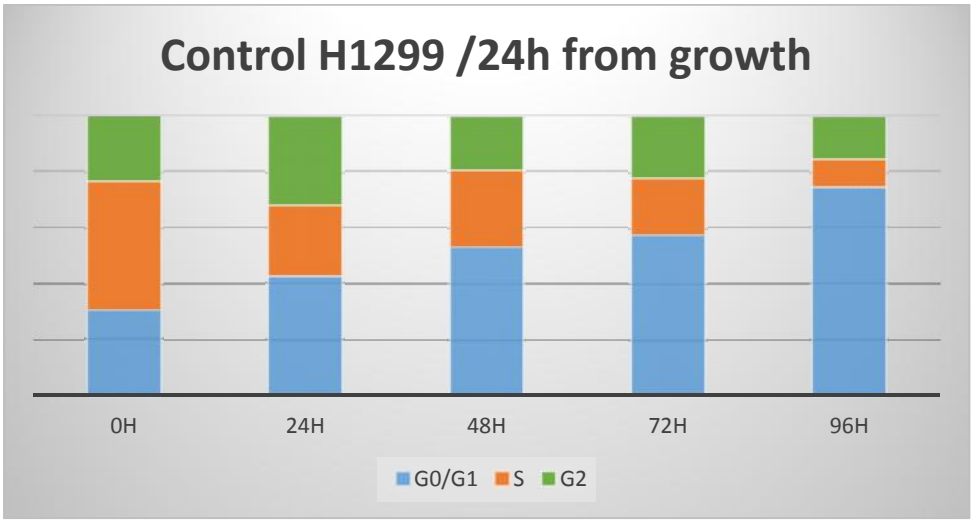

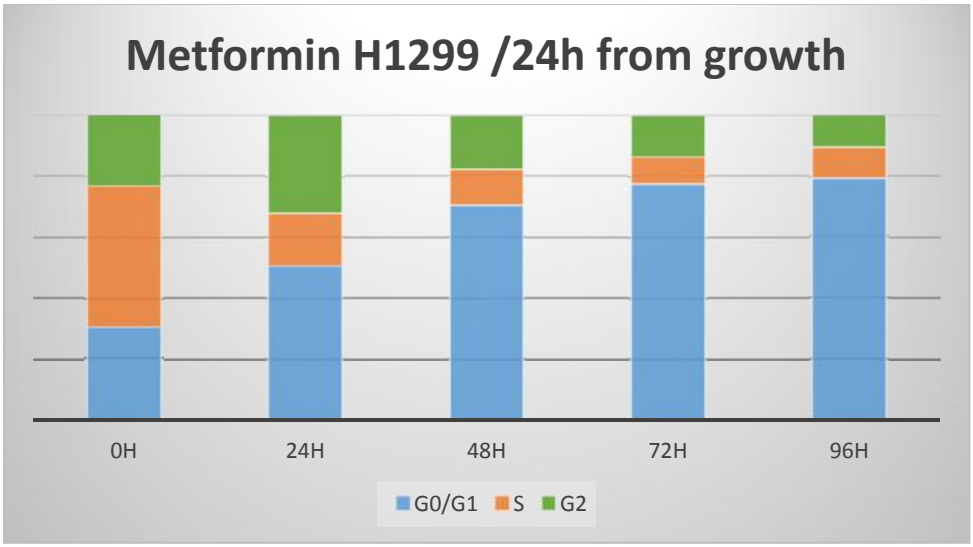

APPENDIX B: LIST OF BIOINFORMATICS RESULTS

List of genes studies and their changes in lung cancer and COPD

Gene	Ave. Normal	SD	Ave. COPD	SD	p	Ave. Cancer	SD	p
AKT1	58.7	16.8	54.8	11.5	0.238	95.0	69.6	0.075
AKT2	24.7	7.5	21.2	5.0	0.019	43.1	24.3	0.014
AKT3	7.1	3.3	9.3	4.8	0.008	3.3	1.8	0.000
alpha tubulin	127.2	60.2	107.7	45.4	0.126	79.7	51.1	0.007
AMPK alpha1	22.9	8.1	30.6	11.5	0.005	13.0	6.1	0.000
AMPK alpha2	0.9	0.5	1.0	0.4	0.485	1.0	1.0	0.601
ATG101	21.4	7.6	19.6	8.5	0.379	37.7	24.6	0.029
ATG12	5.3	3.6	4.4	2.3	0.051	5.7	4.7	0.530
ATG13	14.2	6.8	13.4	2.2	0.451	17.3	4.5	0.058
ATG14	8.0	2.6	8.5	1.5	0.305	7.0	1.8	0.116
ATG16L1	7.3	1.6	6.7	1.0	0.039	13.0	6.6	0.007
ATG16L2	24.2	13.4	22.9	10.2	0.960	32.8	57.4	0.466
ATG2A	5.0	1.3	4.9	1.1	0.690	8.6	1.8	0.000
ATG3	21.7	6.2	21.3	9.0	0.841	26.0	13.5	0.270
ATG4A	6.8	2.2	7.4	1.1	0.128	5.8	2.2	0.131
ATG4B	27.7	13.1	16.6	7.3	0.000	53.4	60.1	0.134
ATG4C	4.5	1.8	5.4	2.9	0.213	3.4	1.9	0.061
ATG5	10.0	2.6	9.9	4.1	0.987	10.2	6.3	0.882
ATG7	7.0	2.8	6.7	3.0	0.915	9.3	5.9	0.241
ATG9A	15.1	4.2	13.8	2.9	0.121	24.1	10.3	0.007
ATG9B	7.2	13.5	2.1	2.3	0.119	28.4	50.0	0.246
BAD	27.0	11.3	18.8	12.0	0.007	62.6	33.7	0.002
BAK1	4.5	2.3	4.2	2.1	0.501	8.0	3.3	0.002
BAX	29.9	39.6	21.7	9.8	0.176	70.2	50.5	0.013
Bcl XL	89.6	22.2	96.5	23.5	0.228	88.0	41.2	0.891
Bcl-2	3.4	4.1	4.0	2.2	0.489	1.6	1.0	0.006
BCL2-L11	6.6	3.1	8.3	3.3	0.041	7.1	3.2	0.670
Beclin1	27.2	9.6	23.9	6.1	0.152	31.4	13.4	0.232
beta-actin	1552.0	920.4	1063.1	669.1	0.012	2350.8	1116.6	0.025
BID	8.2	4.2	7.7	2.4	0.520	25.5	22.0	0.012
Caspase1	18.7	8.0	18.7	11.5	0.994	17.8	10.5	0.766
Caspase10	5.5	1.7	6.8	1.2	0.000	6.2	2.2	0.270
Caspase12	1.5	1.0	1.3	0.8	0.673	0.1	0.1	0.000
Caspase14	0.1	0.0	0.0	0.0	0.401	0.2	0.2	0.119
Caspase2	7.5	2.2	7.7	1.0	0.614	12.0	7.3	0.041
Caspase3	11.3	3.7	18.4	9.3	0.001	12.9	6.9	0.417
Caspase4	43.8	14.6	56.0	17.6	0.005	42.5	16.3	0.794

Caspase5	1.0	0.6	1.2	1.3	0.675	0.5	0.5	0.008
Caspase6	6.9	2.3	5.7	1.5	0.002	10.1	6.0	0.068
Caspase7	18.6	5.3	17.4	5.2	0.384	11.4	3.9	0.000
Caspase8	15.4	5.6	19.2	6.5	0.018	12.4	4.3	0.041
Caspase9	7.2	3.1	6.1	2.3	0.096	12.7	10.5	0.075
Cytochrome C	19.4	10.4	23.9	8.4	0.051	20.8	13.2	0.718
FADD	7.3	2.3	6.6	1.7	0.124	18.7	9.6	0.001
FILP	21.6	6.9	33.6	20.2	0.007	28.4	21.0	0.254
FIP200/ATG17	8.8	3.1	8.7	2.5	0.832	5.2	2.1	0.000
GAP-DH	195.2	203.7	190.0	75.7	0.875	1440.6	1143.8	0.001
HIF1A	31.4	19.3	56.2	40.4	0.007	36.3	15.8	0.341
HIF2A	276.4	180.1	265.4	168.4	0.796	66.3	33.6	0.000
LC3B	21.9	8.2	19.9	3.3	0.137	20.7	12.4	0.743
MCL1	168.6	92.9	297.2	128.7	0.000	155.4	71.9	0.576
mTOR	8.5	2.0	8.1	0.9	0.239	12.9	5.5	0.010
NOXA	4.7	9.3	6.1	3.7	0.363	4.6	3.6	0.954
P53	18.3	12.7	23.2	10.9	0.072	21.3	7.6	0.225
P62	171.1	49.4	140.9	44.1	0.010	327.5	243.9	0.033
PIK3CA	4.4	1.3	5.3	1.5	0.014	2.3	1.0	0.000
PIK3CB	7.7	2.0	7.9	1.8	0.707	8.5	4.0	0.482
PIK3CD	8.4	7.4	7.9	3.5	0.926	12.3	9.3	0.872
PIK3CG	1.9	1.6	2.8	1.8	0.029	1.8	1.8	0.871
PTEN	11.2	3.6	14.0	3.6	0.003	5.8	2.0	0.000
PUMA	3.4	1.7	3.2	1.7	0.671	10.6	8.1	0.006
ULK1	11.1	4.3	9.6	4.2	0.147	23.0	13.5	0.006
VPS13A	5.4	2.5	4.5	1.6	0.096	5.1	3.9	0.828
VPS13B	7.2	3.2	7.1	1.3	0.765	6.3	2.1	0.213
VPS13C	25.7	8.2	30.6	6.1	0.006	12.3	4.2	0.000
VPS13D	17.9	6.0	13.3	6.2	0.002	9.4	6.1	0.000
VPS35	17.7	6.8	19.3	5.2	0.271	20.2	9.4	0.380
Fas receptor	13.67	6.15	17.78	5.29	0.010	7.01	4.02	0.000
Kras	8.05	2.86	11.18	3.89	0.001	8.48	5.70	0.790
IGF1	2.13	1.97	5.70	5.34	0.003	2.19	1.79	0.913
C-RADD	10.66	5.35	7.22	2.24	0.000	6.35	2.32	0.000
RIPK1	12.07	3.00	12.85	1.95	0.185	13.32	7.38	0.546
Lamin A	147.44	113.74	165.64	90.53	0.459	331.49	261.91	0.022
APAF1	7.02	2.49	8.19	2.11	0.039	6.47	4.82	0.689
PARP	17.04	13.04	17.08	2.61	0.987	26.61	13.35	0.027
ROCK	8.88	3.24	11.39	3.45	0.004	5.42	2.71	0.000
GAS	0.92	0.61	0.93	0.64	0.722	0.77	0.37	0.004
Acinus	38.12	14.98	37.99	11.42	0.968	80.36	75.72	0.058

DFF45	5.49	3.51	6.78	1.98	0.048	9.20	4.32	0.009
PRAS40	7.01	3.74	8.39	6.86	0.194	57.17	67.86	0.015
Raptor	5.01	3.26	5.36	1.53	0.539	8.04	3.11	0.004
ERK2	12.80	5.82	11.72	2.15	0.256	10.07	5.12	0.103
ERK1	30.38	9.36	21.76	6.23	0.000	41.21	13.15	0.010
EGFR	10.68	4.00	12.36	4.79	0.142	13.35	12.08	0.430
ROS	11.43	5.86	14.97	9.47	0.022	8.82	7.46	0.275
ALK	0.12	0.13	0.09	0.12	0.364	0.06	0.05	0.089
vps15	11.74	7.48	8.14	3.91	0.009	12.83	7.41	0.634
vps34	4.95	4.17	4.90	2.07	0.951	11.38	10.11	0.035
TSC1	6.70	2.16	7.02	1.42	0.453	5.50	2.54	0.123
TSC2	18.36	10.28	13.26	3.86	0.009	43.47	36.63	0.019
LKB1	16.61	7.91	11.58	4.28	0.001	29.67	15.23	0.007
RHEB	8.23	3.73	8.92	2.05	0.310	10.03	4.60	0.197
EGF	0.52	0.55	0.46	0.27	0.581	1.50	1.61	0.067
DFF40	2.37	0.94	2.05	0.66	0.090	3.45	1.73	0.042

APPENDIX C: PROGRAMMING SCRIPTS

1-Program in R to read RNA-Seq tabular results (after Tophat/Cufflinks), files of transcript expression are tagged with three letters and put in working directory with a CSV file of isoform ensemble id and name.

```
## Program for reading tabular CVS fies for gene expression
## list of genes in a file called gene.csv
listfile= list.files(pattern = "*.tabular")
Genes=read.csv("Genes.csv",stringsAsFactors = FALSE)
Results=NULL
## read all files, all genes, and but the value of FPKM in Results, save CSV
for (afile in listfile) {
  mydata=read.table(afile, sep = "\t",header = TRUE,stringsAsFactors = FALSE)
  a=NULL
  ## Read every gene in the list, and get FPKM
  for (GenesA in Genes[[1]]){
    b = subset(mydata,tracking_id==GenesA)
    a[length(a)+1]= b[["FPKM"]]
  }
    ##add the genes to the results
  Results=cbind(Results,a)
}
##Name cols and rows
row.names(Results)=Genes[[2]]
colnames(Results)=substr(listfile,0,4)


## Save
write.csv(Results,"results.csv")
```

2- In Python 2.7: Counting number of transcriptome with “ATG” (AUG) and where the first “ATG” in 5’UTR exist. Data were downloaded from BioMart hg19.

```
#Counter function
def CountATG(seq):
    seq=seq+" "
    s=0
    for i in range (len(seq)-3,0,-1):
        t=seq[i:i+3]
        if t=="ATG":
            s= len(seq)-i-3
            break
    return (s)
#Prepare data, variables and import re
import re
f=open('c:\mart_export.txt')
Gen=[]
x=''
sequ=''
cont=0
temp=''
SeqLib={}
LenLib=[]
a=[]
#Count
for line in f:
    x= line[:-1]
    if x[0:1]==">":
        if sequ!="" or sequ!='Sequence unavailable':
            SeqLib[temp]=sequ
            a= re.split(ur'''>*\|*\|*\|*\|*''', temp)
            t=CountATG(sequ)
            a.append(t)
```

```
#Continue Script 2
            LenLib.append(a)
        Gen.append(x)
        temp=x[1:]
        sequ=''
    else:
        sequ= sequ+x

SeqLib.clear()
print (LenLib)
#Saving
f1=open('c:/results.txt','w+')
for tt in LenLib:
    f1.write(str(tt)+'\n')
f1.close()

f2=open('c:/BigData.txt','w+')
for tt in LenLib:
    if tt[0]!='':
        if tt[4]=='protein_coding':
            t1=tt[0]
            f2.write(str(t1)+'\n')
            t1=tt[2]
            f2.write(str(t1)+'\n')
            t1=tt[3]
            f2.write(str(t1)+'\n')
            t1=tt[5]
            f2.write(str(t1)+'\n')
f2.close()
#Continue Script 3 in R
```

3- In R: Plotting the results of the count of ATG in transcriptome

```
## Font for Graph

windowsFonts(A = windowsFont("Times New Roman"))

## Read count data

f="e:/AUG_TOTAL.txt"

file1=read.table(f,header = FALSE)

file1=read.csv(f,header = FALSE)

## Prepare variables

d=table(file1)

acu=90273

resu=d[2:300]

for (i1 in 2:300)

  {

   acu=acu-d[i1]

  resu[i1-1]=acu

 }

## Plot line and add shadow for area under graph

plot(resu/902.77,type="l",col=c("red"),family="A",ylab="Percent of transcriptome
with no AUG",xlab="Distance from initiation codon
(bp)",ylim=c(0,100),xlim=c(0,300),lwd=3,main="Percentage of transcriptome with no
AUG in 5'UTR next to initiation codon")

for (i in 1:299){ lines(y=c((resu[i]/90273*100),0),x=c(i,i),col='gray')}

def=rep(0,300)

def[1]=100

## Expected if ATG was random (1:64)

for (i2 in 2:300)

{

  def[i2]=def[i2-1]*63/64

  }

for (i in 1:299){ lines(y=c((def[i]),0),x=c(i,i),col='blue')}
```

References

[1] N. Mizushima, "Autophagy: process and function," *Genes & Dev,* no. 21, pp. 2861-2873, 2007.

[2] W.-w. Li, J. Li and J.-k. Bao, "Microautophagy: lesser-known self-eating," *Cellular and Molecular Life Sciences,* vol. 69, no. 7, pp. 1125-1136, 2012.

[3] S. Kaushik and A. Cuervo, "Chaperone-Mediated Autophagy," *Methods Mol Biol,* no. 445, p. 227–244, 2008.

[4] B. Levine and D. J. Klionsky, "Development by Self-Digestion: Molecular Mechanisms and Biological Functions of Autophagy," *Developmental Cell,* vol. 6, no. 4, p. 463–477, 2004.

[5] D. J. Klionsky, "The molecular machinery of autophagy: unanswered questions," *Journal of Cell Science,* no. 118, pp. 7-18, 2005.

[6] J. Kim, M. Kundu, B. Viollet and K.-L. Guan, "AMPK and mTOR regulate autophagy through direct phosphorylation of Ulk1," *Nature Cell Biology,* no. 13, p. 132–141, 2011.

[7] S. Wullschleger, R. Loewith and M. N. Hall, "TOR Signaling in Growth and Metabolism," *Cell,* vol. 124, no. 3, p. p471–484, 2006.

[8] L. Wang, J. C. Lawrence, Jr, T. W. Sturgill and T. E. Harris, "Mammalian Target of Rapamycin Complex 1 (mTORC1) Activity Is Associated with Phosphorylation of Raptor by mTOR," *J Biol Chem,* vol. 284, no. 22, p. 14693–14697, 2009.

[9] I. G. Ganley, D. H. Lam, J. Wang, X. Ding, S. Chen and X. Jiang, "ULK1·ATG13·FIP200 Complex Mediates mTOR Signaling and Is Essential for Autophagy," *The Journal of Biological Chemistry,* no. 284, pp. 12297-12305, 2009.

[10] N. Hosokawa, T. Sasaki, S. Iemura, T. Natsume, T. Hara and N. Mizushima, "Atg101, a novel mammalian autophagy protein interacting with Atg13," *Autophagy,* vol. 5, no. 7, pp. 973-9, 2009.

[11] M. G. Lin and J. H. Hurley, "Structure and function of the ULK1 complex in autophagy," *Current Opinion in Cell Biology,* no. 39, p. 61–68, 2016.

[12] R. C. Russell, Y. Tian, H. Yuan, H. W. Park, Y.-Y. Chang, J. Kim, H. Kim, T. P. Neufeld, A. Dillin and K.-L. Guan, "ULK1 induces autophagy by phosphorylating Beclin-1 and activating VPS34 lipid kinase," *NATURE CELL BIOLOGY,* no. 15, p. 741–750, 2013.

[13] E. Wirawan, S. Lippens, T. V. Berghe, A. Romagnoli, G. M. Fimia, M. Piacentini and P. Vandenabeele, "Beclin1: A role in membrane dynamics and beyond," *Autophagy,* vol. 8, no. 1, pp. 6-17, 2012.

[14] R. T. Marquez and L. Xu, "Bcl-2:Beclin 1 complex: multiple, mechanisms regulating autophagy/apoptosis toggle switch," *Am J Cancer Res.,* vol. 2, no. 2, p. 214–221, 2012.

[15] S. Randall-Demllo, M. Chieppa and R. Eri, "Intestinal Epithelium and Autophagy: Partners in Gut Homeostasis," *FRONTIERS IN IMMUNOLOGY,* no. 4, p. 301, 2013.

[16] N. Mizushima, T. Yoshimori and Y. Ohsumi, "Role of the Apg12 conjugation system in mammalian autophagy," *The International Journal of Biochemistry & Cell Biology,* vol. 35, no. 5, p. 553–561, 2003.

[17] "MBL life science," 2006. [Online]. Available: http://ruo.mbl.co.jp/bio/g/product/autophagy/autophagy.html.

[18] H. Weidberg, E. Shvets, T. Shpilka, F. Shimron, V. Shinder and Z. Elazar, "LC3 and GATE-16/GABARAP subfamilies are both essential yet act differently in autophagosome biogenesis," *EMBO J.,* vol. 29, no. 11, p. 1792–1802, 2010.

[19] J. A. Diehl, D. S. Haines and S. Y. Fuchs, "The Role of Ubiquitin in Autophagy-Dependent Protein Aggregate Processing," *Genes Cancer,* vol. 1, no. 7, p. 779–786, 2010.

[20] T. Lamark, V. Kirkin, I. Dikic and T. Johansen, "NBR1 and p62 as cargo receptors for selective autophagy of ubiquitinated targets," *Cell Cycle,* vol. 8, no. 13, pp. 1986-90, 2009.

[21] G. Bjørkøy, T. Lamark, S. Pankiv, A. Øvervatn, A. Brech and T. Johansen, "Monitoring autophagic degradation of p62/SQSTM1," *Methods Enzymol,* no. 452, pp. 181-97, 2009.

[22] S. Pankiv, T. H. Clausen, T. Lamark, A. Brech, . J.-A. Bruun, H. Outzen, A. Øvervatn, G. Bjørkøy and T. Johansen, "p62/SQSTM1 Binds Directly to Atg8/LC3 to Facilitate Degradation of Ubiquitinated Protein Aggregates by Autophagy," *The Journal of Biological Chemistry,* no. 282, pp. 24131-24145, 2007.

[23] Y. Ichimura, T. Kumanomidou, Y.-s. Sou, T. Mizushima, J. Ezaki, T. Ueno, E. Kominami, T. Yamane, K. Tanaka and M. Komatsu, "Structural Basis for Sorting Mechanism of p62 in Selective Autophagy," *The Journal of Biological Chemistry,* no. 283, pp. 22847-22857, 2008.

[24] A. K. G. Velikkakath, T. Nishimura, E. Oita, N. Ishihara and N. Mizushima, "Mammalian Atg2 proteins are essential for autophagosome formation and important for regulation of size and distribution of lipid droplets," *Mol. Biol. Cell,* vol. 23, no. 5, pp. 896-909, 2012.

[25] H. Tamura, M. Shibata, M. Koike, M. Sasaki and Y. Uchiyama, "Atg9A Protein, an Autophagy-related Membrane Protein, Is Localized in the Neurons of Mouse Brains," *J Histochem Cytochem,* vol. 58, no. 5, p. 443–453, 2010.

[26] J.-Y. Tang, E. Hsi, Y.-C. Huang, N. C.-H. Hsu, Y.-K. Chen, P.-Y. Chu and C.-Y. Chai, "ATG9A overexpression is associated with disease recurrence and poor survival in patients with oral squamous cell carcinoma," *Virchows Arch,* no. 463, p. 737–742, 2013.

[27] J. M. Gump and A. Thorburn, "Autophagy and apoptosis: what is the connection?," *7 Trends in Cell Biology,* vol. 21, no. 7, pp. 387-92, 2011.

[28] A. Ashkenazi, "Directing cancer cells to self-destruct with pro-apoptotic receptor agonists," *Nature Reviews Drug Discovery,* vol. 7, pp. 1001-1012, 2008.

[29] L. Ouyang, Z. Shi, S. Zhao, F. Wang, T. Zhou, B. Liu and J. Bao, "Programmed cell death pathways in cancer: a review of apoptosis, autophagy and programmed necrosis," *Cell Proliferation,* vol. 45, no. 6, p. 487–498, 2012.

[30] G. Mariño, M. Niso-Santano, E. H. Baehrecke and G. Kroemer, "Self-consumption: the interplay of autophagy and apoptosis," *NATURE REVIEWS: MOLECULAR CELL BIOLOGY,* vol. 15, pp. 81-94, 2014.

[31] B. Levine and J. Abrams, "p53: The Janus of autophagy?," *Nature Cell Biology,* no. 10, pp. 637 - 639, 2008.

[32] E. Tasdemir, M. Chiara Maiuri, E. Morselli, A. Criollo, M. D'Amelio, M. Djavaheri-Mergny, F. Cecconi, N. Tavernarakis and G. Kroemer, "A dual role of p53 in the control of autophagy," *Autophagy,* vol. 4, no. 6, pp. 810-4, 2008.

[33] E. Schmukler, Y. Kloog and R. Pinkas-Kramarski, "Ras and autophagy in cancer development and therapy," *Oncotarget,* vol. 5, no. 3, p. 577–586, 2014.

[34] P. Jiang and N. Mizushima, "Autophagy and human diseases," *Cell Research,* no. 24, p. 69–79, 2014.

[35] A. C. Society, "American Cancer Society: Cancer Facts and Figures 2016.," Atlanta, Ga, 2016.

[36] Z. Chen, C. M. Fillmore, P. S. Hammerman, C. F. Kim and K.-K. Wong, "Non-small-cell lung cancers: a heterogeneous set of diseases," *Nature Reviews Cancer,* no. 14, pp. 535-546, 2014.

[37] "American Cancer society," 1998-2000. [Online]. Available: http://www.cancer.org/cancer/lungcancer-non-smallcell/detailedguide/non-small-cell-lung-cancer-survival-rates.

[38] R. A. Barnard, D. P. Regan, R. J. Hansen, P. Maycotte, A. Thorburn and . D. L. Gustafson, "Autophagy inhibition delays early but not late stage metastatic disease," *J Pharmacol Exp Ther,* 2016.

[39] E. Brega and G. Brandao, "Non-Small Cell Lung Carcinoma Biomarker Testing: The Pathologist's Perspective," *Front Oncol,* vol. 4, p. 182, 2014.

[40] "The Health Consequences of Smoking—50 Years of Progress: A Report of the Surgeon General," GA: U.S. Department of Health and Human Services, Centers for Disease Control and Prevention, National Center for Chronic Disease Prevention and Health Promotion, Office on Smoking and Health, Atlanta, 2014.

[41] J. J. Jaboin, M. Hwang and B. Lu, "AUTOPHAGY IN LUNG CANCER," *Methods Enzymol,* no. 453, p. 287–304., 2009.

[42] W. Gao, J. Jin, J. Yin, S. Land, A. Gaither-Davis, N. Christie, J. Luketich, J. Siegfried and P. Keohavong, "KRAS and TP53 mutations in bronchoscopy samples from former lung cancer patients," *Mol Carcinog,* 2016.

[43] S. W. Ryter and A. M. Choi, "Autophagy in lung disease pathogenesis and therapeutics," *Redox Biology,* vol. 4, p. Pages 215–225, 2015.

[44] "Mayo clinic," [Online]. Available: http://www.mayoclinic.org/.

[45] Z.-H. Chen, H. P. Kim, F. C. Sciurba, S.-J. Lee, C. Feghali-Bostwick, D. B. Stolz, R. Dhir, R. J. Landreneau, M. J. Schuchert, S. A. Yousem, K. Nakahira, J. M. Pilewski, J. S. Lee, Y. Zhang, S. W. Ryter and A. M. K. Choi, "Egr-1 Regulates Autophagy in Cigarette Smoke-Induced Chronic Obstructive Pulmonary Disease," *Plos one,* 2008.

[46] S. Fujii, H. Hara, J. Araya, N. Takasaka, J. Kojima, S. Ito, S. Minagawa, Y. Yumino, T. Ishikawa, T. Numata, M. Kawaishi, J. Hirano, M. Odaka, T. Morikawa, S. Nishimura, K. Nakayama and K. Kuwano, "Insufficient autophagy promotes bronchial epithelial cell senescence in chronic obstructive pulmonary disease," *OncoImmunology,* vol. 1, no. 5, pp. 630-641, 2012.

[47] R. M. Tuder and I. Petrache, "Pathogenesis of chronic obstructive pulmonary disease," *The Journal of Clinical Investigation,* vol. 122, no. 8, pp. 2749-2755, 2012.

[48] D.-H. Yu, . R. A. Waterland, . P. Zhang, D. Schady, M.-H. Chen, . Y. Guan, M. Gadkari and L. Shen, "Targeted p16Ink4a epimutation causes tumorigenesis and reduces survival in mice," *J Clin Invest,* vol. 124, no. 9, pp. 3708-3712, 2014.

[49] " dbSNP: Short Genetic Variants," NCBI, [Online]. Available: http://www.ncbi.nlm.nih.gov/SNP.

[50] R. U. MARTIN, "ESTUDIO MOLECULAR DE LA ENFERMEDAD ÓSEA DE PAGET: Thesis doctoral," University of Salamanca, 2016.

[51] T. Hanada, N. N. Noda, Y. Satomi, Y. Ichimura, Y. Fujioka, T. Takao, F. Inagaki and Y. Ohsumi, "The Atg12-Atg5 Conjugate Has a Novel E3-like Activity for Protein Lipidation in Autophagy," *The Journal of Biological Chemistry,* vol. 282, pp. 37298-37302, 2007.

[52] M. Songane, J. Kleinnijenhuis, B. Alisjahbana, E. Sahiratmadja, I. Parwati, M. Oosting, T. S. Plantinga, L. A. B. Joosten, M. G. Netea, T. H. M. Ottenhoff, E. van de Vosse and R. van Crevel, "Polymorphisms in Autophagy Genes and Susceptibility to Tuberculosis," *PLoS ONE,* vol. 7, no. 8, p. e41618, 2012.

[53] A. Murthy, Y. Li, I. Peng, M. Reichelt, A. K. Katakam, R. Noubade, M. Roose-Girma, J. DeVoss, L. Diehl, R. R. Graham and M. v. L. Campagne, "A Crohn's disease variant in Atg16l1 enhances its degradation by caspase 3," *Nature,* vol. 506, p. 456–462, 2014.

[54] E. Boada-Romero, I. Serramito-Gómez, M. P. Sacristán, D. L. Boone, R. J. Xavier and F. X. Pimentel-Muiños, "The T300A Crohn's disease risk polymorphism impairs function of the WD40 domain of ATG16L1," *Nature Communications,* vol. 7, p. 11821, 2016.

[55] Y. Suzuki, D. Ishihara, M. Sasaki, H. Nakagawa, H. Hata, T. Tsunoda, M. Watanabe, T. Komatsu, T. Ota, T. Isogai, A. Suyama and S. Sugano, "Statistical Analysis of the 5' Untranslated Region of Human mRNA Using "Oligo-Capped" cDNA Libraries," *Genomics,* vol. 64, no. 3, p. 286–297, 2000.

[56] B. Y. Chung, C. S. Simons, A. E. Firth, C. M. B. Brown and R. P. Hellens, "Effect of 5'UTR introns on gene expression in Arabidopsis thaliana," *BMC Genomics,* vol. 7, no. 120, pp. 2164-2167, 2006.

[57] F. Mignone, C. Gissi, S. Liuni and G. Pesole, "Untranslated regions of mRNAs," *Genome Biology,* vol. 3, no. 3, pp. reviews0004-reviews0004.10, 2002.

[58] M. Kozak, " At least six nucleotides preceding the AUG initiator codon enhance translation in mammalian cells," *Journal of Molecular Biology,* vol. 196, no. 4, pp. 947-50, 20 Aug 1987.

[59] H. Zur and T. Tuller, "New Universal Rules of Eukaryotic Translation Initiation Fidelity," *Plos computational biology,* vol. 9, no. 7, p. e1003136, 2013.

[60] I. Rogozin, A. Kochetov, F. Kondrashov, E. Koonin and L. Milanesi, "Presence of ATG triplets in 5' untranslated regions of eukaryotic cDNAs correlates with a 'weak' context of the start codon," *Bioinformatics,* vol. 17, no. 10, pp. 890-900, 2001.

[61] S. Dvir, "Deciphering the rules by which 5'-UTR sequences affect protein expression in yeast," *Proc Natl Acad Sci U S A,* vol. 110, no. 30, pp. 2792-801, 2013.

[62] N. Ghilardi, A. Wiestner, M. Kikuchi, A. Ohsaka and R. C. Skoda, "Hereditary thrombocythaemia in a Japanese family is caused by a novel point mutation in the thrombopoietin gene," *British Journal of Haematology,* vol. 107, no. 2, p. 310–316.

[63] K. Damjanovich, C. Langa, F. J. Blanco, J. McDonald, L. M. Botella, C. Bernabeu, W. Wooderchak-Donahue, D. A. Stevenson and P. Bayrak-Toydemir, "5'UTR mutations of ENG cause hereditary hemorrhagic telangiectasia," *Orphanet Journal of Rare Diseases,* vol. 6, p. 85, 2011.

[64] T. Matthes, P. Aguilar-Martinez, L. Pizzi-Bosman, R. Darbellay, L. Rubbia-Brandt, E. Giostra, M. Michel, T. Ganz and P. Beris, "Severe hemochromatosis in a Portuguese family associated with a new mutation," *BLOOD,* vol. 104, no. 7, pp. 2181-2183, 2004.

[65] O. Semler, L. Garbes, K. Keupp, D. Swan, K. Zimmermann, J. Becker, S. Iden, B. Wirth, P. Eysel, F. Koerber, E. Schoenau, S. K. Bohlander, B. Wollnik and C. Netzer, "A mutation in the 5'-UTR of IFITM5 creates an in-frame start codon and causes autosomal-dominant osteogenesis imperfecta type V with hyperplastic callus," vol. 91, p. 349–357, 2012.

[66] D. M. Ryan , J. Salit, M. S. Walters, T. L. Vincent, F. Agosto-Perez, J. G. Mezey and R. G. Crystal, "Smoking-Induced Alternative Splicing Of Transcript Variants In Human Airway Basal Cells At COPD Risk Locus 19q13.2," *LATE BREAKING ABSTRACTS IN DISEASE SUSCEPTIBILITY AND PATHOGENESIS,* pp. A6609-A6609, 2014.

[67] P. J. Gardina, T. A. Clark, B. Shimada, M. K. Staples, Q. Yang, J. Veitch, A. Schweitzer, T. Awad, C. Sugnet, S. Dee, C. Davies, A. Williams and Y. Turpaz, "Alternative splicing and differential gene expression in colon cancer detected by a whole genome exon array," *BMC Genomics,* vol. 7, p. 325, 2006.

[68] C. Ghigna, C. Valacca and G. Biamonti, "Alternative Splicing and Tumor Progression," *Curr Genomics,* vol. 9, no. 8, p. 556–570, 2008.

[69] C. J. David and J. L. Manley, "Alternative pre-mRNA splicing regulation in cancer: pathways and programs unhinged," *Genes & Dev,* vol. 24, pp. 2343-2364, 2010.

[70] X. M. Ma and J. Blenis, "Molecular mechanisms of mTOR-mediated translational control," *Nature Reviews Molecular Cell Biology,* vol. 10, pp. 307-318, 2009.

[71] G. Panasyuk, I. Nemazanyy, A. Zhyvoloup, V. Filonenko, D. Davies, M. Robson, R. B. Pedley, M. Waterfield and I. Gout, "mTORbeta splicing isoform promotes cell proliferation and tumorigenesis," *The Journal of Biological Chemistry,* vol. 284, pp. 30807-30814, 2009.

[72] Z. Alharbi, "Identification and characterization of novel mTOR splicing isoforms," Doctoral thesis, UCL (University College London), 2015.

[73] M. J. Morgan, G. Gamez, C. Menke, A. Hernandez, J. Thorburn, F. Gidan, L. Staskiewicz, S. Morgan, C. Cummings, P. Maycotte and A. Thorburn, "Regulation of autophagy and chloroquine sensitivity by oncogenic RAS in vitro is context-dependent," vol. 10, no. 10, pp. 1814-1826, 2014.

[74] Y. Hu, L. R. Carraro-Lacroix, A. Wang, C. Owen, E. Bajenova, P. N. Corey, J. H. Brumell and I. Voronov, "Lysosomal pH Plays a Key Role in Regulation of mTOR Activity in Osteoclasts," *Journal of cellular biochemistry,* vol. 117, no. 2, p. 413–425, 2015.

[75] Y. Zou, Y.-H. Ling, J. Sironi, E. L. Schwartz, R. Perez-Soler and B. Piperdi, "The autophagy inhibitor chloroquine overcomes the innate resistance of wild-type EGFR non-small-cell lung cancer cells to erlotinib," *J Thorac Oncol,* vol. 8, no. 6, p. 693–702, 2013.

[76] Z. J. Yang, C. E. Chee, S. Huang and F. A. Sinicrope, "The Role of Autophagy in Cancer: Therapeutic Implications," *Mol Cancer Ther ,* vol. 10, p. 1533, 2011.

[77] "FDA approves Farydak for treatment of multiple myeloma," FDA News Release, 2015.

[78] J. M. Klein, A. Henke, M. Sauer, M. Bessler, K. S. Reiners, A. Engert, H. P. Hansen and E. P. von Strandmann, "The Histone Deacetylase Inhibitor LBH589 (Panobinostat) Modulates the Crosstalk of Lymphocytes with Hodgkin Lymphoma Cell Lines," *Plos one,* 2013.

[79] M. Gandesiri, S. Chakilam, J. Ivanovska, N. Benderska, M. Ocker, P. Di Fazio, M. Feoktistova, H. Gali-Muhtasib, M. Rave-Frank, O. Prante, H. Christiansen, M. Leverkus, A. Hartmann and R. Schneider-Stock, "DAPK plays an important role in panobinostat-inducedautophagy and commits cells to apoptosis under autophagydeficient conditions," *Apoptosis,* vol. 17, no. 12, pp. 1300-1315, 2012.

[80] J. P. Laubach, P. Moreau, J. F. San-Miguel and P. G. Richardson, "Panobinostat for the Treatment of Multiple Myeloma," *Clin Cancer Res,* vol. 21, no. 21, pp. 4767-4773, 2015.

[81] K. Y. Hur and . M.-S. Lee, "New mechanisms of metformin action: Focusing on mitochondria and the gut," *Journal of diabitis investigation,* no. 6, pp. 600-609, 2015.

[82] Y. Feng, C. Ke, Q. Tang, H. Dong, X. Zheng, W. Lin, J. Ke, J. Huang, S.-C. Yeung and H. Zhang, "Metformin promotes autophagy and apoptosis in esophageal squamous cell carcinoma by downregulating Stat3 signaling," *Cell Death and Disease,* no. 5, 2014.

[83] H. LIU, C. SCHOLZ, C. ZANG, J. H. SCHEFE, P. HABBEL, A.-C. REGIERER, C.-O. SCHULZ, K. POSSINGER and J. EUCKER, "Metformin and the mTOR Inhibitor Everolimus (RAD001) Sensitize Breast Cancer Cells to the Cytotoxic Effect of Chemotherapeutic Drugs In Vitro," *Anticancer Research,* vol. 32, no. 5, pp. 1627-1637, 2012.

[84] T. Tomic, T. Botton, M. Cerezo, G. Rober, F. Luciano, A. Puissant, P. Gounon, M. Allegra, C. Bertolotto, J.-M. Bereder, S. Tartare-Deckert, P. Bahadoran, P. Auberger, R. Ballotti and S. Rocchi, "Metformin inhibits melanoma development through autophagy and apoptosis mechanisms," *Cell Death Dis,* vol. 2, no. 9, p. e199, 2011.

[85] M. Saville, J. Lietzau, J. Pluda, W. Wilson, R. Humphrey, E. Feigel, S. Steinberg, S. Broder, R. Yarchoan, J. Odom and . I. Feuerstein, "Treatment of HIV-associated Kaposi's sarcoma with paclitaxel," *The Lancet,* vol. 346, no. 8966, p. 26–28, 1995.

[86] R. Bharadwaj and H. Yu, "The spindle checkpoint, aneuploidy, and cancer," *Oncogene,* no. 23, p. 2016–2027, 2004.

[87] R. Veldhoen, S. Banman, D. Hemmerling, R. Odsen, T. Simmen, A. Simmonds, D. Underhill and I. Goping, "The chemotherapeutic agent paclitaxel inhibits autophagy through two distinct mechanisms that regulate apoptosis," *Oncogene,* vol. 32, no. 6, pp. 736-46, 2013.

[88] S. Calvo, . D. Pagliarini and V. Mootha, "Upstream open reading frames cause widespread reduction of protein expression and are polymorphic among humans," *PNAS,* vol. 106, no. 18, p. 7507–7512, 2009.

[89] A. E. J. Massa, "CÁNCER DE PULMÓN Y CITOCINAS: VARIANTES CLÍNICAS Y GENÉTICAS," Salamanca, 2011.

[90] D. S. D. P. OTERO, "ESTUDIO DE LOS POLIMORFISMOS DE GENES," UNIVERSIDAD DE SALAMANCA, Salamanca, 2008.

[91] Sambrook J and Russel D, Molecular Cloning: A Laboratory Manual, 3rd edition ed., vol. 3, New York, NY, USA: Cold Spring Harbor Laboratory Press.

[92] D. Blankenberg, A. Gordon, G. Von Kuster, N. Coraor, J. Taylor, A. Nekrutenko and the Galaxy Team, "Manipulation of FASTQ data with Galaxy," *Bioinformatics,* vol. 26, no. 14, pp. 1783-1785, 2010.

[93] C. Trapnell, L. Pachter and S. L. Salzberg, "TopHat: discovering splice junctions with RNA-Seq," *Bioinformatics,* vol. 25, no. 9, pp. 1105-1111, 2009.

[94] D. Kim, G. Pertea, C. Trapnell, H. Pimentel, R. Kelley and S. L. Salzberg, "TopHat2: accurate alignment of transcriptomes in the presence of insertions, deletions and gene fusions," *Genome Biology,* vol. 14, no. 4, p. R36, 2013.

[95] C. Trapnell, A. Roberts, L. Goff, G. Pertea, D. Kim, D. R. Kelley, H. Pimentel, S. L. Salzberg, J. L. Rinn and L. Pachter, "Differential gene and transcript expression analysis of RNA-seq experiments with TopHat and Cufflinks," *Nat Protoc,* vol. 7, no. 3, p. 562–578, 2012.

[96] E. Afgan, D. Baker, M. v. den Beek, D. Blankenberg, D. Bouvier, M. Čech, J. Chilton, D. Clements, N. Coraor, C. Eberhard, B. Grüning, A. Guerler, J. Hillman-Jackson, G. Von Kuster, E. Rasche, N. Soranzo, N. Turaga, J. Taylor, A. Nekrutenko and J. Goecks, "The Galaxy platform for accessible, reproducible and collaborative biomedical analyses: 2016 update," *Nucleic Acids Research.*

[97] M. Wolfien, C. Rimmbach, U. Schmitz, J. J. Jung, S. Krebs, G. Steinhoff, R. David and O. Wolkenhauer, "TRAPLINE: a standardized and automated pipeline for RNA sequencing data analysis, evaluation and annotation," *BMC Bioinformatics,* vol. 17, p. 21, 2016.

[98] A. R. Gruber, R. Lorenz, S. H. Bernhart, R. Neuböck and I. L. Hofacker, "The Vienna RNA Websuite," *Nucleic Acids Res,* vol. 36, pp. W70-W74, 2008.

[99] Y. DING, C. Y. CHAN and C. E. LAWRENCE, "RNA secondary structure prediction by centroids in a Boltzmann weighted ensemble," *RNA,* vol. 11, pp. 1157-1166, 2005.

[100] R. Foty, "A Simple Hanging Drop Cell Culture Protocol for Generation of 3D Spheroids," *J Vis Exp,* vol. 51, p. 2720, 2011.

[101] N. Sunaga, . D. S. Shames, L. Girard, M. Peyton, J. E. Larsen, H. Imai, J. Soh, M. Sato, N. Yanagitan, K. Kaira, Y. Xie, A. F. Gazdar, M. Mori and J. D. Minna, "Non–Small Cell Lung Cancers Suppresses Tumor Growth and Sensitizes Tumor Cells to Targeted Therapy," *Mol Cancer Ther,* vol. 10, no. 2, pp. 336-346, 2011.

[102] "Cancer Cell Line Encyclopedia," Broad-Novartis, 2015. [Online]. Available: http://www.broadinstitute.org/ccle/home.

[103] F. Végran, R. Boidot, E. Solary and S. Lizard-Nacol, "A Short Caspase-3 Isoform Inhibits Chemotherapy-Induced Apoptosis by Blocking Apoptosome Assembly," *PLoS ONE,* vol. 6, no. 12, p. e29058, 2011.

[104] M.-E. Huot, G. Vogel, A. Zabarauskas, C. T.-A. Ngo, J. Coulombe-Huntington, J. Majewski and S. Richard, "The Sam68 STAR RNA-Binding Protein Regulates mTOR Alternative Splicing during Adipogenesis," *Molecular Cell,* vol. 46, no. 2, p. 187–199, 2012.

[105] J. R. Molina, P. Yang, S. D. Cassivi, S. E. Schild and A. A. Adjei, "Non–Small Cell Lung Cancer: Epidemiology, Risk Factors, Treatment, and Survivorship," *Mayo Clin Proc,* vol. 83, no. 5, p. 584–594, 2008.

[106] Q. GUO, Z. LIU, L. JIANG, M. LIU, J. MA, C. YANG, L. HAN, K. NAN and X. LIANG, "Metformin inhibits growth of human non-small cell lung cancer cells via liver kinase B-1-independent activation of adenosine monophosphate-activated protein kinase," *Mol Med Rep,* vol. 13, no. 3, p. 2590–2596, 2016.

[107] N. WU, C. GU, H. GU, H. HU, Y. HAN and Q. LI, "Metformin induces apoptosis of lung cancer cells through activating JNK/p38 MAPK pathway and GADD153," *Neoplasma,* vol. 58, no. 6, pp. 482-490, 2011.

[108] Q. GUO, Z. LIU, L. JIANG, M. LIU, J. MA, Y. CHENGCHENG, L. HAN, K. NAN and X. LIANG, "Metformin inhibits growth of human non-small cell lung cancer cells via liver kinase B-1-

independent activation of adenosine monophosphate-activated protein kinase," *Mol Med Rep,* vol. 13, no. 3, p. 2590–2596, 2016.

[109] A. J. Lakhter, R. P. Sahu, Y. Sun, W. Kaufmann, E. J. Androphy, J. B. Travers and S. R. Naidu, "Chloroquine Promotes Apoptosis in Melanoma Cells by Inhibiting BH3 domain Mediated PUMA Degradation," *J Invest Dermatol,* vol. 133, no. 9, p. 2247–2254, 2013.

[110] J. Y. Guo, H.-Y. Chen, R. Mathew, J. Fan, A. M. Strohecker, G. Karsli-Uzunbas, J. J. Kamphorst, G. Chen, J. M. Lemons, V. Karantza, H. A. Coller, R. S. DiPaola, C. Gelinas, J. D. Rabinowitz and E. White, "Activated Ras requires autophagy to maintain oxidative metabolism and tumorigenesis," *Genes & Dev,* no. 25, pp. 460-470, 2011.

[111] M. Chaurasia, A. N. Bhatt, A. Das, B. S. Dwarakanath and K. Sharma, "Radiation-induced autophagy: mechanisms and consequences," *Free Radic Res,* vol. 50, no. 3, pp. 273-290, 2016.

[112] K. Buffen, M. Oosting, J. Quintin, A. Ng, J. Kleinnijenhuis, V. Kumar, E. van de Vosse, C. Wijmenga, R. van Crevel, E. Oosterwijk, A. Grotenhuis, S. Vermeulen, L. Kiemeney, F. van de Veerdonk, G. Chamilos, R. Xavier, J. van der Meer, M. Netea and L. Joosten, "Autophagy controls BCG-induced trained immunity and the response to intravesical BCG therapy for bladder cancer," *PLoS Pathog,* 2014.

[113] T. S. Plantinga, E. van de Vosse, A. Huijbers, M. G. Netea, L. A. B. Joosten, J. W. A. Smit and R. T. Netea-Maier, "Role of Genetic Variants of Autophagy Genes in Susceptibility for Non-Medullary Thyroid Cancer and Patients Outcome," *Plos one,* 2014.

[114] R. Usategui-Martín, J. García-Aparicio, L. Corral-Gudino, I. Calero-Paniagua, J. Del Pino-Montes and R. González Sarmiento, "Polymorphisms in Autophagy Genes Are Associated with Paget Disease of Bone," *PLOS one,* 2015.

[115] K. Xie, C. Liang, Q. Li, C. Yan, C. Wang, Y. Gu, M. Zhu, F. Du, H. Wang, J. Dai, X. Liu, G. Jin, H. Shen, H. Ma and Z. Hu, "Role of ATG10 expression quantitative trait loci in non-small cell lung cancer survival," *You have full text access to this content,* 2016.

[116] K. M. Burghardt, V. Avinashi, C. Kosar, W. Xu, P. W. Wales, Y. Avitzur and A. Muise, "A CARD9 Polymorphism Is Associated with Decreased Likelihood of Persistent Conjugated Hyperbilirubinemia in Intestinal Failure," *Plos one,* 2014.

[117] C. Ciccacci, C. Perricone, F. Ceccarelli, S. Rufini, D. Di Fusco, C. Alessandri, F. Romana Spinelli, E. Cipriano, G. Novelli, G. Valesini, P. Borgiani and F. Conti, "A Multilocus Genetic Study in a Cohort of Italian SLE Patients Confirms the Association with STAT4 Gene and Describes a New Association with HCP5 Gene," *PLoS One,* vol. 9, no. 11, 2014.

[118] C. Capela, A. D. Dossou, R. Silva-Gomes, G. Emmanuel Sopoh, M. Makoutode, J. Filipe Menino, A. Gabriel Fraga, C. Cunha, A. Carvalho, F. Rodrigues and J. Pedrosa, "Genetic

Variation in Autophagy-Related Genes Influences the Risk and Phenotype of Buruli Ulcer," *PLoS Negl Trop Dis,* vol. 10, no. 4, p. e0004671, 2016.

[119] T. S. Plantinga, L. A. Joosten and M. G. Netea, "ATG16L1 polymorphisms are associated with NOD2-induced hyperinflammation," *Autophagy,* vol. 7, no. 9, 1074-1075.

[120] K. G. Lassen, P. Kuballa, K. L. Conway, K. K. Khushbu K. Patel, C. E. Becker, J. M. Peloquin, E. J. Villablanca, J. M. Norman, T.-C. Liu, R. J. Heath, M. L. Becker, . L. Fagbami, H. Horn, J. Mercer, O. H. Yilmaz, J. D. Jaffe, A. F. Shamji, A. K. Bhan, S. A. Carr, M. J. Daly, H. W. Virgin, S. L. Schreiber, T. S. Stappenbeck and R. J. Xavier, "Atg16L1 T300A variant decreases selective autophagy resulting in altered cytokine signaling and decreased antibacterial defense," *PNAS,* vol. 111, no. 21, p. 7741–7746, 2014.

[121] J. Y. Guo, H.-Y. Chen, R. Mathew, J. Fan, A. M. Strohecker, G. Karsli-Uzunbas, J. J. Kamphorst, G. Chen, J. M. Lemons, V. Karantza, H. A. Coller, R. S. DiPaola, C. Gelinas, J. D. Rabinowitz and E. White, "Activated Ras requires autophagy to maintain oxidative metabolism and tumorigenesis," *Genes Dev,* vol. 25, no. 5, pp. 460-70, 2011.

[122] R. Lock, S. Roy, C. M. Kenific, J. S. Su, E. Salas, S. M. Ronen and J. Debnath, "Autophagy facilitates glycolysis during Ras-mediated oncogenic transformation," *Mol Biol Cell,* vol. 22, no. 2, pp. 165-78, 2011.

[123] S. Yang, X. Wang, G. Contino, M. Liesa, E. Sahin, H. Ying, A. Bause, Y. Li, J. M. Stommel, G. Dell'Antonio, J. Mautner, G. Tonon, M. Haigis, O. S. Shirihai, C. Doglioni, N. Bardeesy and A. C. Kimmelman, "Pancreatic cancers require autophagy for tumor growth," *Genes Dev,* vol. 25, no. 7, pp. 717-29, 2011.

[124] Y.-L. Hu, M. DeLay, A. Jahangiri, A. M. Molinaro, S. D. Rose, W. S. Carbonell and M. K. Aghi, "Hypoxia-induced autophagy promotes tumor cell survival and adaptation to antiangiogenic treatment in glioblastoma," *Cancer Res,* vol. 72, no. 7, pp. 1773-83, 2012.

[125] J. Wegrzyn, T. Drudge, F. Valafar and V. Hook, "Bioinformatic analyses of mammalian 5'-UTR sequence properties of mRNAs predicts alternative translation initiation sites," *BMC Bioinformatics,* vol. 9, p. 232, 2008.

[126] A. Bisio, S. Nasti, J. Jordan, S. Gargiulo, L. Pastorino, A. Provenzani, A. Quattrone, P. Queirolo, G. Bianchi-Scarrà, P. Ghiorzo and A. Inga, "Functional analysis of CDKN2A/p16INK4a 5'UTR variants predisposing to melanoma," *Human Molecular Genetics,* vol. 19, no. 8, pp. 1479-91, 2010.

[127] D. R. Morris and A. P. Geballe, "Upstream Open Reading Frames as Regulators of mRNA Translation," *Mol. Cell. Biol,* vol. 20, no. 23, pp. 8635-8642, 2000.

[128] P. Flicek, M. R. Amode, D. Barrell, K. Beal, K. Billis, S. Brent, D. Carvalho-Silva, P. Clapham, G. Coates, S. Fitzgerald, L. Gil, C. García Girón, L. Gordon, T. Hourlier, S. Hunt, N. Johnson, T.

Juettemann, A. K. Kähäri, S. Keenan, E. Kulesha, F. J. Martin, T. Maurel, W. M. McLaren, D. N. Murphy, R. Nag, B. Overduin, M. Pignatelli, B. Pritchard, E. Pritchard, H. S. Riat, M. Ruffier, D. Sheppard, K. Taylor, A. Thormann, S. J. Trevanion, A. Vullo, S. P. Wilder, M. Wilson, A. Zadissa, B. L. Aken, E. Birney, F. Cunningham, J. Harrow, J. Herrero, T. J. Hubbard, R. Kinsella, M. Muffato, A. Parker, G. Spudich, A. Yates, D. R. Zerbino and S. M. Searle, "Ensembl 2014," *Nucl. Acids Res.,* vol. 42, no. D1, pp. D749-D755, 2014.

[129] K. Spriggs, M. Bushell and A. Willis, "Translational Regulation of Gene Expression during Conditions of Cell Stress," *Mol Cell,* vol. 40, p. 228–237, 2010.

[130] X. M. Ma and J. Blenis, "Molecular mechanisms of mTOR-mediated translational control," *Nature Reviews Molecular Cell Biology,* vol. 10, pp. 307-318, 2009.

[131] C. Kevil, P. Carter, B. Hu and A. DeBenedetti, "Translational enhancement of FGF-2 by eIF-4 factors, and alternate utilization of CUG and AUG codons for translation initiation," *Oncogene,* no. 11, pp. 2339-2348, 1995.

[132] L. Lackey, E. McArthur and A. Laederach, "Increased Transcript Complexity in Genes Associated with Chronic Obstructive Pulmonary Disease," *PLoS One,* vol. 10, no. 10, p. e0140885, 2015.

[133] G. S. Omenn, A. K. Yocum and R. Menon, "Alternative Splice Variants, a New Class of Protein Cancer Biomarker Candidates: Findings in Pancreatic Cancer and Breast Cancer with Systems Biology Implications," *Disease Markers,* vol. 28, pp. 241-251, 2010.

[134] A. Mühlethaler-Mottet, M. Flahaut, K. Balmas Bourloud, K. Nardou, A. Coulon, J. Liberman, M. Thome and N. Gross, "Individual caspase-10 isoforms play distinct and opposing roles in the initiation of death receptor-mediated tumour cell apoptosis," *Cell Death and Disease,* vol. 2, p. e125, 2011.

[135] S. Rao, L. Tortola, T. Perlot, G. Wirnsberger, M. Novatchkova, R. Nitsch, P. Sykacek, L. Frank, D. Schramek, V. Komnenovic, V. Sigl, K. Aumayr, G. Schmauss, N. Fellner, S. Handschuh, M. Glösmann, P. Pasierbek, M. Schlederer, G. P. Resch, Y. Ma, H. Yang, H. Popper, L. Kenner, G. Kroemer and J. M. Penninger, "A dual role for autophagy in a murine model of lung cancer," *Nature Communications,* vol. 5, p. 3056, 2014.

[136] Y. Geng, L. Kohli, B. J. Klocke and K. A. Roth, "Chloroquine-induced autophagic vacuole accumulation and cell death in glioma cells is p53 independent," *Neuro Oncol,* vol. 12, no. 5, p. 473–481., 2010.

[137] G. Manic, F. Obrist, G. Kroemer, I. Vitale and L. Galluzzi, "Chloroquine and hydroxychloroquine for cancer therapy," *Molecular & Cellular Oncology,* vol. 1, no. 1, p. e29911, 2014.

[138] R. K. Amaravadi, D. Yu, J. J. Lum, T. Bui, M. A. Christophorou, G. I. Evan, A. Thomas-Tikhonenko and C. B. Thompson, "Autophagy inhibition enhances therapy-induced apoptosis in a Myc-induced model of lymphoma," *J Clin Invest.,* vol. 117, no. 2, p. 326–336, 2007.

[139] X. Liang, J. Tang, Y. Liang, R. Jin and X. Cai, "Suppression of autophagy by chloroquine sensitizes 5-fluorouracil-mediated cell death in gallbladder carcinoma cells," *Cell & Bioscience,* vol. 4, no. 10, 2014.

[140] S. Avniel-Polak, G. Leibowitz, Y. Riahi, B. Glaser, D. Gross and S. Grozinsky-Glasberg, "Abrogation of Autophagy by Chloroquine Alone or in Combination with mTOR Inhibitors Induces Apoptosis in Neuroendocrine Tumor Cells," *Neuroendocrinology,* 2015.

[141] E. Firat, A. Weyerbrock, S. Gaedicke, A.-L. Grosu and G. Niedermann, "Chloroquine or Chloroquine-PI3K/Akt Pathway Inhibitor Combinations Strongly Promote γ-Irradiation-Induced Cell Death in Primary Stem-Like Glioma Cells," *PLoS One,* vol. 7, no. 10, p. e47357, 2012.

[142] N. Echeverry, G. Ziltener, D. Barbone, W. Weder, R. A. Stahel, V. C. Broaddus and E. Felley-Bosco, "Inhibition of autophagy sensitizes malignant pleural mesothelioma cells to dual PI3K/mTOR inhibitors," *Cell Death and Disease,* vol. 6, p. e1757, 2015.

[143] M. Gandesiri, S. Chakilam, J. Ivanovska, N. Benderska, M. Ocker, P. Di Fazio, M. Feoktistova, H. Gali-Muhtasib, M. Rave-Fra, O. Prante, H. Christiansen, M. Leverkus, A. Hartmann and R. Schneider-Stock, "DAPK plays an important role in panobinostat-induced autophagy and commits cells to apoptosis under autophagy deficient conditions," *Apoptosis,* vol. 17, p. 1300–1315, 2012.

[144] D. C. Rubinsztein, P. Codogno and B. Levine, "Autophagy modulation as a potential therapeutic target for diverse diseases," *Nature Reviews Drug Discovery,* vol. 11, pp. 709-730, 2012.

[145] M. C. Crisanti, A. F. Wallace, V. Kapoo, F. Vandermeers, M. L. Dowling, L. P. Pereira, K. Coleman, B. G. Campling, Z. G. Fridlender, G. D. Kao and S. M. Albelda, "The HDAC inhibitor panobinostat (LBH589) inhibits mesothelioma and lung cancer cells in vitro and in vivo with particular efficacy for small cell lung cancer," *Mol Cancer Ther,* vol. 8, pp. 2221-2231, 2009.

[146] T. Yan-Fang, L. Zhi-Heng, X. Li-Xiao, F. Fang, L. Jun, L. Gang, C. Lan, W. Na-Na, D. Xiao-Juan, S. Li-Chao, Z. Wen-Li, X. Pei-Fang, Z. He, F. Xing, W. Jiang and P. Jiang, "Molecular Mechanism of the Cell Death Induced by the Histone Deacetylase Pan Inhibitor LBH589 (Panobinostat) in Wilms Tumor Cells," *PLoS One,* vol. 10, no. 7, p. e0126566, 2015.

[147] C. Fischer, K. Leithner, C. Wohlkoenig, F. Quehenberger, A. Bertsch, A. Olschewski, H. Olschewski and A. Hrzenjak, "Panobinostat reduces hypoxia-induced cisplatin resistance of

non-small cell lung carcinoma cells via HIF-1α destabilization," *Molecular Cancer,* vol. 14, no. 4, 2015.

[148] P. G. Richardson, R. L. Schlossman, M. Alsina, D. M. Weber, S. E. Coutre, C. Gasparetto, S. Mukhopadhyay, M. S. Ondovik, M. Khan, C. S. Paley and S. Lonial, "PANORAMA 2: panobinostat in combination with bortezomib and dexamethasone in patients with relapsed and bortezomib-refractory myeloma," *Blood,* vol. 122, pp. 2331-2337, 2013.

[149] A. Takahashi, F. Kimura, A. Yamanaka, A. Takebayashi, N. Kita, K. Takahashi and T. Murakami, "Metformin impairs growth of endometrial cancer cells via cell cycle arrest and concomitant autophagy and apoptosis," *Cancer Cell International,* vol. 14, no. 53, 2014.

[150] Q. GUO, Z. LIU, L. JIANG, M. LIU, J. MA, C. YANG, L. HAN, K. NAN and X. LIANG, "Metformin inhibits growth of human non-small cell lung cancer cells via liver kinase B-1-independent activation of adenosine monophosphate-activated protein kinase," *Mol Med Rep,* vol. 13, no. 3, p. 2590–2596, 2016.

[151] I. Monastyrska, E. Rieter, D. J. Klionsky and F. Reggiori, "Multiple roles of the cytoskeleton in autophagy," *Biol Rev Camb Philos Soc,* vol. 84, no. 3, pp. 431-48, 2009.

[152] H. LIU, C. SCHOLZ, C. ZANG, J. H. SCHEFE, P. HABBEL, A.-C. REGIERER, C.-O. SCHULZ, K. POSSINGER and J. EUCKER, "Metformin and the mTOR Inhibitor Everolimus (RAD001) Sensitize Breast Cancer Cells to the Cytotoxic Effect of Chemotherapeutic Drugs In Vitro," *Anticancer Research,* vol. 32, no. 5, pp. 1627-1637, 2012.

[153] R. Rao, R. Balusu, W. Fiskus, U. Mudunuru, S. Venkannagari, L. Chauhan, J. E. Smith, S. L. Hembruff, K. Ha, P. Atadja and K. N. Bhalla, "Combination of pan-histone deacetylase inhibitor and autophagy inhibitor exerts superior efficacy against triple-negative human breast cancer cells," *Mol Cancer Ther,* vol. 11, no. 4, pp. :973-83, 2012.

[154] K. Matsunaga, T. Saitoh, K. Tabata, H. Omori, T. Satoh, N. Kurotori, I. Maejima, K. Shirahama-Noda, T. Ichimura, T. Isobe, S. Akira, T. Noda and T. Yoshimori, "Two Beclin 1-binding proteins, Atg14L and Rubicon, reciprocally regulate autophagy at different stages," *Nature Cell Biology,* no. 11, pp. 385 - 396, 2009.

[155] H. Chial, "Proto-oncogenes to Oncogenes to Cancer," *Nature Education,* vol. 1, no. 1, p. 33, 2008.

[156] H. Chial, "Tumor Suppressor (TS) Genes and the Two-Hit Hypothesis," *Nature Education,* vol. 1, no. 1, p. 177, 2008.

[157] C. GM, "Tumor Suppressor Genes," in *The Cell: A Molecular Approach*, Sunderland, Sinauer Associates, 2000.

[158] J. Geradts, K. M. Fong, P. V. Zimmerman, R. Maynard and J. D. Minna, "Correlation of Abnormal RB, p16ink4a, and p53 Expression with 3p Loss of Heterozygosity, Other Genetic Abnormalities, and Clinical Features in 103 Primary Non-Small Cell Lung Cancers," *Clin Cancer Res,* vol. 5, p. 791–800, 1999.

[159] E. L. Kim, R. Wüstenberg, A. Rübsam, C. Schmitz-Salue, G. Warnecke, E.-M. Bücker, N. Pettkus, D. Speidel, V. Rohde, W. Schulz-Schaeffer, W. Deppert and A. Giese, "Chloroquine activates the p53 pathway and induces apoptosis in human glioma cells," *Neuro Oncol,* vol. 12, no. 4, p. 389–400, 2010.

[160] K. Sobczak and W. Krzyzosiak, "Structural Determinants of BRCA1 Translational Regulation," *The Journal of Biological Chemistry,* no. 277, pp. 17349-17358, 2002.

[161] P. Araujo, K. Yoon, D. Ko, A. Smith, M. Qiao, U. Suresh, S. Burns and L. O. F. Penalva, "Before It Gets Started: Regulating Translation at the 5′ UTR," *Comparative and Functional Genomics,* vol. 2012, 2012.

[162] J. Andrews, I. Levenson and B. Oliver, "New AUG initiation codons in a long 5′ UTR create four dominant negative alleles of the Drosophila C2H2 zinc-finger gene ovo," no. 207, p. 482–487, 1997.

[163] G. Scheper, M. van der Knaap and C. Proud, "Translation matters: protein synthesis defects in inherited disease," *Nature Reviews Genetics,* vol. 8, pp. 711-723, 2007.

[164] A. K. G. Velikkakath, T. Nishimura, E. Oita, N. Ishihara and N. Mizushima, "Mammalian Atg2 proteins are essential for autophagosome formation and important for regulation of size and distribution of lipid droplets," *Mol Biol Cell,* vol. 23, no. 5, p. 896–909, 2012.

[165] Y. Shao, Z. Gao, P. A. Marks and X. Jiang, "Apoptotic and autophagic cell death induced by histone deacetylase inhibitors," *Cell Biology,* vol. 100, no. 52, p. 18030–18035, 2004.

[166] A. M. Schläfli, O. Adams, J. A. Galván, M. Gugger, S. Savic, L. Bubendorf, R. A. Schmid, K.-F. Becker, M. P. Tschan, R. Langer and S. Berezowska, "Prognostic value of the autophagy markers LC3 and p62/SQSTM1 in early-stage non-small cell lung cancer," *Oncotarget,* 2016.